**ADDIS ABABA UNIVERSITY**
**SCHOOL OF GRADUATE STUDIES**
**SCHOOL OF EARTH SCIENCES**

# GEOLOGY, GEOCHEMISTRY AND GENESIS OF ULA ULO NICKEL DEPOSIT, ADOLA BELT, SOUTHERN ETHIOPIA

**WUBEGZIER KEBEDE ADAMU**

**A thesis submitted to the School of Graduate Studies of Addis Ababa University in partial fulfillment of the requirements for the degree of Master of Science in Resource Geology (Mineral Deposit)**

**May 30, 2018**
**Addis Ababa, Ethiopia**

**ADDIS ABABA UNIVERSITY**
**SCHOOL OF GRADUATE STUDIES**
**SCHOOL OF EARTH SCIENCES**

# GEOLOGY, GEOCHEMISTRY AND GENESIS OF ULA ULO NICKEL DEPOSIT, ADOLA BELT, SOUTHERN ETHIOPIA

**WUBEGZIER KEBEDE ADAMU**

**ADVISOR: WORASH GETANEH (PhD)**
**CO-ADVISOR: MULUGETA ALENE (PhD)**

**A thesis submitted to the School of Graduate Studies of Addis Ababa University in partial fulfillment of the requirements for the degree of Master of Science in Resource Geology (Mineral Deposit)**

**May 30, 2018**
**Addis Ababa, Ethiopia**

# Declaration of Originality

I hereby declare that the thesis is my original master‘s degree work under the supervision of Dr. Worash

Getaneh and Dr. Mulugeta Alene, School of Earth Sciences, Addis Ababa University during the year 2018. I further declare that this work has not been presented or submitted to any other university or institution for the award of any degree or diploma. All sources and materials used for the thesis have been duly acknowledged.

Wubegzier Kebede Adamu _____ _____

Signature Date

This is to certify that the above declaration made by the candidate is correct to the best of my knowledge and belief.

Dr. Worash Getaneh _____ _____

Signature Date

Dr. Mulugeta Alene _____ _____

Signature Date

# Abstract

The study area is located in the Neoproterozic metavolcano-sedimentary assemblages of Megado belt within Adola belt of southern Ethiopia. Nickel mineralization is hosted and confined by serpentinites. The country rocks are tremolite talc schist and talc tremolite schists. Geochemistry of the host rock and country rocks is studied. All units shows LILE Enrichment (Ba/Yb)n is 2.92 (serpentinite), 1.2(talc schist), 3.84 (tremolite schist) and 3.2 (amphibolite). Because these LILEs are fluid mobile and easily assimilated from the subducting slab as compared HFSEs. REEt calculated as serpentinite (0.7 – 1.84 ppm), talc schist (2.69 ppm) and tremolite schist (2.79) while amphibolite has REEt (6.18). (La/Yb) c.n values are serpentinite (4.2), talc schist (6.6), tremolite schist (3.7) and amphibolite (8.1). Slight enrichment of LILE and LREE and depletion of HFSE and HREE for both serpentinite, talc tremolite schist and amphibolite is due to assimilation and dehydration of subducting slab. Magmatic evolution undergone without amphibole intervention and plagioclase crystallization. Both ultramafic and mafic rocks are crystallized from similar origin. The geochemical signature of both the mafic and ultramafic rocks is similar to alkaline thoeliitic and island arc thoeliitic bonnieite. Tectonic discrimination shows island arc boninite andesite affinity. Meta sedimentary rocks are also common in the study area. These are quartzite, meta psmmite and graphite schist. Both metavolcanic and metasedimentary rocks are metamorphosed to greenschist facies. Because the mineral assemblages are antigorite, lizardite, talc, tremolite, actinolite, chlorite, epidote, sericite and hornblende. The rocks are aligned NS and dips towards $70^0$ towards W. The deposit is zoned into two. These are oxide zone and saprolite zone. Oxide zone is upper portion of the lateritic column while saprolite covers the lower part. The occurrence of the mineralization in these zones is variable. Inferred resources estimation is done for these zones separately. The source of the Ni is serpentinites. The metal is leached from oxide zone and serpentinites and precipitated in the saprolite as garnierites. The mineralogy of these garnierites is studied. Both serpentine-like and talc-like garnierites are observed. Other ore minerals observed are chromite and magnetite. The genesis is formulated based on geochemical and mineralogical characteristic of garnierites. The deposit model is ultramafic hosted lateritic nickel deposit hosted. Ore body Morphology, extent, mineralogy and geochemistry are studied and explained.

*Key words: Ula Ulo Nickel deposit, Serpentinites, Lateritic Nickel deposit, Garnierite, Talc-like and Serpentine-like garnierite.*

# Acknowledgment

This research is done by the contribution of different organizations like Addis Ababa University, ALS (Australian laboratory services), University of Naples, and Taiwan Institute of Chemistry. Firstly, I would like to thank Addis Ababa University for giving me an opportunity for studying Master's degree and funding the research. Secondly, ALS (Australian laboratory services) for geochemical analysis and University of Naples and Taiwan institute of chemistry for XRD analysis.

I am very grateful for my advisors Dr. Worash Getaneh and Dr. Mulugeta Alene for their repetitive follow up, constructive comments, encouragement and tireless support. I had no words to express my deepest gratitude to Mr. Amogne workie for XRD analysis at Taiwan institute of chemistry and Mr. Yemane Kelmwork for XRD analysis at university of Naples. School of Earth Science and All academic staffs have a contribution on this research.

My acknowledgement goes to my family (Metekie Yebeltal (mom), Nestanet Dechasa (my love), Hargewine Meharie (sister) and Sintayehu Kebede (sister) for their encouragement and unforgettable support. For their kindly collaboration during field work in this challenging time, as well I should thank Haya Dima administrations and local community.

# Tables of contents

# List of figures

# List of tables

ACRONYM

| | |
|---|---|
| ALS | Australian laboratory services |
| ICP-MS | Inductively Coupled Plasma Mass Spectroscopy |
| ICP- AES | Inductively Coupled Plasma Atomic Emission Spectroscopy |
| XRD | X- Ray Diffraction |
| INSG | International Nickel Study Group |
| TMEP | Training for mineral exploration program |
| Act | Actinolite |
| Alb | Albite |
| Ant | Antigorite |
| Bt | Biotite |
| Chl | Chlorite |
| CPx | Clinopyoxene |
| Epd | Epidote |
| Hbl | Hornblend |
| Olv | Olivine |
| Plg | Plagioclase |
| Qtz | Quartz |
| Ser | Sericite |
| Serp | Serpentine |
| Tac | Talc |
| Tre | Tremolite |
| LOI | Loss on ignition |
| HREE | Heavy Rare Earth Element |
| LILE | Large Ion Lithophile Element |
| LREE | Light Rare Earth Element |
| HFSE | High Field Strength Element |
| TAS | Total Alkali Silica |

# Chapter - I

# Introduction

## 1.1. Background Information

Southern Ethiopia is the first place to be studied and explored for Ni exploitation (Jelenc, 1966b). This mineralization is related to metamorphosed and obducted ophiolite during subduction. Jelenc (1966b) is the first to state the presence of dikes of mafic - ultramafic composition within Adola metasediments. These dikes have been assumed to have a potential to host Ni and Cr. Nickel is present within the crystal lattices of olivine and other ferromagnesian minerals in trace concentration. Solomon (2003) added that the host rock of this nickel mineralization is metamorphic equivalent of peridotite. Nickel occurrences in the region are many but the major ones are Budussa, Kenticha, Dubicha Gudda, Dubicha Mika, Wollabo, Burjiji, Ula Ulo and Tulla. They are grouped as chromite containing serpentinite (e.g., Budussa, Kenticha, Dubicha Gudda, Dubicha Mika, and Wollabo) and serpentinite without eluvial chromite (e.g., Burjii, Ula Ulo and Tulla) (Jelenc, 1966b). The reason behind this variation requires detailed study. The mineralogy of these serpentinite bodies is lizardite and antigorite with chrysotile (Clark, 1978). Ore mineralogical studies on the garnierite veins show pimelite (Solomon, 2003) affinity. Surficial nickel mineralization is formed by lateritic soil development. Concentration of metals in unweathered peridotite is uneconomical (Nickel (0.1- 0.3 %), cobalt (0.02 %), and copper (0.998 %)) (Solomon, 2003). The main accessory mineral is magnetite with nickel of unknown chemical structure (Jelenc, 1964).

Nickel exploration in the region dates back to 1950's (Jelenc, 1964). Detailed exploration activity was conducted at Ula Ulo, Kenticha, Kilta, Big Dubicha, Lolotu, and Tulla (Jelenc, 1964). Reserves of some of these deposits have been evaluated. From all of these occurrences, Ula Ulo is the largest reserve containing 2,298,863ton at 1.41 % Ni proved reserves (Ministry of Mines (MOM), 1964). Some drilling data on Ula Ulo showed as much as 4% Ni in the area within garnierite veins (Jelenc, 1964).The proposed research will be conducted on Ula Ulo – Haya Dima on which serpentinite hosted nickel mineralization is located.

## 1.2. Geographic Setting of the Study Area

### 1.2.1. Location and Accessibility

The research is conducted in the Adola belt, a narrow belt of meta-volcano sedimentary rocks of Neoproterozic age. The geographic boundaries of the study area are 481000 – 486000 Easting, and 607890 – 611000 Northing. It is located at 612 km far from Addis Ababa along the road Addis Ababa – Hager Mariam (asphalted) – Dawa (all weathered)- Haya Dima (all weathered)- Ula Ulo (all weathered). Another route of 607 km is available along Addis Ababa – Kibermengst (asphalted) – Haya Dima (all weathered) – Ula Ulo (all weathered). Administration wise, the study area is located in Oromia regional state, Gujii zone, Agga Wouii woreda (Haya Dima) administration as shown in Fig 1.1a and b.

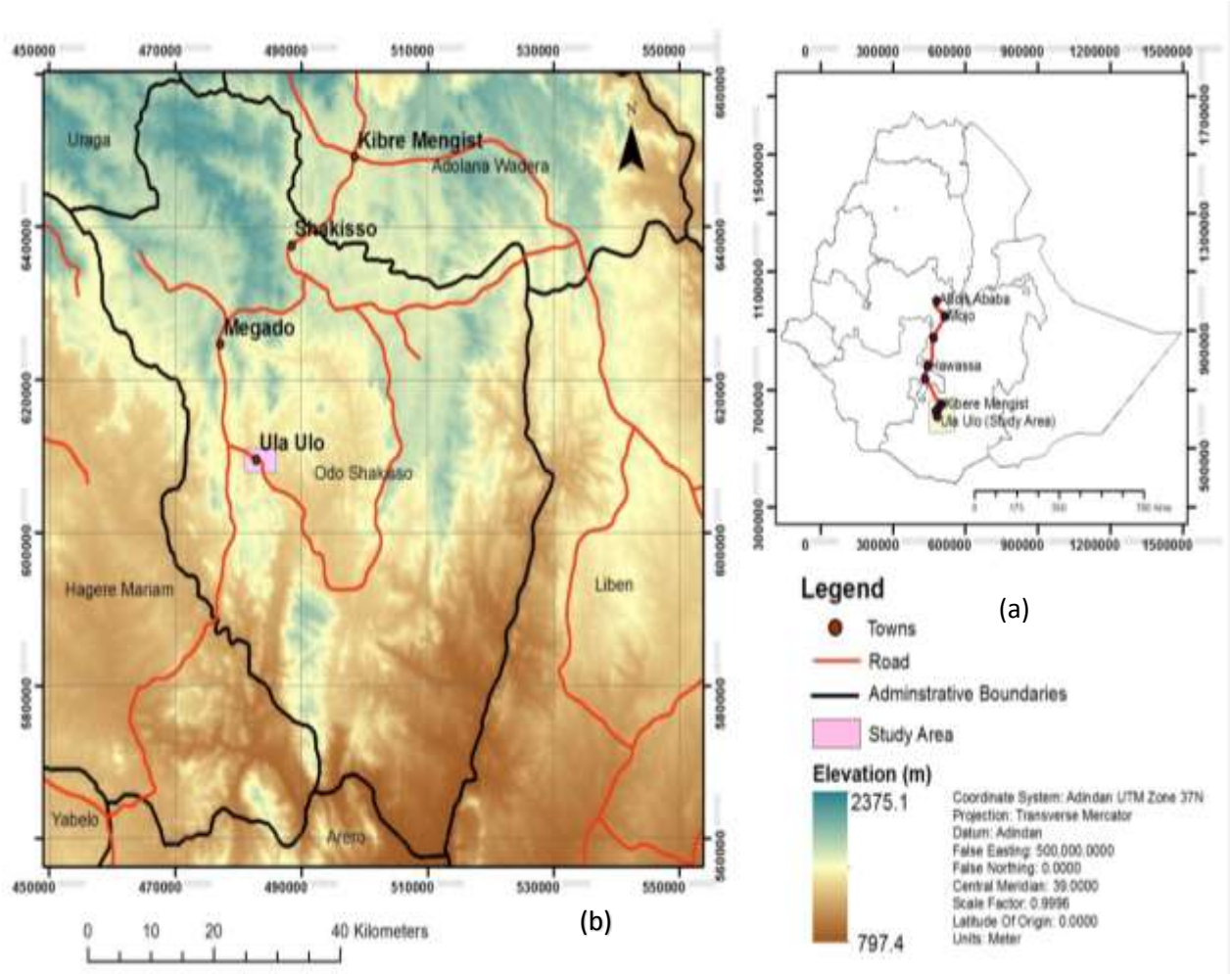


*Fig 1.1 Location map of the study area*

### 1.2.2. Physiography and Drainage

The elevation (fig 1.2) of the area is below 2000 meter above sea level except some places (Kumdo and Worseti), but the variation on the relief is prominent since the region is polydeformed. These folding resulted cliff forming ridges (1700 meter above sea level) to relatively low land areas (1400 meter). The ridges are mainly composed of mafic ultramafic sequences (e.g. Ula Ulo, Kilta, Kenticha, Werseti, Kumudo and Wosho) while the low lands are either high grade gneisses and/or metasediments.

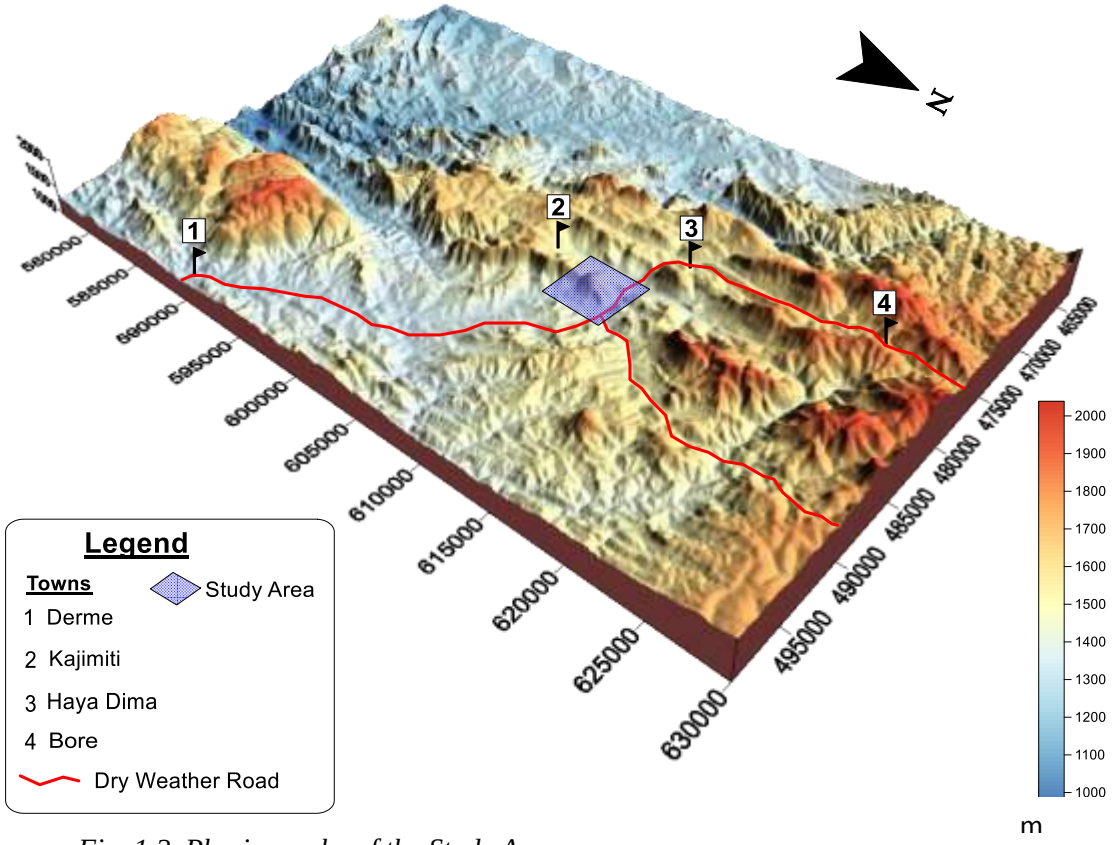


*Fig. 1.2. Physiography of the Study Area*

Major rivers found in the area are Mormora, Chemoga, Haya Dima and Dawa (Fig 1.3). These all are persistent for the whole season. Down the catchment, all the rivers merge and form Dawa river top left of the photo which is the major tributary of river Genale. These rivers are very important for the local people because they serve as a source of placer gold. Major placer mining sites in the region are along these rivers. Awata river in Bedakissa area served as placer mining site since the imperial period. Haya Dima and Dawa rivers, the most closest, to the study

area are also major placer mining sites. Mormora and Chemoga river play a role of producing electrical power for Adola Gold Enterprise (Megado). Kenticha Tantalum Mine uses Mormora river for mineral processing.

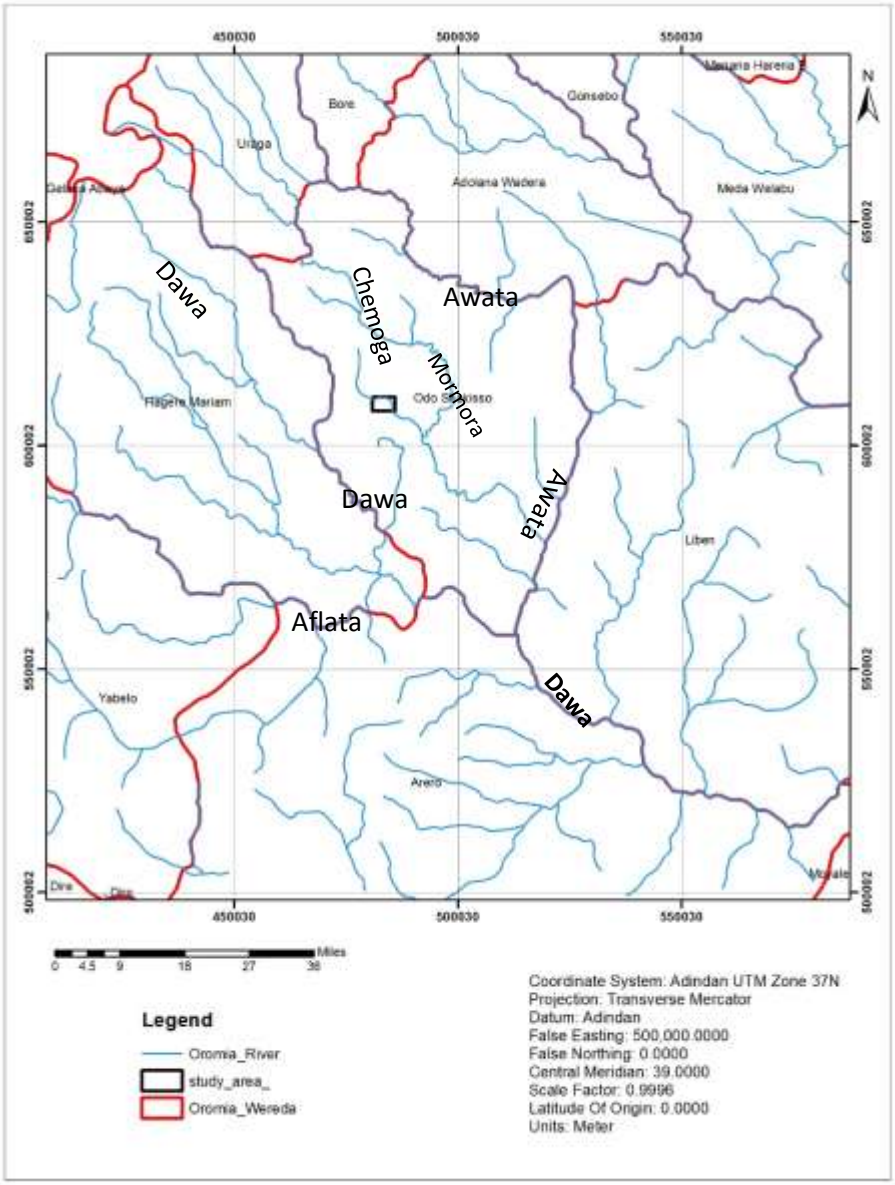


*Fig 1.3. Drainage map of the study area including Dawa, Mormora and Awata rivers.*

### 1.2.3. Vegetation and Climate

The climate is classified as tropical savanna wet having an average temperature of 19.9 $^{0}$c and average annual precipitation of 922 mm (https://en.climate-data.org/location/508527/). The maximum temperature is 29.6 $^{0}$c in February and the minimum temperature is 10.6 $^{0}$c in

December. The maximum precipitation is recorded in March- May and September – October (Fig. 1.4).

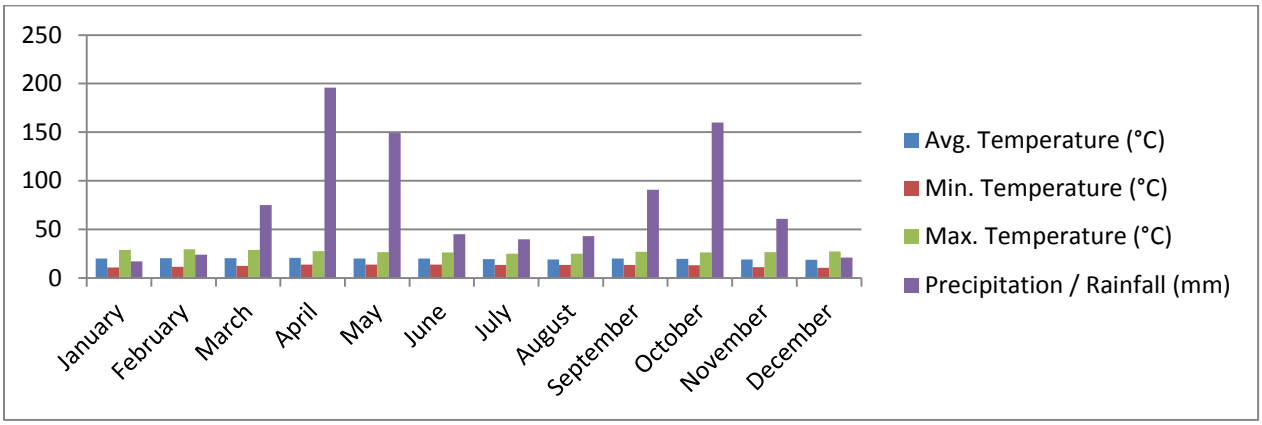


Fig 1.4 Climate and Weather data of the study area *(https://en.climate-data.org/location/508527/; accessed on march 2, 2018)*

Deep weathering and subsequent soil development, minimal human intervention and the availability of rain resulted in the presence of thick forest cover. Most trees are endemic. These are Dodonaea angustifolia, Podocarpus flactus, and African olive. Towards Kenticha the vegetation cover is sparse (Fig 1.5. a). Along the road to Kajimiti valley the forest cover is dense (Fig 1.6. b). Serpentinite ridges are devoid of vegetation with only short Dodonaea angustifolia trees (Fig 1.5. c). In recent times the population growth cause for illegal repopulation which is severely damaging the forest cover of the area.

**(a)**

**(b)**

**(c)**

*Fig 1.5 Field photographs showing (a) a panoramic view of Kenticha Tantalum Mine; (b) dense forest covers along the road to kajimiti; (c) xerophytic vegetation of the study area.*

### 1.2.4. Population and settlements

According to the national censes conducted in 2007, the population of the woreda (Odo Shakisso) is 206, 372 (107, 224 males and 99,148 females) from these, the urban population accounts 33,643 (18,047 males and 15,596 females) and the rural population is 172,729 (89,177 males and 83,552 females) (CSA, 2007). Their religion is (56.6 %) protestant, (14 %) orthodox christan, (11.4 %) Islam, (10.6 %) traditional, (1.8 %) catholic, and (5 %) others. In Gujii zone different languages are spoken by the local people. These are Afan Oromo (77.9 %), Gedeogna (14.15 %), Amharic (4.31 %), Guragegna (3.1 %), Solomaligna (1.6 %) and Sidamigna (0.8 %) (CSA, 2007).

The area is sparsely populated in rural areas and outside placer mining sites. But around the cities and the placer mining sites (in the local language they call it Worfa) it is densely populated. Major cities are Haya Dima, Megado, Dermi, Kenticha, Dawa and Shakisso.

The economy of the people is dependent on placer gold mining, animal husbandry, coffee plantation and small agriculture. Major placer mining sites are Worfa (1 and 2), Kajimiti, Bore (upper and lower), Dolovia, Bedakissa and others. The region (Borena) is well known for its cattle. Therefore, there is a market chain through which the farmers are able to sell their cattle. Coffee plantation is restricted to some localities in the study area (e.g. Chaketa, Wollena and Megado).

(a) (b)

*Fig 1.6 Field photographs showing vegetation and cattle's; (a) cows and oxen, (b), camels.*

### 1.3. Statement of the problem

Previous studies on the nickel mineralization of Ula Ulo area targeted concentration of Ni in the surficial weathering medium and genesis of nickel mineralization was inferred based on Ni % in unaltered serpentinite and unaltered peridotite . These are 0.5 and 0.3 % Ni respectively (Jelenc, 1966b). But such interpretation could lead to wrong conclusion about genesis of the mineralization since depletion of Ni in the host rock will be an indication of accumulation of Ni at the base of the ultramafic body as magmatic sulfide deposit (Ridely, 2012; Misra, 1999). The genesis of Ni mineralization could also be linked to Serpentinization and metamorphism process (Eckstrand, 1975; Donaldson, 1981; Levitte and Kent, 1968). The proposed Ula Ulo lateritic nickel mineralization was also not studied in detail. Summaries were made from interpolation of results from different localities (e.g. using Big Dubicha drilling data for interpretation of Ula Ulo (Levitte and Kent, 1968)). In reality, even within small distance there is a clear difference between serpentinite of Kenticha and Ula Ulo which are selectively enriched by Cr and Ni respectively (Jelenc, 1966b).

The proposed research will identify an ore forming process so that uncertainties about the genesis of nickel mineralization will be clarified. Moreover, data from mineralogical, geochemical, geological and structural investigations collectively will update present level of knowledge on geochemistry and geology of rocks in Ula Ulo area.

## 1.4. Objective of the research

### 1.4.1. General objective

The main objective of this research is to understand the geology, geochemistry and genesis of nickel mineralization at Ula Ulo area.

### 1.4.2. Specific objectives

In order to achieve the above mentioned main objective the following specific objectives are formulated.

1. Produce geological map at a scale of 1: 10, 000.
2. Determine the geochemistry of the host rock and mineralized body.
3. Ore mineralogy investigation.
4. Explain the genesis of the mineralization.
5. Delineate the ore body and estimate the reserve

## 1.5. Methodology

### 1.5.1. Introduction

This research is conducted using three major methods: geological mapping, geochemical studies, and mineralogical studies. The research was conducted in four major phases.

### 1.5.2. Phase one

The first phase is pre field preparation (collection of relevant information about the study area) and literature review (reviewing previous works and theoretical (conceptual) frameworks of nickel mineralization). This phase helped to widen the understanding on the study area and nickel mineralization. Topographic maps were purchased from Ethiopian map agency. Moreover, other necessary field materials (like hammer, compass, clinometer and GPS) were prepared for the fieldwork.

### 1.5.3. Phase two

Phase two was devoted to field work during which primary data were collected. The data collected include geological (geological mapping), structural (description and measurement), mineralization (samples) and geochemistry (samples).

#### 1.5.3.1. Geological mapping

Geological mapping is done to record geological information observed during the field work. The output is a two dimensional geological map at scale of 1:10,000. During the first field work the following tasks are done

- In the field, lithological, textural, weathering, topographic (relief) and structural studies are done. The primary data with supportive photographs were collected.
- Measurements of the primary (bedding) and secondary (foliation and joints) features were done.

The second field work is done to fill some information gaps. The draft map that is produced based on the first field work was reviewed and confirmed.

#### 1.5.3.2. Sampling

Forty one representative fresh samples are collected. These samples are categorized into three. The first are lithological samples collected for host rock and country rock for mineralogical studies. Nine Samples from six lithological units are selected for petrographic study. Three samples are selected from the serpentinite unit for alteration and facies identification. Twelve geochemical samples are selected for geochemical analysis. Out of these seven are from the serpentinite unit to understand the genesis of the mineralization, the ore grade and the geochemistry of the host rock. The remaining five are from the Amphibolite unit (one sample), veins (two samples), talc unit (one sample) and tremolite unit (one sample).

### 1.5.4. Phase three

Phase three is post field data analysis and interpretation. Twelve rock samples were collected for geochemical analysis. These samples are collected from the whole lithologic units (see table 5.1).These samples were crushed and grinded to 75 micron mesh size in ALS laboratory (Addis Ababa). The analysis ICP-MS and ICP- AES are done in ALS laboratory, Ireland. ICP-MS analysis is done for trace element and rare earth elements collectively 30 element package. Prior to ICP-MS analysis the samples were fused by lithium borate fusion. The fusion enables complete dissolution of refractory lithophile elements. These fused bead need to be digested by four acids for ICP-AES whole rock package (thirteen elements) analysis. Ore grade nickel and base metals (twelve elements) done by four acid digestion ICP-AES (ALS, 2018).

Mineralogical samples (thin sections and polished sections) are prepared in Ethiopian geological survey laboratory. Nine thin sections, three from the serpentinite, are prepared. Two Polished sections are prepared with dimensions of 45mm * 24mm. Ore petrographic study using Nikon ore microscopes was done at Addis Ababa University. Six samples are analyzed by XRD analysis in Taiwan Institute of Chemistry (five samples) and university of Naples (one sample). From the analysis the host rock and the ore zone is mineralogy is characterized. Ore petrographic studies are done to understand the mineral assemblage and ore – gangue association. For this purpose two polished sections with dimension of 42 mm* 26 mm were prepared in Ethiopian geological survey laboratory.

### 1.5.5. Phase four

This phase is presentation of the research to the scientific community. For presentation I used different software packages. These are ArcGIS, MapInfo professional, Surfer, and Match XRD. ArcGIS is used for geological mapping and resource calculation, MapInfo used for stratigraphic column production, Surfer used for Modeling and geological cross section production and Match XRD used for mineral phase and composition identification. Report writing were done from the starting date to the finalization of the work. Progressive report submitted in February and final report produced in eight chapter scheme. These are introduction, literature review, regional geology, local geology, geochemistry, mineralization of the deposit, discussion and conclusion.

## 1.6. Material

Materials required for the research are;

- Field equipment's (i.e. Garmin GPS, Compass and Clinometer, Geological Hammer and Chisel, and Rock Sample Holding Kits.
- Software (i.e. ArcGIS software, MapInfo professional, Toolkit petrography, Petrograph beta, Surfer software, Match XRD data plotter, Adobe illustrator and Sterionet)
- Stationeries

## 1.7. Previous works

The Nickel exploration on the region was first driven by the local peoples. Because they have taken samples to Ministry of Mine after looking unusual a green stain on the serpentinites (Jelenc,

1964). These initiated nickel exploration program in 1957/58 (Jelenc, 1965). The exploration targeted (Jelenc, 1965; Jelenc, 1963; Jelenc, 1964 and some references there in) a discovery of new occurrences and to make a reconnaissance survey on Ula Ulo, Big Dubicha, Lolotu, Tulla and Ujima ridges. Side by side to the reconnaissance survey some explorations were done on Tulla and Kenticha serpentinite bodies. This exploration later advanced to drilling. Extensive drillings are done on Kilta- Tulla- Ula Ulo.

Technological samples (50kg each) were collected from pits of Ula Ulo and Tulla (Jelenc, 1963). These samples are used to characterize the technological property of the mineralization for better utilization.

Initial reserve was calculated in 1963 for Tulla and Ula Ulo. These are 583, 500 tons @ 1.14 % Ni and 2, 161, 250 tons @ 1.35 % Ni respectively (Jelenc, 1963). The average depth of mineralization in Tulla is 6.57 meter. The maximum grade is 1.8 % Ni, observed on the depth between 1.4 – 3.0 meter containing. Down the depth; the grade decreases up to 18 meter. Below the depth of 24.5 meter the nickel concentration is below 0.5 % in Tulla (Jelenc, 1964).

Ula Ulo ridge on other hand is rounded serpentinite body; diameter is 300 meter and is enriched by garnierite veins in its western slope. Extensive shallow drillings, 1500 meter, were done in 1964. The average depth of these boreholes is 6.61 meter (Jelenc, 1964). The average grade is calculated to be 1.5 % Ni and the cutoff grade considered was 1 %. The tonnage is 2,000,000 ton. In some part of the deposit, the grade riches up to 4.5 % Ni. Accessory minerals are magnetite (crystalline and amorphous), and travorite. Some analyses done on the amorphous magnetite showed 0.9% Ni and 0.44 % Cr. Veins of magnetite are 2 – 5 mm wide. The morphology of Ula Ulo is circular with diameter of 300meter (Jelenc, 1964). At this point mineral assemblage of the nickel bearing garnierite veins was not known (Jelenc, 1964).

Jelenc (1964) also discussed and explained about the geology and genesis of the nickel - chromium deposits of Sidamo province. The nickel bearing lens shaped serpentinites are hosted by chlorite – talc schist. The talc schist is bounded by gneiss. Jelenc (1964) has divided the serpentinite bodies in to two as western and eastern alignment. These alignments are chromite barren and chromite containing serpentinite bodies. The chromite barren serpentinites are Burjiji, Ula Ulo, kilta and Tulla. Chromite containing serpentinites are Kenticha, and Dubicha. The genesis of the chromite mineralization is related to weathering of the serpentinite bodies. On

other hand nickel mineralization, in the residual soil, is originated from lattices of silicate minerals.

According to Jelenc (1966) these serpentinite bodies are mostly lizardite and a result of alteration of peridotite. Garnierite veins in Tulla and Saddle are following the fissures of the altered serpentinites. The concentration of nickel in the region is estimated by Jelenc (1966) and Bentor (1967) as 1-3 % Ni with Co (0.02 to 0.05%) and Cr (0.5 -1.6%). The morphology of these veins is variable (i.e. sinister, cottage, incrustation and stock works). The reserve classification on Ula Ulo is done in 1966. The proved reserve is 2, 317, 086 tons @ 1.37 % Ni with average depth of 4.70 m (Jelenc, 1966b). Probable reserve is estimated as 994, 450 tons @ 1.35 Ni. The possible reserve is 500,000 tons.

Valicn and Yehwalwork (1967) prepare a geological map and megascopic description of Ula Ulo, Kilta, and Tulla prospects. On their map they displayed nickel bearing serpentinites those are found in Adola between the geographic coordinate of $5^0$ 35'N - $6^0$35'N and $38^0$45'E – 39 $^0$ 05' E. They identified the predominant lithologies, chlorite-talc schist (altered and limonitized), chlorite schist (with barren white quartz and 1-3 cm thick magnetite), chlorite – epidote schist (containing 1m thick quartz veins), quartizitic and graphitic schists and serpentinites. These schists are oriented NS and dipping $60^0$ to the west. Nickel found in the form of pimelite on variably (Ni, Fe and Si) enriched saprolitic and podolithic soil horizons. From the surface to down depth the horizons are Fe-rich cap rock (Ni) barren, Ni-rich weathered serpentine and fresh (Ni barren) serpentine. Ore body dimension estimated as 600 meter width x 1000 meter long and 200 height (Valicn and Yehwalwork, 1967). Residual Ni deposit at Ula Ulo riches 70 % of the surface area with concentration of 0.82 % Ni and minimum depth of 1meter (Valicn and Yehwalwork, 1967). They also done chemical analysis on Ula Ulo, 10 representative samples, shows 0.66 -1.82 % Ni, 0.01 -0.02 % Co, 6.60 – 11.31 Fe, 0.28 – 0.79 % $Cr_2O_3$ , 20.72 -28.63 % MgO, 42.95 – 54.60 % $SiO_2$ , 0.16 – 0.28 $Al_2O_3$, 0.01- 0.05 Ca. the ore reserve is 3,000, 000 ton @ 1.60 Ni with cutoff grade 0.8 % Ni.

Bentor (1967) and Jelenc (1966) stated nickel mineralization on the region riches up to 1-3 % with Co (0.02 to 0.05%) and Cr (0.5 -1.6%). Analysis of garnierite veins revealed that pale vane green color (1.26 Wt % Ni) with small veins of grey material.

Drilling at Big Dubicha (289 meter) and at Tula (79.6 meter) indicated the presence of garnierite, calcite and azurite veins with disseminated chalcopyrite. The fresh peridotite encountered after 143 meter (Hamerla, 1977).

# Chapter – II

# Literature review

## 2.1. Introduction

Nickel ($^{28}_{58}$ Ni) is an element with electron configuration of [Ar] $4s^2 3d^8$. It has low thermal and electrical conductance with high resistance to deterioration. These properties make nickel to be required in the different industries. The main applications are for the production of stainless steel (~65%), metal alloys (~20%) and plating (~9%) (INSG, 2018).

According to Fleischer (1953) and Cornwall (1949) the nickel content of the earth's crust is 0.008-0.02 weight percent. Nickel is the fifth abundant element of the earth. Primordial earth's fractionation causes segregation of Sidrophile and Chalcophile elements to the earth's core. This fractionation also enriched earth's mantle relative to earth's crust up to 0.3 % in peridotite and dunite (Misra, 1999). Therefore magmas formed by partial melting of mantle peridotite and dunite are more enriched by nickel than magmas formed by crustal anatexis. The formation of a magmatic nickel sulfide deposit relied on sulfur saturation and segregation of the immiscible melt (Ripley and Li, 2013).

Nickel deposits are classified as magmatic, structure related and sedimentary deposits (Dills, 2010). Magmatic Nickel sulfide deposits are formed by gravity driven settling of nickel bearing immiscible sulfide melt from mafic or ultramafic magma (Naldrett, 1999; Cornwall, 1949; Keays, 1995). These sulfide melt contains chalcophile elements, Ni – Fe- Cu, resulting in the formation of sulfide minerals like pyrrhotite, pentlandite and chalcopyrite (Dills, 2010; Cornwall, 1949).

Naldert (2013) summarized the possibilities for the formation magmatic sulfide deposits. These are accumulation of sulfur in the system without silicate crystallization. This is possible only if there is sulfur addition. Addition can by crustal contamination or magma mixing. Crustal contamination is efficient if there is sulfur bearing rocks (e.g. anhydrite or gypsum). The second requirement is restricted flow. This is possible if there is a conduit. Additional to the above two requirement there should be also interaction between the sulfur and the magma. Reaction enables

the sulfide to scavenge and accumulate Ni. This is related to the absence of sulfide maturation and depletion of nickel on the crystallizing phase (olivine and pyroxene).

Structure related deposits are formed in continental rifts. They contain five element (Ni-Co-As-Ag-Bi) associations. Their genesis is related to deposition of paragentically differentiated sulfide ores in fissure veins (Staude et.al, 2012; Dills, 2010).

Sedimentary nickel deposits are formed by deep intensive weathering of ultramafic rocks. The weathering happened when there is humid tropical to sub-tropical climatic conditions (Cornwall, 1949; Butt, 2013). Cornwall (1949) identified two families of lateritie: nickelfirous iron laterites and nickel silicate types. Nickelfirous iron laterites are weathered serpentinites whereas nickel silicate types are hydrous silicate garnierite of talc and antigorite affinity. Three possible ore types of lateritic regolith are oxides, hydrous magnesium silicates and clay silicates (Butt, 2013). The oxide deposits are the upper most part of the soil profile containing iron oxide minerals such as goethite. Goethite holds Ni either by substitution or adsorption. The lower portion of the lateritie profile contains hydrous magnesium silicates or garnierites. These garnierite veins fill the cracks of saprolite zones (Gaudin et.al, 2005). Smectite and saponite are dominant ore minerals of clay silicate lateritic deposits.

Serpentinization can transform olivine to heazlewoodite + awaurite + Ni rich magnetite at low S content and to millerite + pyrite + Ni poor magnetite if the sulfur level is high (Filippidis, 1982). Nickel sulfide minerals (e.g. Godlevskite, Violarite or Barvoite) are common on serpentinized peridotite with high sulfur fugacity (Eckstrand, 1975 in Misra, 1999).

### 2.2. Models of Nickel Deposits

Mineral deposit models are developed based on information on the genesis, grade and tonnage of a given deposit (Berger et al 2002). These models are classified as descriptive, grade and tonnage, and genetic models (Cox and Singer, 1986). Genetic models are collection of characteristics of the deposit (Cox and Singer, 1986; Berger et al 2002). Descriptive model of nickel are Stillwater Ni-Cu, Norilsk Cu- Ni- PGE, Komatitic Ni- Cu, intrusive dunite Ni – Cu, synorogenic- synvolcanic Ni- Cu, vein (limasol forest type) Co- Ni, and lateritic Ni deposits (Cox and Singer,1986). Later dills (2010) classified nickel deposits into three groups. These are magmatic, structure related and sedimentary.

Magmatic deposits are subdivided into five models according to the place of crystallization (e.g. basal, pipe and rift (extrusive)) and the mineral commodity it contain ( e.g. Ni – Cu, Ni- Cu- Co and Ni – Cu – PGE/PGM). These deposits are formed by discrimination and assembling of sulfide droplets. The magmatic deposits result from Komatitic and picritic magmas (Keays, 1995; Naldert, 2013). These magmas are formed from unmixed mantel magma. If sulfur saturation is achieved these magmas host Ni – Cu- Co mineralization (Redman and Keays, 1985; Keays, 1995). Plenty of Ni – Co deposits are formed by this process (e.g., Sudbury, Still water and Kamblada) (Cox and Singer, 1986; Dills, 2010). Ore mineral assemblage of magmatic Ni-Cu deposits includes pentlandite, pyhhrotite and magnetite. The grade of these deposits riches up to 3.4 % Ni (Cox and Singer, 1986). Vein type deposits are strata bound epigenetic veins of five elements (Ni-Co-As-Ag-Bi) association. These deposits are commonly associated with continental rifting (e.g. Freiberg and Biber in Germany). These hydrothermal related deposits are high grade and low tonnage holding Ag in native form (Burisch et al., 2017).

Lateritic nickel - cobalt deposits are the result of chemical weathering (Marsh and Anderson, 2011). The mineralization is surficial and accumulate from the original higher concentration of nickel in olivine (0.2- 0.4%) (Brand et al., 1998). Therefore, these deposits are considered as sedimentary deposits. In such deposits nickel shows a green cast (Long, 2014). The green cast (color) is related to the grade (Brindley and Hang, 1973). This cast is helpful for exploration and mining geologists to easily recognize the deposit. Nickel laterites can be formed by direct and multiphase genesis (Butt, 2013).

Lateritic deposits have five major zones. These are duricrust (oxidized) zone, limonite zone, ferruginous saprolite, quartz and smectite zone and saprolite peridotite zone (Eliopoulos et al 2012). Sometimes the cap rock will be removed and these zones are reduced to four. The ore mineral assemblage of these types of deposits can be oxide lateritie, clay silicate and hydrous magnesium silicate (Longo, 2014). Butt (2013) listed the ore minerals associated to lateritic ore deposits as oxide ore, hydrous silicate ore and clay ore (table 2.1). Out of these garnierite (hydrous magnesium silicates) are high grade.

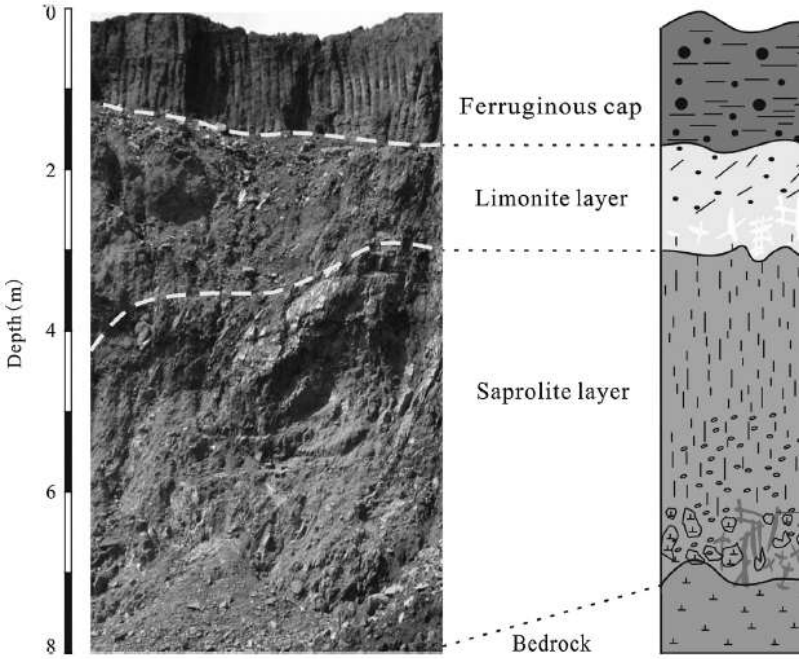


*Fig. 2.1 Field photograph of vertical exposure and correlated lateritic profile (after Wei Fu, 2014).*

.

**oxide ore**

| | | | |
|---|---|---|---|
| Goethite | Oxide | α-(Fe3+)O(OH) | 2% Ni, 0.2% Co |
| Asbolane | Oxide | (Ni2+,Co3+)xMn4+(O,OH)4.nH2O | 16% Ni, >4% Co |
| Lithiophorite | Oxide | (Al,Li)Mn4+O2(OH)2 | 1% Ni, ~7% Co |

**Mg- silicate ore**

| | | | |
|---|---|---|---|
| Ni lizardite -népouite | Serpentine | (Mg,Ni)3Si2O5(OH)4 | 6–33% Ni |
| 7Å garnierite | Serpentine | Variable, poorly defined | 15% Ni |
| Nimite | Chlorite | (Ni5Al)(Si3Al)O10(OH)8 | 17% Ni |
| 14Å garnierite | Chlorite | Variable, poorly defined | 3% Ni |
| Falcondoite | Sepiolite | (Ni,Mg)4Si6O15(OH)2.6H2O | 24% Ni |
| Kerolite-willemseite | Talc | (Ni,Mg)3Si4O10(OH)2 | 16–27% Ni |
| 10Å garnierite | Talc | Variable, poorly defined | 20% Ni |

**clay (silicate ore)**

| | | | |
|---|---|---|---|
| Nontronite | Smectite | Na0.3Fe23+(Si,Al)4O10(OH)2.nH2O | ~4% Ni |
| Saponite | Smectite | (Ca/2,Na)0.3(Mg,Fe2+)3(Si,Al)4O10 (OH2).4H2O | ~3% Ni |

*Table 2.1 Nickel ore minerals in lateritic deposits (after Butt, 2013).*

### 2.3. Serpentinization

Serpentinite is a rock composed of serpentine minerals. The process that transformed the parent ultramafic rock to serpentinite is called serpentinization. Serpentinization happened at low temperature and in presence of sulfur and water. This reaction transforms olivine to serpentine + brucite + Ni-magnetite + sulfides (Fillipidas, 1982). A review by Moody (1976) presented that serpentine minerals are commonly lizardite, chrysotile and antigorite. Chrysotile is further classified as orthochrysotile (a = 5.34 Å, b= 9.23 Å, c= 14.63 Å.), parachrysotile and clinochrysotile (a= 5.34 Å, b= 9.2 Å and c = 14.65 Å) (Whittaker and Zussman, 1956). Lizardite and chrysotile are polymorphs. Antigorite indicates prograde metamorphism of elevated pressure and temperature while brucite, lizardite and chrysotile are formed under lower temperature and pressure (Moody, 1976). The following reactions indicate the progressive reaction that results in the formation of antigorite (Evans, 2010).

**Foresterite + H2O → Antigorite + Brucite**

**Foresterite + Talc + H2O → Antigorite**

**Foresterite + Enstatite + H2O → Antigorite**

**Foresterite + SiO2 (aq) + H2O → Antigorite**

Other associated ferroalloys formed by serpentinization include awaurite, pentlandite, magnetite and ferrit –chromite (chromian-spinel) (Ashley, 1975). Chromites (relict) are surrounded by ferrit-chromite. Magnetite is also replaced chromite.

Compositional difference is also present within serpentine minerals. This variation is clearly described by Moody (1976). Three end members are identified. Al- serpentines are lizardite group containing septechlorite and amesite. Fe- serpentines are greenalite and cornstidite. Ni-serpentines can be lizardite group garnierite, nepouite or chrysotile group garnierite and percorite.

Three kinds of textures are common on serpentine minerals. These are psudomorphic textures (on relict olivine amphibole and pyroxenes), non psudomorphic texture (interlocking) and veins (Wicks and Whittaker, 1977). These textures are used to discriminate one serpentine mineral from the other. Mesh and hour glass textures are also common textures on serpentinites.

Serpentinization could lead to the formation of a deposit (Stefano et al., 1988). Because during Serpentinization there is remobilization and new mineral and phase generation. These minerals will have an ability of hosting an economical mineral deposit.

### 2.4. Garnieritization

Garnierite is a collective name for Ni-containing non crystalline phyllosicates. These minerals could contain different silicate minerals including serpentine, stevensite, smectite, talc, sepiolite, smectite and chlorite (Faust, 1966; Brindley and Hang, 1973; Springer, 1974; Brindley, 1978; cited from Longo, 2014).

Classification of garnierite is proposed by Brindley and Maksimovic (1974) as 1:1 layer and 2: 1 layer. 1:1 layer garnierites are serpentine like including chrysotile-percorite, lizardite-nepouite and amesite-nimesite. 2:1 layer garnierites are talc like talc-willmesite, kerolite-pimelite and chlorite-nimite. The identification is possible using XRD techniques since these garnierite minerals shows either 7 Å and l0 Å reflection (Brindley and Hang, 1973). Depending on this basal reflection they are divided as talc like (10 Å) and serpentine like (7Å). Keroliet is a mixture of talc like (β-Keroliet) and serpentine like (α- Keroliet) (Brindley and Hang, 1973). The concentration of nickel in Keroliet is up to 20 %.

Longo (2014) made a five-fold classification of Falcondo garnierites as type I, II, III and IV. Type I garnierite are pale green + yellowish garnierite's thin (mm) veins with a diffraction signature of 7.26 and 7.30 Å. In petrography these garnierite are yellow mixtures. It is dominated by serpentine like phase. Type-II garnierite is aquamarine garnierite which is commonly found as encrustation. This garnierite had two diffraction picks those are narrow pick (7.27–7.31 Å) and wider pick (9.95–10.14 Å). These values show that the mineral is an aggregate of both phases. Quartz veins are commonly associated to these type serpentinites. Type III garnierite is deep green garnierite with diffraction spacing at 7.30–7.38 Å and at 9.86–10.46 Å. It is green in optical microscope. This type is the aggregate of talc like and serpentine like garnierite mineral. Type IV garnierite is green (bluish) garnierite containing saprolite fragments. Its diffraction spacing is at 9.58–10.02 Å. This type is considered as only talc like. The fifth and the last garnierite type is Type V garnierite. This garnierite is highly fragile fragmented whitish pale green garnierite.

.

# Chapter III

# Regional geology

## 3.1. Geological setting

Physiographic regions of Ethiopia are divided into four, western plateau, south eastern plateau, Main Ethiopian Rift and Afar depression (Mengesha et.al, 1999). These regions consist of three major lithological units. These are the Precambrian basement, early tertiary and Cenozoic volcanic and Mesozoic and Paleozoic sedimentary rocks.

Kazmin (1971; 1975) classified the Ethiopian Precambrian basement into lower complex (Archean age), middle complex (lower Proterozoic) and upper complex (upper Proterozoic and younger). The lower complex is a gneissic terrain containing Burjii gneiss, Arero group and Konso gneiss. Arero group further is sub divided to Yavello gneiss, Awata gneiss and Alghe gneiss. Middle complex comprises Wadera group. Upper complex is classified as Adola, Mormora and Kajimitti group. But later a review on Precambrian Geology of Ethiopia by Asrat et al. (2001) stated the oversimplification and geochronological inconsistency of Kazmin's threefold classification based on the work of the following authors on granitoids (Ayalew et al., 1990, Gichile, 1991; Worku and Schandelmeir, 1996; Teklay et al., 1998; Yibas, 2002). The age classification of Kazmin revised because all the three complexes are formed coevally during the Pan African Orogeny (Stern, 1994) and the difference in their lithological variety and grade of metamorphism was due to their tectonic and weathering history. Two types of collisions are registered in the southern Ethiopia (Stern, 1994 as cited in Tsegie, 2005). These are Himalayan style collision of Mozambique belt and oblique collision of Arabian Nubian Shield. Finally the old threefold classification was revised and corrections made by De Wit and Chewaka (1981) classification. Two blocks (volcano sedimentary terrain and gneissic terrains) is the acceptable classification (Asrat et al., 2001; Kozyerv et al, 1995).

Multi-phase Neoproterozic assembly of Gondwana formed East African, Brasiliano, Kuungan and Damaran orogenies (Meert et al., 2008; Abdelsalam et al., 2008). East African Orogeny displays a complete willson cycle which took place for 500 Ma during Neoproterozic time

(Stern, 1994). This event includes rifting of Rodina, closure of Mozambique Ocean, Accretion, and Orogeny (Stern, 1994; Blasband et al., 2000; Greiling et al., 2000 as cited in Johnson and Woldehimanote, 2003). Two major structures of Ethiopia basement complex are Arabian Nubian shield (ANS) and Mozambique Belt (MB) (Kazmin et al., 1978; Asrat et al., 2001). Arabian Nubian Shield is mantle derived juvenile low grade arc complex which is exposed in all metamorphic terrains of Ethiopia (Teklay et al, 1998; Asrat et al, 2001). Mozambique Belt rather is reworked crustal material which is exposed in high grade metamorphic terrains (southern, eastern, and western) (Asrat et al., 2001).

### 3.2. Precambrian Geology of southern Ethiopia

The earliest work of Lebling (1940) classified Precambrian rocks of southern Ethiopia as gneissic, granitoids and ‘‘green’’ rock terrenes. Later Jelenc (1966) classified Adola rocks into Gariboro series (older) and Adola series. Gariboro consists of granitic gneisses, actinolite schist and mica schist. Adola is north south (NS) trending volcano-sedimentary (green schist) rocks respectively. These works are later modified by (Kazmin, 1972; Kazmin et al., 1978; Gilboy, 1970; Chatter, 1971) to three fold classification as lower, middle and upper complex. Schmerold (1988a) proposed a five-fold litho structural classification for Adola basement rocks. These are Western Basement, Metavolcano-sedimentary Belt, Central Basement, Ultramafic Belt and Eastern Basement. Worku and Yifa (1992) modified these classifications into Western Gneissic Domain, Metavolcano-sedimentary Domain, Burjiji Gariboro Domain, Ultrabasic Domain and Eastern Gneissic Domain. Two fold generalization was made by Gebrehab (1992) as Gneissic terrain and greenstone belt. This generalization is also supported by Asrat et al. (2001) and Yibas et al. (2002).

### 3.3. Stratigraphy of Adola belt

Three fold classification of Adola belt proposed by different authors (e.g. Chatter, 1971; Gillboy, 1970). These are lower, middle and upper complexes. Chater (1971) and Gillboy (1970) described the contact between the middle and upper complex as tectonic contact. Kazmin (1972) differentiated the three complexes based on sedimentation gaps (Kozyerv et al, 1985). Later the works of Kozyerv et al. (1985) supports the tectonic classification and summarized the geology of Adola into middle and upper complexes.

Middle complex contains Awata group and Mormora group (Zembaba formation, Aflata formation and Kenticha formation). The upper complex includes Adola group (Chaketa formation, Finkelcha formation) and kajimitti beds. Awata group consists of Bora and Buluka formations. Bora formation has a thickness of 1250 meter and their lithological composition is gneisses of interchangeable biotite-hornblende and hornblende – biotite gneisses. Buluka formation overlays Bora formation conformably and its thickness is 1560 meter. This formation is migmatized biotite Amphibolite gneisses showing homogeneity throughout the thickness.

Mormora group is a second sedimentary cycle (Kozyerv et al., 1985) characterized by rhythmic stratification of psmmatic and pellitic – carbonate rock. From lower part to the upper part the pellitic proportion increases and psmmatic proportion decreases. Zembaba formation is 1300 meter thick fine grained quartzo feldsphatic gneisses. This unit is referred as Wadera group by Kazmin (1972). This formation conformably is overlain by 1943 meter thick pssammio-pelitic assemblage of Aflata formation. Kenticha formation is the upper most succession of Mormora group which is graphitic and micaceous schist containing patches of marble. The thickness of the Kenticha formation is 1470 meter. The formation is overlain by younger Adola groups of the upper complex.

Upper complex contains Megado graben syncline (Kozyerv et al., 1985). It contains Adola group and Kajimitti beds with unconformable contact. Adola groups are further subdivided into Chaketa and Finkelcha formation. Chaketa formation comprises volcanoclastic and intercalating amphibolite schist, actinolite chlorite schist, metaquartzite and amphibolite. At the bottom part amphibolite-actinolite schist dominates, whereas at the top quartzite and graphitic schist are abundant. The thickness of this formation is 850 m at Chaketa spot. Based on Petrographic investigations and chemical analysis, Kozyerv et al (1985) classified the origin of these rocks as low alkaline thoeliitic magma. These magmas doesn't undergone removal of potassium. The rocks formed are gabbro- amphibolite. Finkelcha formation is the thickest (1110 m) terriginous sediment found at the southern core of the Megado Graben syncline.

Recent works by TMEP (1986-1990) modified these stratigraphic sequence into the following simplified stratigraphy as presented by Gebrehab (1992).

| | |
|---|---|
| | Tertiary basalt<br>Unconformity |
| Greenstone Belts | Post tectonic granitoids<br>Minor tonalitic gneisses<br>Upper metasedimentary group<br>✓ Metaturbidite (meta conglomerate), Metasandstone, Metagraywackes<br>✓ Semi politic Schists with felsic clasts<br>✓ graphitic quartzite |
| | Mafic – ultramafic rocks<br>✓ Mafics dominantly metagabroos, locally layered<br>✓ Ultramafics (serpentinite-talc carbonate rocks)<br>Syn-tectonic granitoids<br>✓ Granite gneiss<br>✓ Granodiorites/ tonalite gneiss<br>Metavolcanics<br>✓ Minor felsic to intermediate rocks<br>✓ Meta basalt/Amphibolite<br>Lower metasedimentary group<br>✓ Semi politic Schists<br>✓ Graphite schist and quartzite<br>✓ Fe- Mn sediments<br>✓ Marble/dolomite<br>Tectonic contact (unconformity ) |
| Gneissic Terrains | Gneisses<br>✓ Minor graphitic and micaceous schists<br>✓ Minor calc silicate fels<br>✓ amphibolite biotite gneisses<br>✓ Biotite, quartz biotite gneisses<br>✓ Quartzo feldsphatic gneisses |

*Table 3.1 Composite stratigraphy of the region*

Generally, Precambrian of southern Ethiopia comprises two tectenostratigraphic units. These are high grade Granite – Gneiss terrains (Mozambique belt) and low grade ophiolite thrust - fold belts (ANS) (Yibas et al., 2002).

### 3.4. Granite -Gneissic Terrain

This terrain are multiply deformed high grade gneisses intruded by syn and post tectonic granitoids (Worku and Yifa, 1992). It bounds two N-S trending parallel belts (Megado belt and Adola belts) (Ghebrehab, 1992). The terrain is classified into two sub terrains (Burjii – Moyale and Adola-Genale) and four complexes (Yibas et al, 2002). According to Tsegie (2006) and Ghebrehab (1992) these terrains are variably enriched by amphibole to biotite gneisses, quartzofeldsphatic gneiss, and granitic gneiss. Based on their lithologic and metamorphic associations, these units are named as Zembaba, Shakisso, and Soda domains by Worku and Schandelmeir (1996). Zembaba domain is located in the eastern side of kenticha mafic ultramafic belt (see fig 3.1), Soda domain located in the western side of Megado belt. While Shakisso domain covers the central part of adola belt in between Megado belt and Kenticha belt.

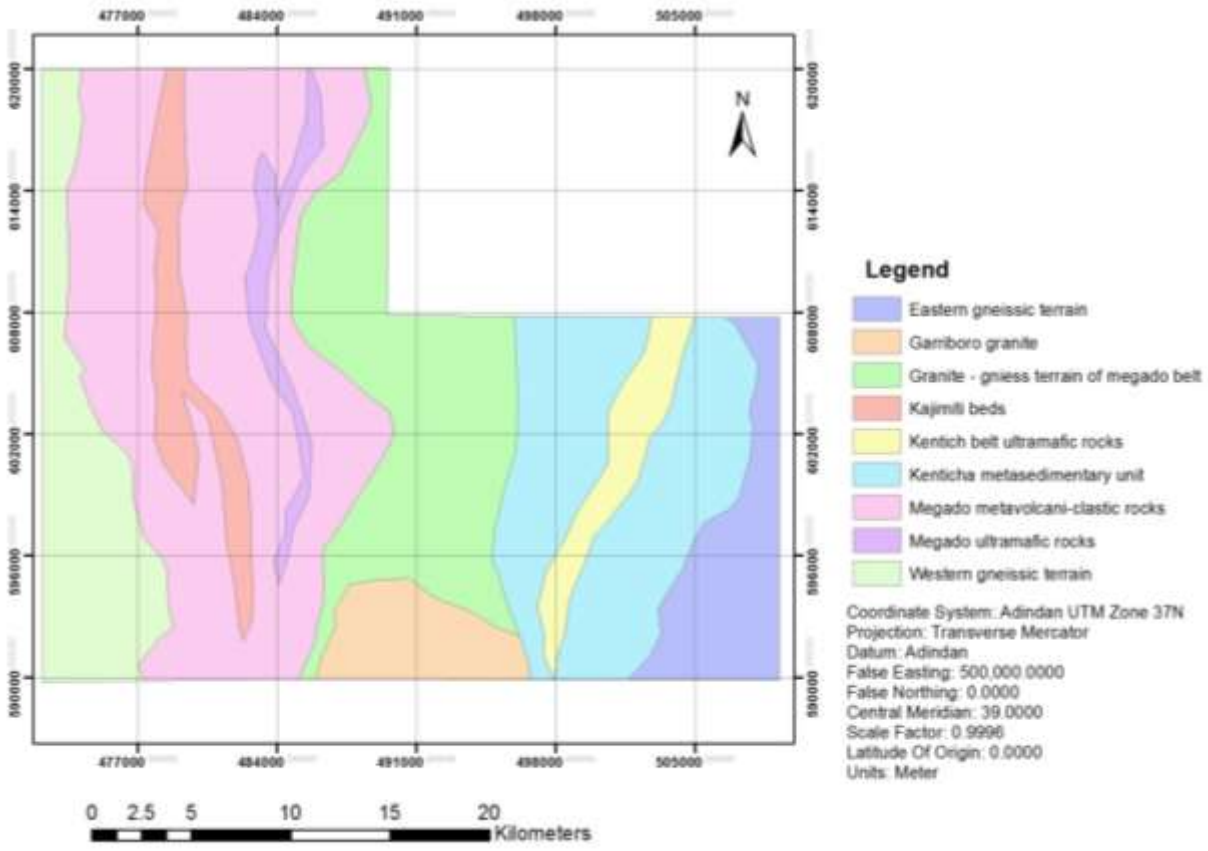


*Fig 3.1 General geological map of Granite- gneiss and meta mafic ultramafic of The Megado belt and Kenticha belt* (modified from TMEP, *1993)*

Lithologically Soda domain comprises of biotite – hornblende gneisses, amphibolites, quartzofeldsphatic gneisses, and kyanite schist. Shakisso domain contains quartzo feldsphatic gneisses, amphibolites/amphibole schist and biotite schists with syn tectonic granites. Zembaba domain instead contains migmatized gneiss and quartzofeldsphatic gneiss.

### 3.5. Mafic –Ultramafic –Sedimentary Ophiolite Belts

There are four parallel ophiolite thrust fold belts. These are Megado, Kenticha, Bulbul and Moyale EL-Kur belts. They are product of subduction remnant obducted ophiolites (Yibas, 2000). The term thrust fold is used to express their deformational history. Mafic rocks (amphibolites) are low- Ti thoeliites and boninites (Yibas, 2000c and the reference there in). Megado belt as explained by Yibas et al (2003) comprises amphibolites, amphibolites schist, gabbro, serpentinite, meta graywacke and meta psmmite. In Megado belt mafic rocks are the dominant lithologies. Kenticha belt consists of greenschist to lower amphibolites facies pellitic and ultramafic rock (Yihunie and Tesfaye, 2002).

Ultramafic rocks are represented by talc-tremolite, serpentinite and talc anthophyllite schist (Yibas et al, 2003). Bulbul is sheared green schist (garnet bearing pellitic and semi pellitic schists) terrain covering the eastern end of Adola belt (Abdelselam et al, 2008; Yihunie and Tesfaye, 2002). Moyale EL- Kur terrain is found at the southern limit of Adola belt at the Ethio-Kenya border with lithologies of metamorphosed mafic, ultramafic and small metasediments (Walsh, 1972; Tolessa et al., 1991; Alene and Barker, 1993; Yibas, 2000).

# Chapter - IV

# Geology of Ula Ulo Nickel deposit

## 4.1. Overview

Ula Ulo nickel deposit is elliptical in shape and is hosted by serpentinite. The serpentinite is classified into three sub groups considering the presence and absence of the nickel mineralization. These sub units are barren serpentinite, stock worked serpentinite, and veined serpentinite. The country rocks for the deposit are talc schist and tremolite schist. Talc schist enclosed the serpentinites except in the south western portion in which tremolite schist enclosed the deposit. Other lithological units are amphibolite, meta-psammite, quartzite and graphite schist. Amphibolites are located in the eastern margin of the study area along the major trust. Meta psammite and quartzite are associated with both the graphitic schist and talc schist in which they form disseminated patches throughout the northern half of the study area. Based on lithological, structural and mineralization variations the rocks in the study area are classified as:

1. Serpentinite
2. Talc-tremolite
3. Amphibolite
4. Meta psmmite
5. Quartzite and
6. Graphite schist

Lithostratigraphy of the study area is interpreted field observation and regional geology. When we cross the study area from east to the west, we found the lithologies in the following sequence. These are amphibolite, talc tremolite schist, serpentinite, talc tremolite schist, quartzite, graphite schist and metapsmmite. Due to multiple phases of deformation these units are inter-fingered and show intercalation. One major thrust on the east portion of the study area which displaced the talc tremolite schist and meta-psmmite over the amphibolite unit. The study area is found on the eastern limb of Megado syncline (Kozyrev et al. 1985). In Megado syncline, when we cross it rim to core, we will encounter younger rocks. From this structural interpretation a chronological relationship of the rock is made. From the oldest to the youngest the relationship is: amphibolite,

talc tremolite schist, serpentinite, quartzite, graphite schist and meta-psammite. The true thickness is calculated as $t = h\ \cos a \sin d + v \cos d$

Where t = true thickness, h = distance between the contacts, **a=** the angle between the measurement angle and the dip direction, **d=** true dip and V = elevation variation. Based on the calculation the thicknesses of the units are as the following amphibolite unit is 332 meter thick, talc tremolite schist unit is 227 meter thick, serpentinte unit is 332 meter thick, quartzite unit is 86 meter, graphite schist unit is 360 meter thick and meta psammite unit is 123 meter thick.

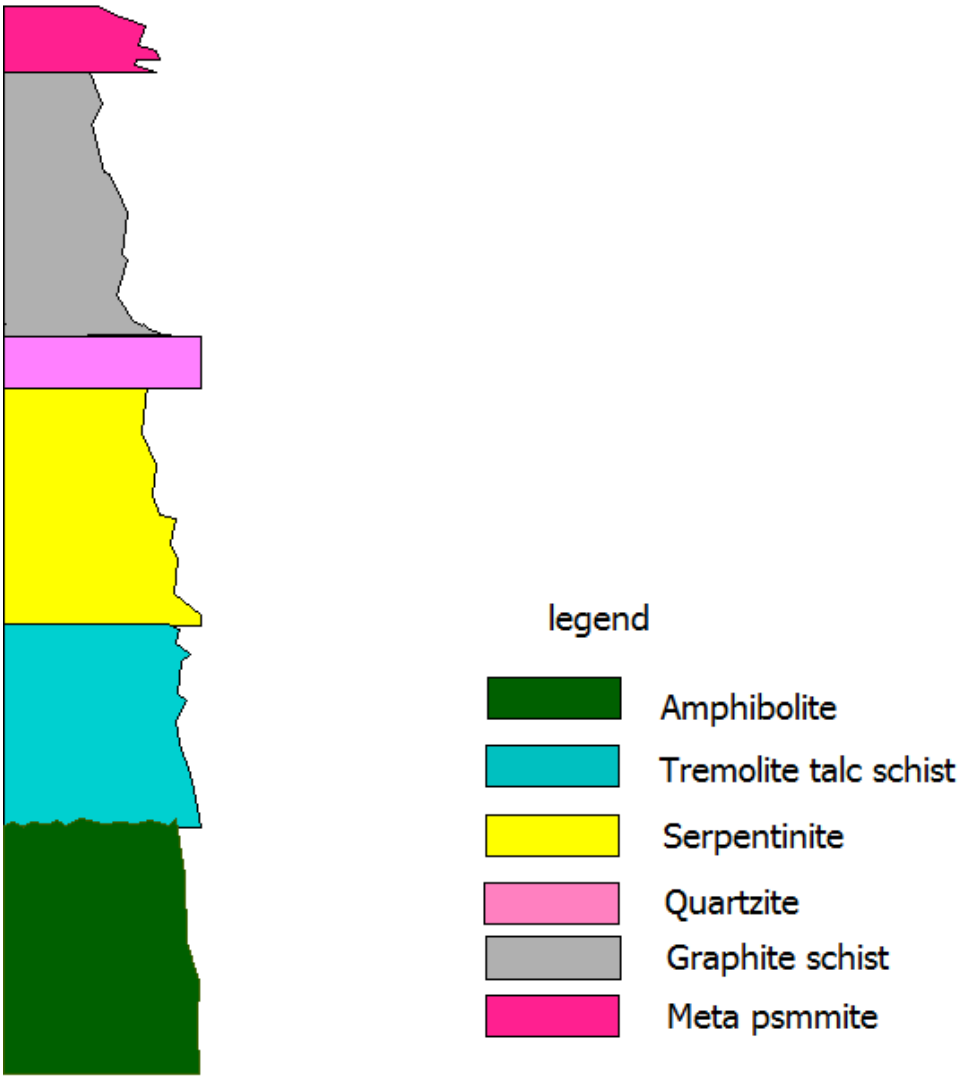


*Fig 4. 1 A composite lithostratigraphy of mafic ultramafic and metasediments of Ula Ulo. The horizontal thickness indicates the intensity of weathering.*

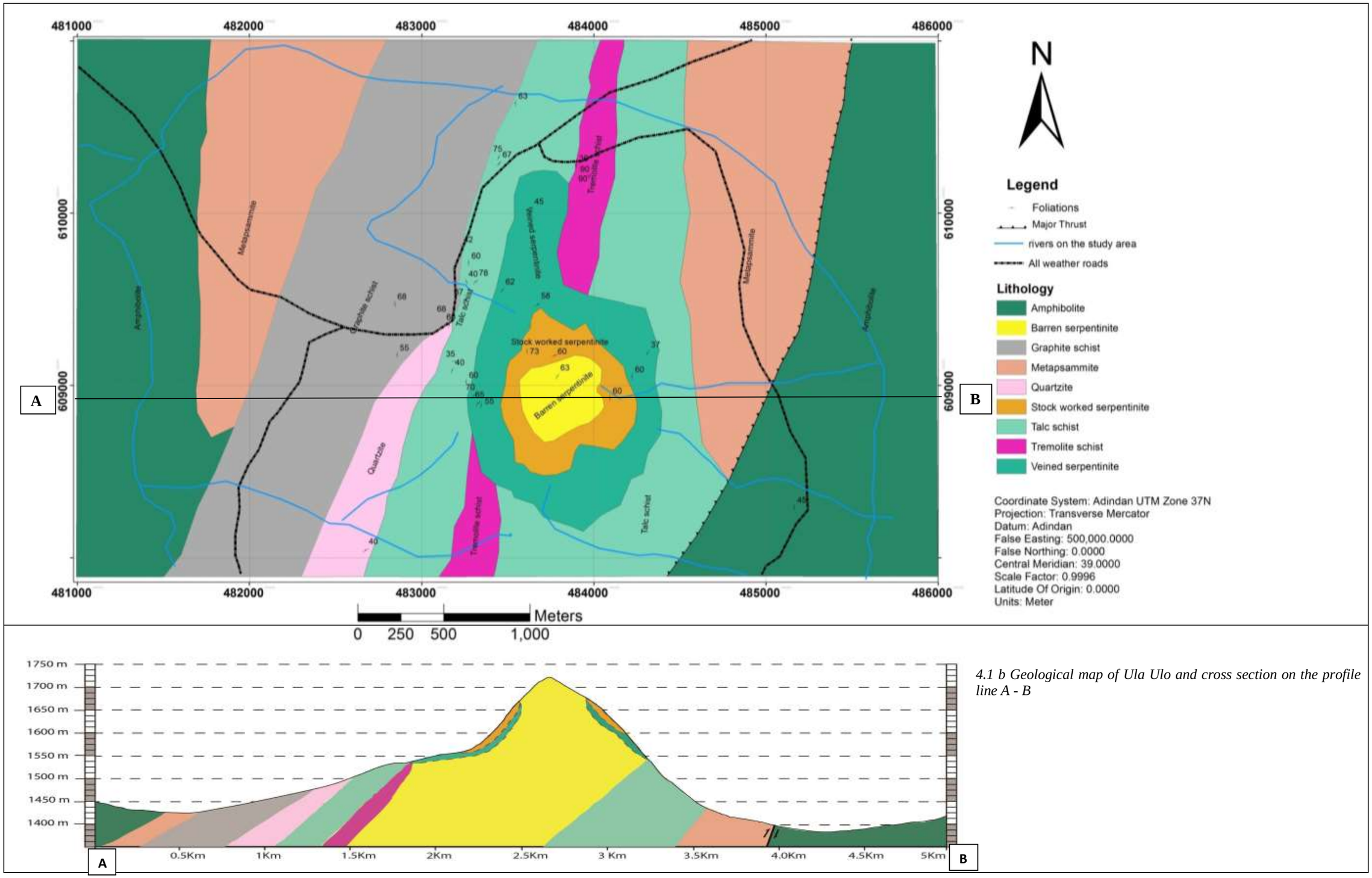


*4.1 b Geological map of Ula Ulo and cross section on the profile line A - B*

### 4.2. The Serpentinite Unit

This unit covers the central portion of Ula Ulo ridge. The unit radially extends from the center forming elliptical outline. From the center (1755 meter above sea level) to the outer portion (1485m above sea level) the elevation decreases. This unit contains three subunits: barren serpentinite (central), stock worked serpentinite (middle) and veined serpentinite (outer). The contacts with these subunits are gradational and conformable. But the contact of the veined serpentinites and the talc unit is sharp and conformable (Fig 4.1 b).

#### 4.2.1. Barren serpentinite

Barren serpentinite is non mineralized portion of the serpentinite unit. This is the core of the serpentinite body covering the peak of Ula Ulo ridge. It is characterized as non foliated and slightly weathered rock (Fig 4.2 a and b). It is medium grained. It contains dark spots of about 3 cm long; which are chromite. The color of rock is mottled yellow to reddish yellow. The texture is granoblastic. In thin section (Fig 4.2 c and d), it shows relict olivine, serpentine, antigorite, clinopyroxene, opaques and quartz. It doesn't show any preferred orientation. This is because of the absence of platy minerals. The mineral serpentine, lizardite (networked serpentine) and antigorite (acicular serpentine) are the dominant phases. Both minerals show first order interference colors. Their color is from dark to dark gray. Veins of serpentinites show undulose extinction.

(a)

(b)

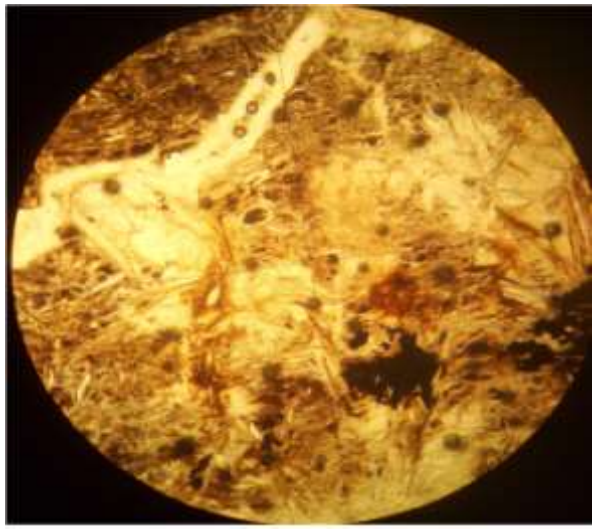

(c)

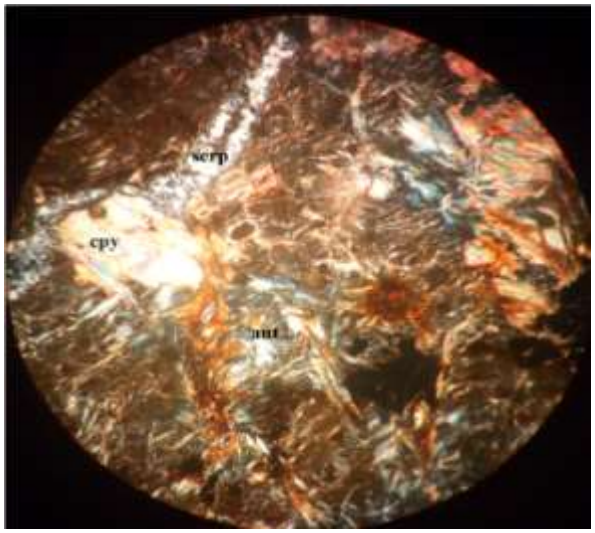


(d)

Fig 4.2 Outcrop and microscopic pictures of Barren serpentinite*; (a) at the top of Ula Ulo ridge ,(b)enlarged picture of a , (c) Thin section (US-01) of barren serpentine (10x) in ppl ( plain polarized light) , (d) and in xpl (cross polarized light).(10X)*

Replacement of olivine by antigorite is common resulting in pseudomorphic texture. The antigorite forms acicular grains with low relief compared to olivine and clinopyroxene. The modal proportion of minerals is quartz (4 to 7%), serpentine (45 to 78%), antigorite (0 -30%), olivine (5-10%), chlorite (2-5%), talc (2-3%), clinopyroxene (5-8%), and opaque (0-5 %) (Fig 4.2 c and d).

### 4.2.2. Stock-worked Serpentinite

This serpentinite is the middle zone of the serpentinite body containing stock works of garnierite and magnetite veinlets. The intensive weathering formed thick red soil containing flakes of remnant serpentinites. The color of the rock is green to reddish green. It is non foliated (Fig 4.3 a) and massive. Veins of magnetite are visible forming thin mesh wire texture on the rock (Fig 4.3 b). The rock is granoblastic containing disseminated spots of dark and light minerals.

The unit consists of quartz (3-7%), serpentine (60-66%), talc (15-26%), olivine (3-7%), chlorite (4-6%), clinopyroxene (0-5%), and opaque (chromite) (0-5%) (Fig 4.3 c and d). The serpentinite shows mesh texture surrounding grains of relict olivine and clinopyroxene. An aggregate of glassy minerals form a vein (probably lizardite). Talc grains are poikiloblastic and highly

anisotropic showing reddish green color in cross polarized light. Green minerals (chlorites) are contained by talc grains.

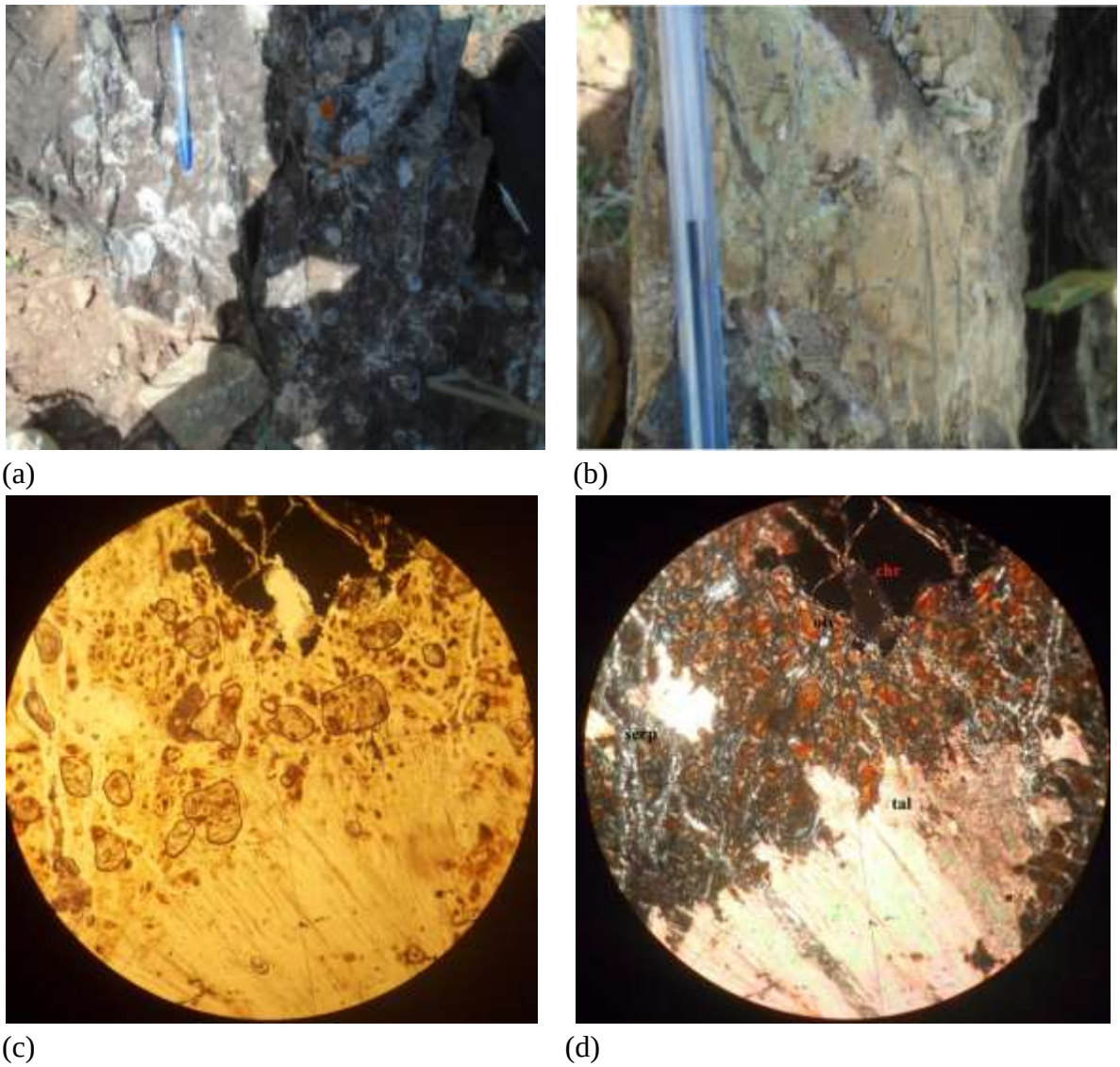


(a) (b)

(c) (d)

Fig 4.3 Outcrop and microscopic pictures of stock worked serpentinite *(a) insitu specimen of a (b), c and d, are microscopic photos of the stock worked serpentinite under ppl and xpl. (10X)*

### 4.2.3. Veined Serpentinite

This unit is the outer zone (lower part) of the serpentinite unit. This unit is intensively veined by garnierite and silica (amorphous quartz) veins (Fig 4.4 a and b). The difference with the middle serpentinite is that in this unit magnetite veins are not common. A green (Fig 4.4 b) and white (Fig 4.4) vein forms a mesh wire texture on the outcrop level. The rocks are massive; none foliated and colored with greenish tint with yellow color. The dominant mineralogical

constituents of this unit are serpentine (65.4%), antigorite (14 %), talc (11.25 %), olivine (4.6 %), quartz (3.2 %), opaque (chromites and magnetite (2.2 %), and clinopyroxene (1.6 %)).

(a) (b)

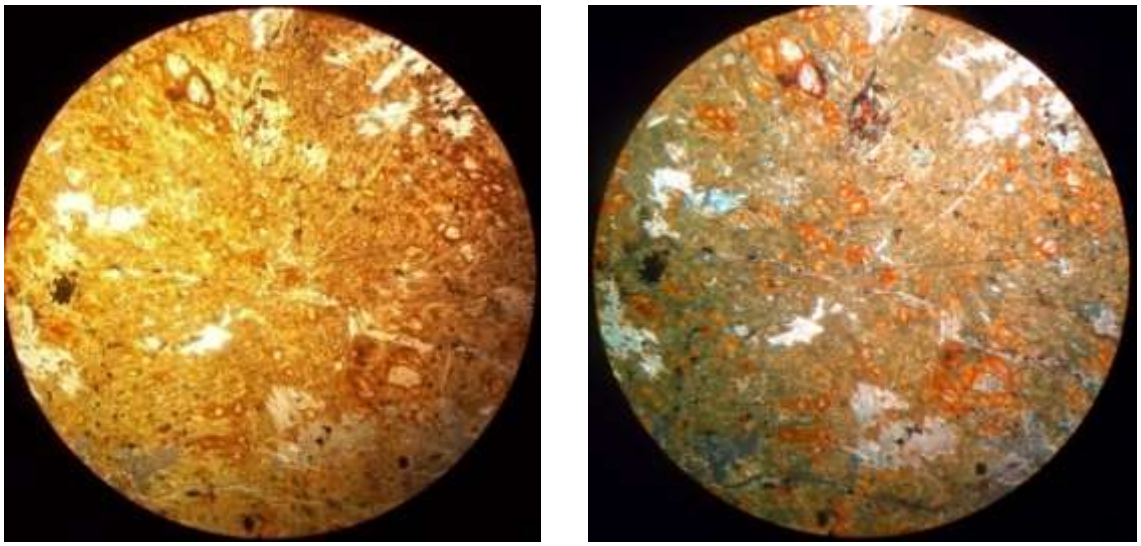

(c) (d)

Fig 4.4 Outcrop and microscopic pictures of veined serpentinite *(a=silica vein, b= garnierite vein containing serpentinites), c and d are thin section photos of veined serpentinite.(10X)*

### 4.3. Talc- Tremolite Unit

This unit covers the largest proportion of the mapped area. It encloses the elliptical serpentinite body extending north south. The contact with the serpentinite unit and graphite is sharp. Two sub units, talc and tremolite units comprise this unit. The contact between these sub units is gradual containing intercalation zone.

### 4.3.1. Tremolite Talc Schist

This unit is overlain by graphite schist and underlained by tremolite schist. Fresh talc schists are colored green and become white and shiny when it is weathered. It is foliated with orientation of NS to 060 and dipping $60^0$ to $87^0$ towards NW. Mineral surfaces are visible showing elongated fibrous minerals. The grain size is variable from fine coarse grained (Fig 4.5 a). Under petrographic microscope its composition is dominated by perfectly cleaved talc mineral grains (up to 94 %) and some tremolite (0-3%) and opaque minerals (up to 2 %). The talc is schistosed (Fig 4.5 a and b) marking the schistosity plane. the tremolite is subparallel to the foliation. The opaques are prophyroblastic and idoblastic (Fig 4.5 a and b). Tremolite is found surrounding the opaque grains.

(a)

(b)

(c)

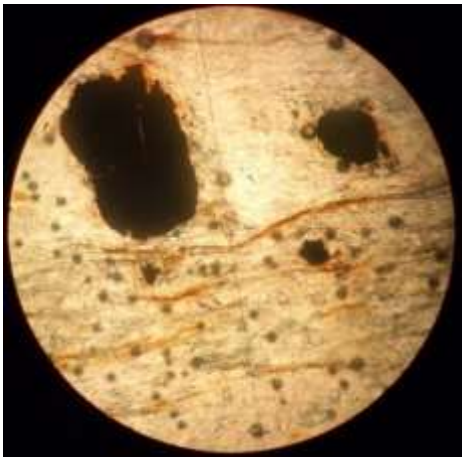

(d)

Fig 4.5 Outcrops and microscopic pictures of talc schist*: (a) coarse grained talc unit at contact with graphite schist), (b) fine grained talc unit at the contact with massive tremolite unit,(c) and (d) are plane polarized and cross polarized pictures of the talc unit.(10X)*

### 4.3.2. Tremolite Schist

This unit is relatively massive with incipient foliation. The color of the rock is deep green (fresh) and red (weathered). Radiating fibrous is observable on hand specimen. Delineation of the contact between this unit and talc schist is made based on the exposure of this unit at the north eastern (Fig 4.6 a) and south western parts (Fig 4.6 b). The unit is underlained by serpentinite unit and overlaid by talc schist. The unit is massive.

*(a)*

*(b)*

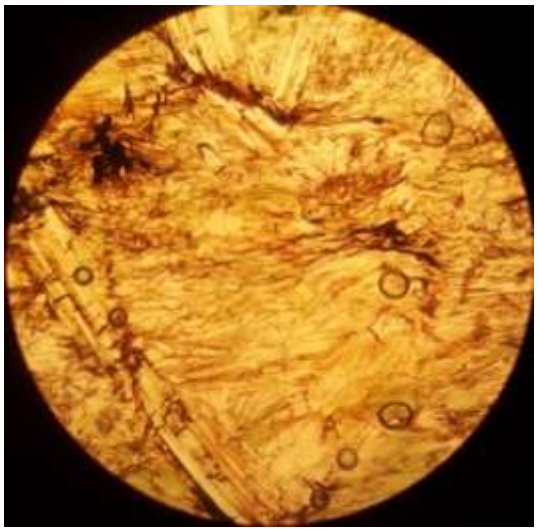

*(c)*

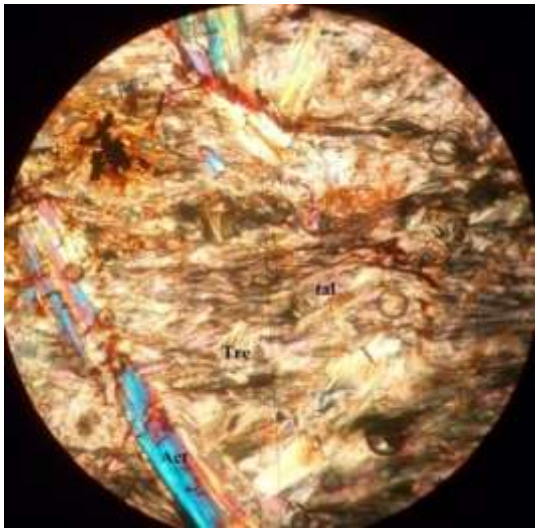


*(d)*

Fig 4.6 Exposure and microscopic picture of tremolite schist unit *(a), and (b )are out crop pictures while (c) is plain polarized light microscopic photo of talc tremolite unit and (d) under cross polarized light.(10X)*

This unit shows dominantly three minerals, acicular tremolite, elongated tabular actinolite and talc. Under plain polarized light (Fig 4.6 c) all the minerals appear white, except the opaques. Tremolite shows acicular cleaveage. Actinolite is prismatic to tabular (Fig 4.6 d). Talc is highly sheared and schistosed. Under cross polarized light (Fig 4.6 d), actinolite is anisotropic showing a peacock color. Talc is slightly anisotropic. Tremolite is isotropic and remains white. The mineralogical composition of the rock is tremolite (30-75%), actinolite (8-30%), talc (7-50%), quartz (2-4%), hornblende (0-20%) and opaque (1-2%).

### 4.4. Amphibolite

The unit occupies the eastern most limit of the study area. This unit found below the talc tremolite and serpentinte unit. This is because of the thrust formed by east west compression. This unit occupies a relatively low lying portion of the study area. The unit is not foliated. Due to deep soil horizon development and forest covers it is difficult to find exposures. The color is deep dark green containing visible crystals of actinolite (elongated) and tremolite (radial fibers) (Fig 4.7 a and b). The contact with talc schist (south east part) and psmmite (north east part) is sharp and tectonic.

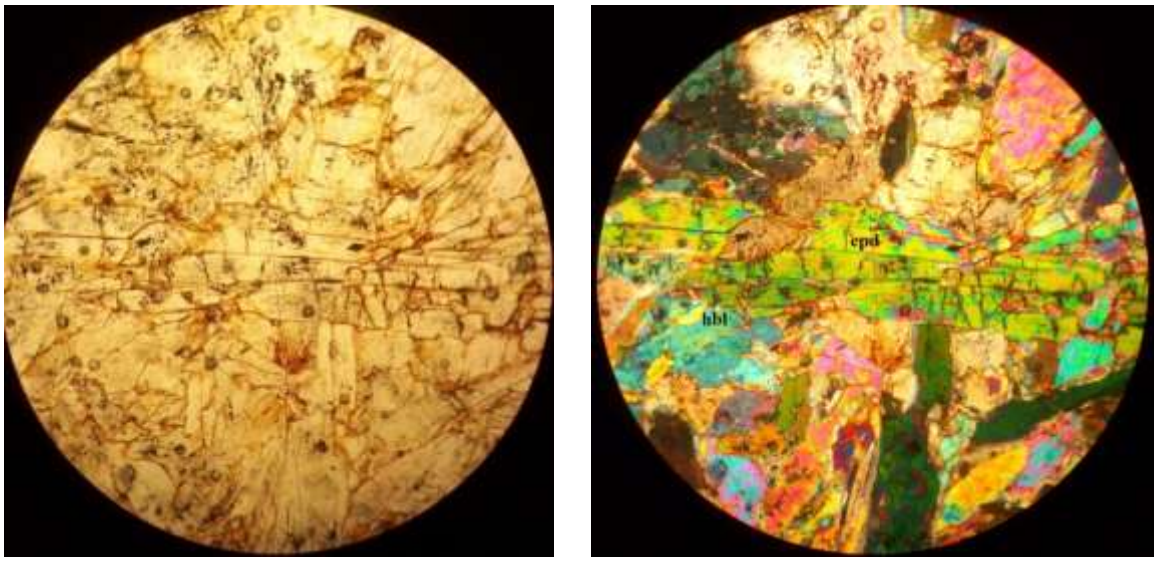


(a) (b)

*Fig 4.7 Microscopic pictures of the amphibolite under ppl and xpl respectively (10X)*

In thin section (Fig 4.7) the rock is dominated by hornblende and epidote. Epidote shows one perfect cleavage where as hornblende displays two cleavages. The modal proportion is plagioclase (0-10%), epidote (25-40%), hornblende (5-20%), sericite (5-45), quartz (5-10%) and biotite (5-20%). Epidotitation and serisitation alterations are dominant. Epidote pseudomorph replaces plagioclase. Porphyroblasts of epidote and hornblende are common.

### 4.5. Meta-Psammite

This unit is exposed on the north eastern part of the study area. The unit is intensively weathered covering a transition between the cliff forming ultramafic units (talc schist unit and serpentinite unit) and flat terrains. The beds are thinly laminated and highly fragile. Biotite grains are visible by naked eye. In the east, the unit is bounded by thrust and amphibolite. The contact of this unit and the amphibolite is sharp and tectonic. In the west the contact with talc is sharp. Throughout the unit there are intercalations of quartzite and biotite schist. Foliations (shistocity) are oriented as $025^0$ / $37^0$ towards NW. Mineral lineation and microfolds are present (fig 4.8 a).

(a)

(b)

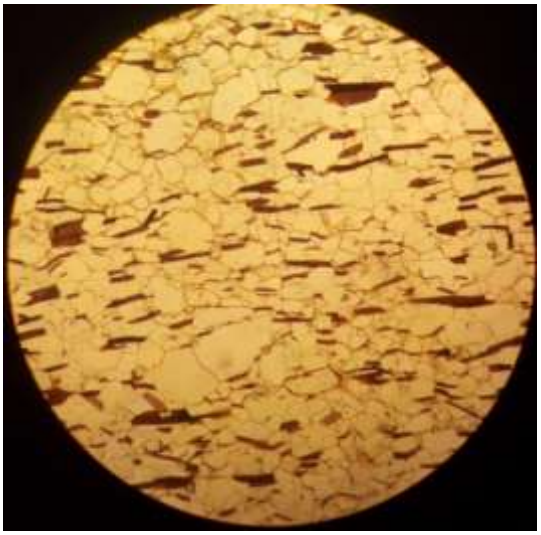

(d)

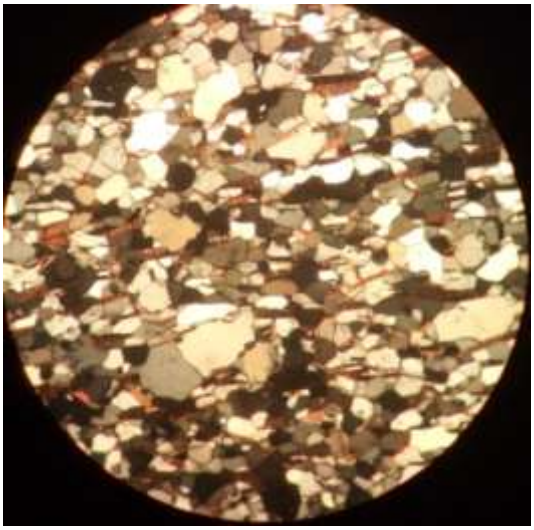

(d)

Fig 4.8 Meta psmmite unit outcrops and photomicrographs; *(a) quartz mineral lineation, (b) micro folds ,(c and d) are microscopic photos of the unit in the ppl and xpl respectively.(10X)*

The unit is composed of quartz (65-80%), biotite (0-5%), potassium feldspar (0-10%), voids (0-3%) and opaques (up to 3%). Quartz and feldspar grains are relatively coarser showing a granoblastic texture. Biotite and opaque grains are delineating the foliation (schistocity) (see Fig 4.8 c).

### 4.6. Quartzite

The unit is exposed in the south western portion of the study area, and is overlaid by graphitic schist and underlined by talc schist. The contacts with talc schist and graphite schist are sharp and gradational respectively. Quartzite unit is non foliated unit containing slightly segregated light and dark bands. The relict sedimentary structures are preserved. These structures are

beddings. The color is variable from pure sugary white to pinkish dark color. Its modal composition is quartz (up to 90%), biotite (2-3%), and opaque (0-8%) (See Fig 4.9 c and d)


(a)


(b)

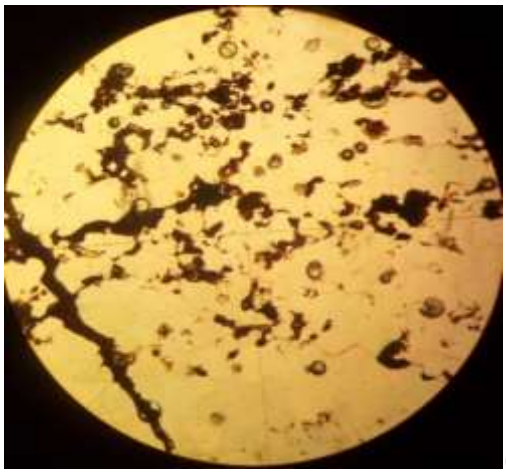
(c)

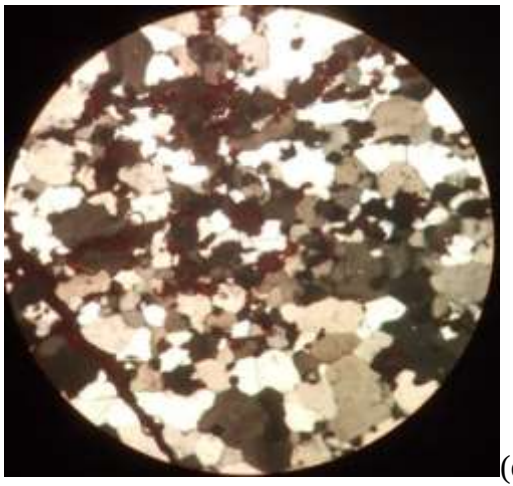
(d)

*Fig 4.9 Outcrop and microscopic pictures of quartzite: (a )outcrop picture, (b) is the when (a) is zoomed, (c) and (d) are plan polarized and cross polarized microscopic photos of the unit respectively.(10X)*

### 4.7. Graphite Schist

This unit covers the western part of the area (almost 25%). The rocks are foliated and variegated in color. The colors observed are reddish gray, greenish grey, dark gray and green. The area is covered by vegetation and plantation compared to the other portions. The grain size is fine and rocks show penetrative planar fabric. Its composition is quartz (20-40%), muscovite (0-40), biotite (10-25), sericite and chlorite (20-25%), and potassium feldspar (0-5%). The unit shows decussate texture (Fig 4.10 b).

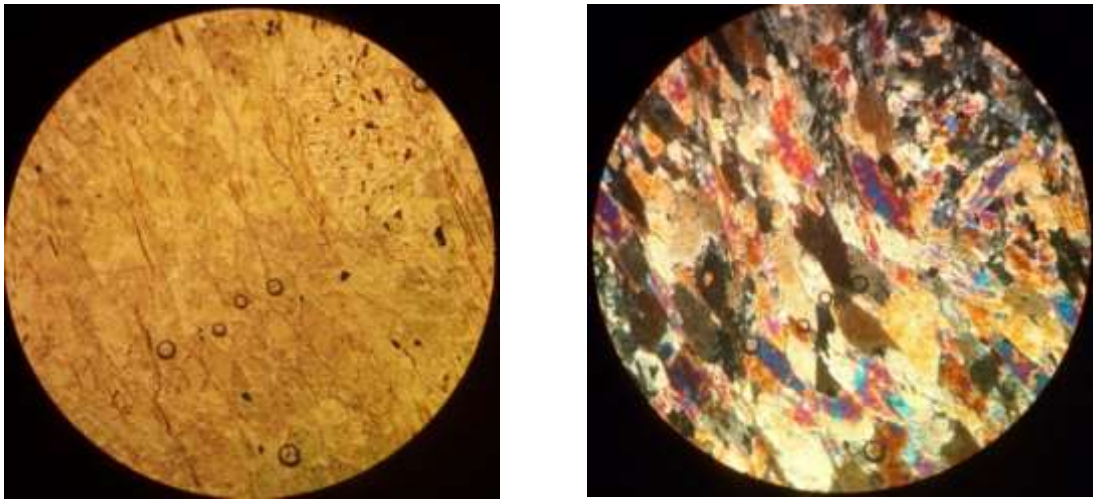

(a) (b)

*Fig. 4.10 microscopic photos of the graphite unit under plain polarized light (a) and cross polarized (light). (10X)*

### 4.8. Alterations

Major alteration types are serpentinization, silicification, sericitization, actinolitization, epidotitation and chloritiztion. Serpentinization (Fig 4.11 a) is the dominant alteration event occurred during metamorphism. This alteration transformed the olivine and pyroxene minerals into serpentine and talc respectively. During mineral grain development different serpentine minerals preferentially grow in different directions. These resulted in the mesh textures.

Silicification (Fig 4.11 b and c) is common on serpentinite and quartzite unit. In veined serpentine sub unit there are silica gel filling veins where the silica content is 91.4 % $SiO_2$ (UNNWV-D2-5) and 98.2 % (UNV-D5-1). These veins are amorphous and milky white. Their orientation is variable and their dip is in most case greater than 70 $^0$ towards NW. In association to these barren quartz veins, there are green veins which are enriched by nickel.

Sericitization (Fig 4.11 e) is common in graphitic mica schist and amphibolite units. In both cases very fine grain mica formed agglomerate texture. Epidotitation (Fig 4.11 d and e) is observed in amphibolite unit. Due to this reaction epidote crystals are developed on the plagioclase mineral grains. Pseudomorphs of plagioclase are very common. Commonly hornblende also replaces olivine and pyroxene crystals. Actinolitization (Fig 4.11 f) is observed in the tremolite schist. Acicular elongated grains developed over radiating fibrous tremolite crystals. Chloritiztion commonly is observed over talc crystals and graphite schist. But these

alterations are very rare in the other lithologies. The following figures depict the above mentioned alteration types.

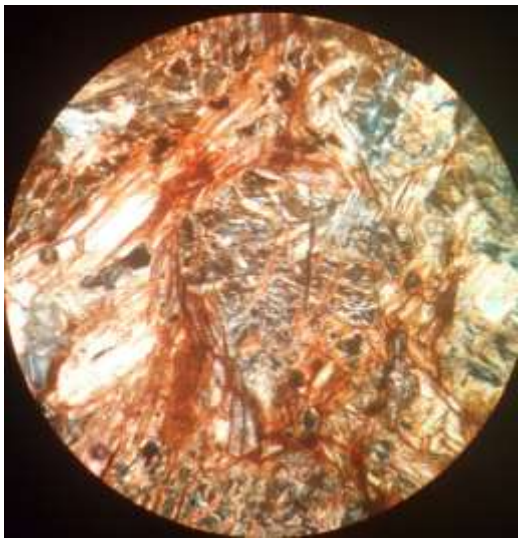

(a)

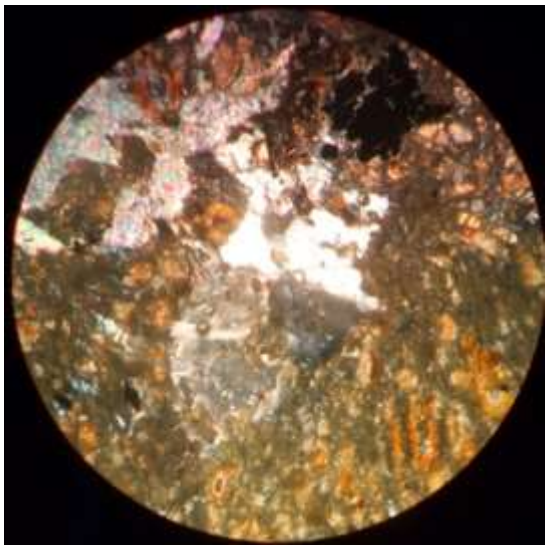

(b)

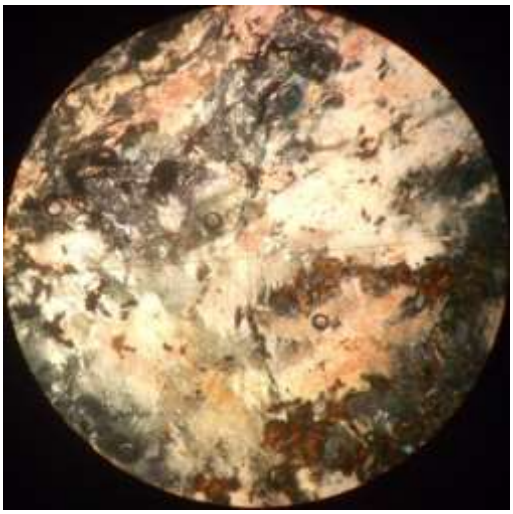

(c)

(d)

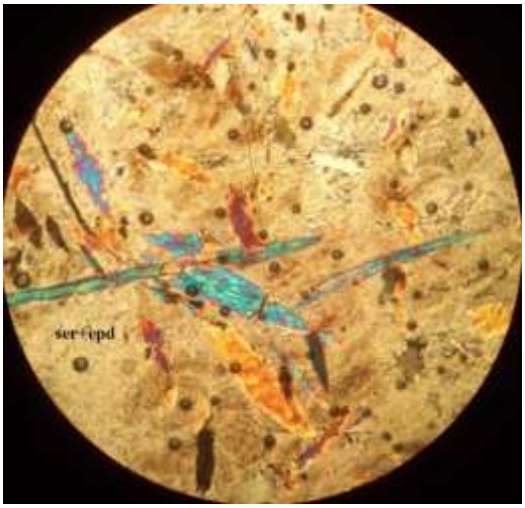


(e)

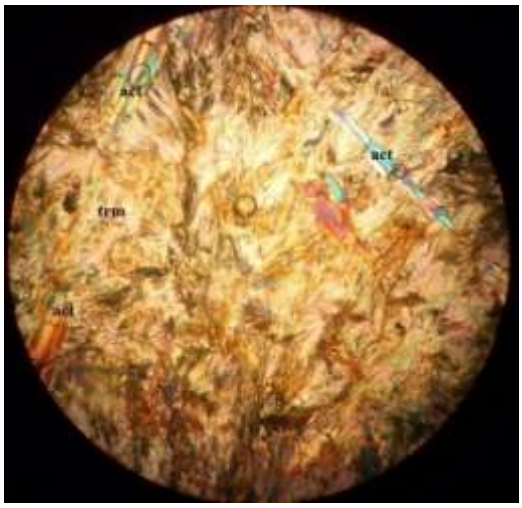


(f)

*Fig. 4.11 Different types of alterations (a) serpentine replacing olivine (serpentinisation), (b) and (c) undulose extinction (silicification) common on stock worked and veined serpentine, (d) biotite partly replacing epidote, (e) sericite and epidote mutually developed over plagioclase (protolith), (f) actinolite grains developed over tremolite grains crossing the foliation.*

### 4.9. Metamorphism

All lithological units are affected by metamorphism. Some lithologies like talc- tremolite schist, Metapsammite and graphitic schist developed preferred orientation (shistocity). However, serpentinite, amphibolite, and quartzite unit are not foliated. Some newly formed metamorphic minerals (e.g. talc and biotite) developed along the foliation plane while others (e.g. tremolite and actinolite) cross the foliation plane. Green minerals (epidote and chlorite) are observed in all lithological units. This suggests that the terrain is metamorphosed to a metamorphic garde of green schist facies. During the field mapping neither gneisses nor phyllites were observed. The rocks are uniformly schistose. Regional metamorphism is characterized by the association regional ductile structures. In the study are all the units are inclined and dipping to the west. These units are aligned due to the presence of east west compression. This compression resulted Megado syncline. The senso strictu the rocks are on the western limb of Megado syncline. Taking this association into consideration the possible type of metamorphism is regional metamorphism.

The presence of relict olivine grains are observed on serpentinites. This information with the absence of epidote or plagioclase supports the ultramafic origin. In some parts, veins of

serpentine are visible containing dark and light mineral grains. In most cases the antigorite forms fibrous acicular textures while replacing the olivine. These indicate that the serpentinized protoliths is peridotite (higher olivine content). The process is called serpentinization. Quartz is mostly recrystalized and show undulose extinction.

The dominant mineral phases of Meta-ultramafic rocks are serpentine, antigorite, talc, actinolite, tremolite, clinopyroxene, olivine (relict), and quartz. Talc and serpentine always replace the olivine and clinopyroxene. Opaques are idioblastic and prophyroblastic disseminated throughout the host lithology. The talc unit shows poikiloblastic texture due to its opaque contents. The metabasic rock (amphibolite) is dominated by hornblende and epidote. Epidote is originated from plagioclase. If the rock is dominated by epidote or plagioclase. It is originaly a basalt.

Primary beddings are observed on the meta psammite unit. This unit also highly fragile. The grains observed are highly sorted sedimentary rocks. This informations supports sedimentary origin. Fragiality is related to low compaction during sedimentation and the absence of cementing materials. The protolith is arkosic sand stone. Quartzite shows sedimentary bedding. This evidence supports sedimentary origin. The composition of this unit is dominantly quartz. The possible protolith is aranitic sandstone. The dominant mineral phases and assemblages observed are

1. Serpentinite unit
   a, Serp+Ant+Olv+CPy+Qtz
   b, Serp+Tal+Ant+Cpx+Chl+Olv
2. Talc – tremolite schist unit
   a, Tac+Tre+Act+Qtz
   b, Tre+Hbl+Tlc+Act
3. Amphibolite unit
   a, Epd+Hbl+Ser+Plg+Qtz
4. Quartzite unit
   a, Qtz+Bt+Alb
5. Psmmite unit
   a, Qtz+Bt
6. Graphite biotite schist
   a, Qtz+Bt+Ser+Alb

## 4.10. Geological structures

In Ula Ulo meta volcano-sedimentary terrains both primary and secondary structures are present. Secondary structures are dominant than primary structures. Primary structures are bedding and laminations on Meta psmmite and quartzite units. These rocks are originated from sedimentary rocks. These sedimentary structures are not fully destroyed by metamorphism. Ductile structures like folding and shear structures are concentrated along the foliated rocks. non foliated rocks on other hand develops brittle structures.

### 4.10.1. Ductile structures

Lega dembi – Aflata shear zone passes through the study area. Some indication of shearing was seen during field works. The orientation of legdambi – aflata shear zone is NS. Though the regional orientation is NS, local variations on schistosity orientation is observed for different lithological units (Fig 4.14).

The azimuth of the foliation of tremolite talc schist ranges from 320 to 047. While its dip ranges from $40^0$ to $87^0$ with a dip direction of NE to NW respectively. Propagation of strike is observed on the contact between talc tremolite schist and tremolite talc schist. As a result anatomizing folds are formed (Fig 12 a). Its orientation is similar to the strike of the tremolite talc schist. These fold plunges to west.

The azimuth of meta psmmite unit is 005-045 and its dip ranges from $45^0$ to $60^0$ to NW. Micro fold is observed in this unit. The fold axis of the micro fold is 045 and plunges $33^0$ towards SE. mineral lineations (Fig 12 b) are found in this unit. Boudnages (Fig 4.12 b) of quartz veins and en echelon veins (Fig 4.12 c) are also present .Their orientation is $035/40^0$ towards NW. These kinematic indicators show the sense of movement of the shear.

Quartzite unit is not foliated but they contain a band of minerals (mineral lineation). These mineral lineations (Fig 12.d) have a trend of NS to 035 and plunge ranges from $40^0$ to $90^0$ towards NW. the azimuth of graphite schists is 353 and its dip is 680 towards NW.

(a)

(b)

(c)

(d)

*Fig 4.12 Field photograph showing different ductile structures found in the study are: (a) = folded tremolite talc schist, (b) = micro folds and badinages, (c) = en echelone veins and (d) is mineral lineation.*

### 4.10.2. Brittle structures

Brittle structures are wide spread in whole lithologic units. This structures shows a variable orientation (Fig 4.14). These are barren quartz veins, chalcedony veins and garnierite veins. Thick barren veins (Fig 4.13 a and b) in tremolite talc schist and meta psmmite units. Both are concordant to the foliation of the rock. Close visual observations confirmed that veins are barren and sugary. Their orientations are $057/78^0$ SE and $015/37^0$ in tremolite talc schist and meta psmmite respectively. Chalcedony veins (Fig 4.13 d) localized to the top part of the serpentinites. Their orientation is similar to garnierite veins. Garnierite veins (Fig 4.14) found in the lower part

of the serpentinite unit. The thickness of these veins is variable. Their orientation is variable and presented on Fig 4.14 b.

(a)

(b)

(c)

(d)

*Fig 4.13 Field photograph showing different types of veins found in the study area*

Joints are the dominant brittle structures found in the area. Different set and orientations are observed as presented on Fig 4. 14 d.

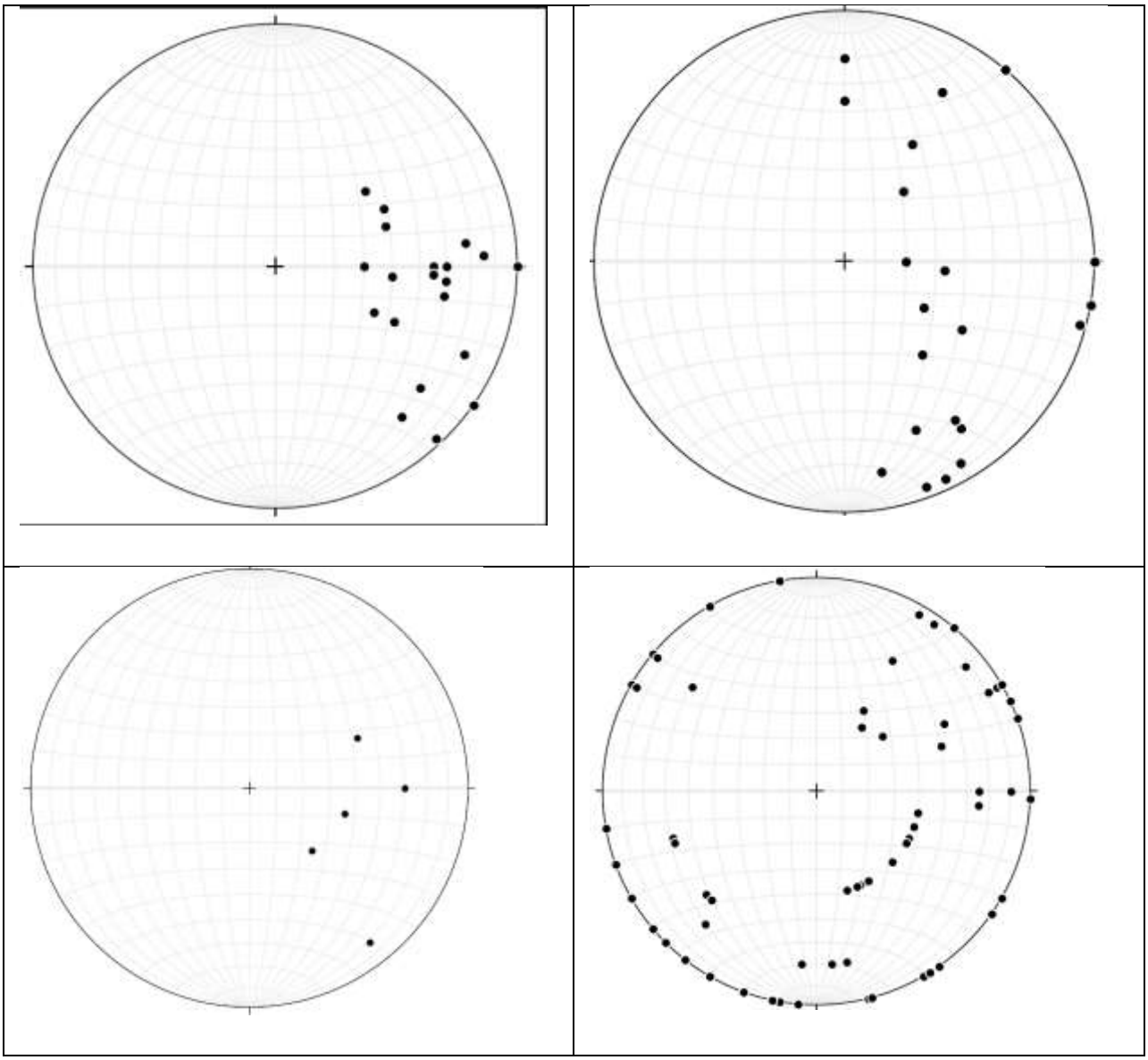

*Fig 4.14 Stereographic projection of structural elements of the area: (a) = foliations, (b) = garnierite veins, (c) = quartz veins and mineral lineations, (d) = joints.*

# Chapter V

# Geochemistry

## 5.1. Introduction

Geochemistry is used to interpret the origin and alteration of the deposit. To achieve this three types of data's are used. These are major element, trace element and LOI. Alteration is interpreted based on the major elements and LOI. Trace elements data are helpful to understand the origin of the deposit. Table 5.1 presents the location of samples collected and analyzed for geochemical investigation.

| *Samples* | *Easting* | *Northing* | *Elevation* | *Description* |
|---|---|---|---|---|
| UNNWV-D2-5 | *0483514* | *0610180* | *1485m* | *Phase 1 Silica vein* |
| UNWS-D5-2 | *0483454* | *0610297* | *1456m* | *Veined serpentine* |
| UCT-D3-2 | *0483471* | *0609561* | *1555m* | *Talc* |
| UCWS-D3-5 | *0483893* | *0609378* | *1659m* | *Stock worked serpentinite* |
| UWTr-D4-3 | *0483332* | *0608905* | *1556m* | *Tremolite* |
| UTFS-D3-6 | *0483756* | *0609059* | *1755m* | *Barren serpentine* |
| UNV-D5-1 | *0483454* | *0610297* | *1456m* | *Phase 2 veins* |
| UWWS-D4-6 | *0483372* | *0608943* | *1566m* | *Veined serpentinite* |
| UEFS-D6-4A | *0483695* | *0608813* | *1669m* | *Pale green serpentinite* |
| UCFS-D3-3 | *0483680* | *0609476* | *1602m* | *Stock worked serpentinte* |
| UEA-D6-6 | *0485164* | *0608302* | *1491m* | *Amphibolite* |
| UEFS-D6-4B | *0483722* | *0608852* | *1676m* | *veined serpentinite* |

*Table 5.1 Geochemical samples and their description*

## 5.2. Analysis results

Table 5.2 presents the result of the geochemical analysis. These results are categorized as major elements, trace elements, base metals and ore grade. Major elements were analyzed by ICP-AES while the trace elements were done by ICP-MS. Twelve rock samples were collected for geochemical analysis.

| **El.** | **core** | **Middle** | **middle** | **outer-east** | **outer east** | **outer-north** | **outer-west** | **vein - outer** | **vein - outer** | **country rocks** | | |
|---|---|---|---|---|---|---|---|---|---|---|---|---|
| | **UTFS-D3-6(serpentine)** | **UCFS-D3-3 (serpentinite)** | **UCWS-D3-5(serpentinite )** | **UEFS-D6-4B(serpentinite)** | **UEFS-D6-4A (serpentinite)** | **UNWS-D5-2(serpentinite)** | **UWWS-D4-6(serpentinite)** | **UNV-D5-1(vein)** | **UNNWV-D2-5 (Vein)** | **UCT-D3-2(talc)** | **UWTr-D4-3(tremolite)** | **UEA-D6-6(amphibolite)** |
| ***Major element (wt. %)*** | | | | | | | | | | | | |
| **$SiO_2$** | 40.6 | 40.7 | 46.9 | 43.1 | 42.2 | 65.2 | 48.8 | 98.2 | 91.4 | 55.1 | 50.3 | 56.1 |
| **$TiO_2$** | <L.D | <L.D | <L.D | <L.D | <L.D | <L.D | <L.D | <L.D | 0.01 | 0.02 | 0.03 | 0.01 |
| **$Al_2O_3$** | 0.13 | 0.13 | 0.47 | 0.07 | 0.09 | 0.3 | 0.2 | 0.04 | 0.08 | 2.73 | 4.48 | 0.93 |
| **$Fe_2O_3$** | 7.46 | 7.69 | 9.79 | 7.59 | 7.26 | 5.67 | 9.45 | 0.84 | 5.42 | 8.11 | 10.35 | 7.11 |
| **FeO** | 6.71 | 6.92 | 8.81 | 6.83 | 6.53 | 5.1 | 8.50 | 0.8 | 4.88 | 7.3 | 9.32 | 6.4 |
| **MnO** | 0.08 | 0.09 | 0.19 | 0.1 | 0.09 | 0.11 | 0.11 | 0.01 | 0.04 | 0.12 | 0.09 | 0.2 |
| **MgO** | 37.1 | 37.1 | 28.9 | 31.2 | 33.1 | 17.55 | 28.4 | 1.05 | 1.26 | 25.2 | 26.8 | 22 |
| **CaO** | 0.01 | 0.01 | 0.04 | 0.04 | 0.02 | 0.06 | 0.03 | <L.D | 0.04 | 1.56 | 0.06 | 8.8 |
| **$Na_2O$** | 0.01 | <L.D | 0.02 | <L.D | <L.D | <L.D | 0.01 | 0.01 | <L.D | 0.12 | 0.03 | 0.12 |
| **$K_2O$** | 0.01 | 0.01 | 0.02 | 0.02 | 0.01 | 0.02 | 0.01 | 0.01 | 0.02 | 0.03 | 0.02 | 0.02 |
| **$P_2O_5$** | <L.D | <L.D | 0.01 | 0.02 | <L.D | 0.01 | <L.D | <L.D | 0.02 | <L.D | 0.01 | 0.01 |
| **$Cr_2O_3$** | 0.36 | 0.39 | 0.38 | 0.38 | 0.32 | 0.29 | 0.37 | 0.07 | 0.09 | 0.53 | 0.43 | 0.45 |
| **NiO** | 0.33 | 0.45 | 1.75 | 4.54 | 3.38 | 2.57 | 1.98 | 0.09 | 0.14 | 0.74 | 0.27 | 0.12 |
| **LOI** | 13.65 | 13.75 | 12.05 | 12.85 | 13.35 | 8.59 | 10.65 | 1.15 | 1.91 | 4.54 | 5.91 | 2.81 |
| **Total** | 99.41 | 99.87 | 98.77 | 95.37 | 96.44 | 97.8 | 98.03 | 101 | 100 | 98.06 | 98.51 | 98.57 |

| ***Trace element(ppm)*** | | | | | | | | | | | | |
|---|---|---|---|---|---|---|---|---|---|---|---|---|
| **Sc** | 4 | 5 | 11 | 4 | 3 | 7 | 7 | <1 | 1 | 15 | 29 | 9 |
| **V** | <L.D | 22 | 13 | <L.D | 12 | <L.D | 22 | <L.D | 21 | <L.D | 66 | 21 |
| **Cr** | 2410 | 2790 | 2600 | 2640 | 2300 | 2240 | 2620 | 440 | 680 | 3610 | 2840 | 3220 |
| **Co** | 118 | 120 | 145 | 126 | 119 | 130 | 130 | 12 | 35 | 77 | 98 | 73 |
| **Ni** | 2630 | 3580 | 13800 | 35700 | 26600 | 15600 | 19800 | | | | | |
| **Cu** | 2 | 2 | 50 | 3 | 3 | 2 | 2 | 1 | 1 | 40 | 59 | 12 |
| **Zn** | 48 | 49 | 52 | 40 | 36 | 42 | 42 | 6 | 11 | 61 | 55 | 58 |
| **Ga** | 0.2 | 0.2 | 0.4 | 0.3 | 0.1 | 0.6 | 0.2 | <L.D | 0.4 | 3.2 | 4 | 1.4 |
| **As** | 5 | <L.D | <L.D | <L.D | 6 | <L.D | <L.D | <L.D | <L.D | <L.D | 15 | 11 |
| **Rb** | <L.D | <L.D | 0.3 | 0.6 | 0.4 | 1.4 | 0.2 | 0.9 | 1.1 | <0.2 | <0.2 | 0.7 |
| **Sr** | 1 | 0.7 | 2.7 | 1.3 | 0.9 | 2.5 | 1.9 | 0.2 | 2.3 | 3.5 | 0.3 | 99.4 |
| **Y** | <L.D | <L.D | <L.D | <L.D | <L.D | <L.D | <L.D | <L.D | 1.8 | 0.7 | 0.5 | 1.3 |
| **Zr** | <L.D | <L.D | 2 | <L.D | <L.D | 2 | 43 | <L.D | 4 | 5 | 12 | 7 |
| **Nb** | 0.3 | 0.2 | 0.5 | 0.3 | 0.3 | 0.4 | 0.3 | 0.4 | 0.7 | 0.9 | 1.2 | 0.8 |
| **Mo** | 1 | 1 | 1 | 2 | 2 | 1 | 1 | 1 | <L.D | 1 | <L.D | 1 |
| **Cd** | <L.D | <L.D | <L.D | 0.7 | 0.7 | 0.6 | 0.6 | <L.D | <L.D | <L.D | <L.D | <L.D |
| **Sn** | <L.D | <L.D | <L.D | <L.D | <L.D | <L.D | <L.D | <L.D | <L.D | <L.D | <L.D | <L.D |
| **Cs** | <L.D | <L.D | 0.02 | 0.03 | 0.03 | 0.12 | 0.04 | 0.17 | 0.11 | <L.D | 0.04 | 0.02 |
| **Ba** | 1.6 | 1.9 | 20.8 | 16.5 | 6 | 11.5 | 9.1 | 2.8 | 25.3 | 6.3 | 1.8 | 6 |
| **La** | 0.7 | 0.7 | 1.2 | 0.8 | 0.9 | 0.9 | 1 | 0.8 | 2.1 | 1.1 | 1.1 | 1.5 |
| **Hf** | <L.D | <L.D | <L.D | <L.D | <L.D | <L.D | 1 | <L.D | <L.D | 0.2 | 0.4 | 0.4 |
| **Ta** | <L.D | <L.D | <L.D | <L.D | <L.D | <L.D | <L.D | <L.D | <L.D | <L.D | <L.D | <L.D |
| **W** | 1 | 1 | 1 | 3 | 3 | 2 | 3 | <1 | 1 | 1 | 1 | 1 |
| **Pb** | <L.D | 2 | 5 | 7 | 3 | 2 | 2 | <L.D | <L.D | 2 | <L.D | 3 |

| | | | | | | | | | | | | |
|---|---|---|---|---|---|---|---|---|---|---|---|---|
| **Ce** | <L.D | <L.D | <L.D | <L.D | <L.D | <L.D | <L.D | <L.D | 2.1 | 0.7 | 0.7 | 1.9 |
| **Pr** | <L.D | <L.D | 0.04 | <L.D | <L.D | 0.07 | <L.D | 0.03 | 0.28 | 0.09 | 0.1 | 0.25 |
| **Nd** | 0.1 | <0.1 | 0.2 | <0.1 | 0.1 | 0.1 | 0.1 | 0.1 | 1.1 | 0.3 | 0.4 | 1.1 |
| **Sm** | <L.D | <L.D | <L.D | <L.D | <L.D | 0.05 | <L.D | <L.D | 0.25 | 0.06 | 0.07 | 0.23 |
| **Eu** | <L.D | <L.D | <L.D | <L.D | <L.D | 0.03 | <L.D | <L.D | 0.05 | 0.04 | <0.03 | 0.37 |
| **Gd** | <L.D | <L.D | <L.D | <L.D | <L.D | <L.D | <L.D | 0.05 | 0.21 | 0.08 | 0.12 | 0.24 |
| **Tb** | <L.D | <L.D | <L.D | <L.D | <L.D | 0.01 | <L.D | 0.01 | 0.03 | 0.02 | 0.02 | 0.04 |
| **Dy** | <L.D | <L.D | <L.D | <L.D | <L.D | <L.D | <L.D | <L.D | 0.19 | 0.13 | 0.07 | 0.28 |
| **Ho** | <L.D | <L.D | 0.01 | <L.D | <L.D | 0.02 | 0.01 | 0.01 | 0.04 | 0.01 | 0.02 | 0.04 |
| **Er** | <L.D | <L.D | <L.D | <L.D | <L.D | 0.06 | 0.04 | <L.D | 0.12 | 0.06 | 0.09 | 0.11 |
| **Tm** | <L.D | <L.D | <L.D | <L.D | <L.D | 0.01 | <L.D | <L.D | 0.02 | <L.D | <L.D | <L.D |
| **Yb** | <L.D | <L.D | <L.D | <L.D | <L.D | 0.09 | <L.D | <L.D | 0.14 | 0.09 | 0.08 | 0.1 |
| **Lu** | <L.D | <L.D | <L.D | <L.D | <L.D | <L.D | 0.01 | <L.D | 0.03 | 0.01 | 0.02 | 0.02 |
| **Hf** | <L.D | <L.D | <L.D | <L.D | <L.D | <L.D | 1 | <L.D | <L.D | 0.2 | 0.4 | 0.4 |
| **Ta** | <L.D | <L.D | <L.D | <L.D | <L.D | <L.D | <L.D | <L.D | <L.D | <L.D | <L.D | <L.D |
| **Pb** | <L.D | 2 | 5 | 7 | 3 | 2 | 2 | <L.D | <L.D | 2 | <L.D | 3 |
| **Th** | <L.D | <L.D | <L.D | <L.D | <L.D | <L.D | <L.D | <L.D | 0.03 | 0.13 | 0.35 | 0.08 |
| **U** | <L.D | <L.D | <L.D | <L.D | <L.D | 0.36 | 0.06 | 0.05 | 0.31 | 0.06 | 0.1 | 0.09 |
| **Tl** | <L.D | <L.D | 10 | <L.D | <L.D | <L.D | <L.D | 10 | <L.D | 10 | <L.D | 10 |

*Table 5.2 Analysis results for major and trace elements*

These samples are collected from the whole lithologic units (see table 5.1).These samples were crushed and grinded to 75 micron mesh size in ALS laboratory (Addis Ababa). The analysis ICP-MS and ICP- AES are done in ALS laboratory, Ireland. ICP-MS analysis is done for trace element and rare earth elements collectively 30 element package. Prior to ICP-MS the samples were fused by lithium borate fusion. The fusion enables complete dissolution of refractory lithophile elements. These fused bead need to be digested by four acids for ICP-AES whole rock package (thirteen elements) analysis. Ore grade nickel and base metals (twelve elements) done by four acid digestion ICP-AES. On the table < sign stand for concentrations which are below the detection limit of the instrument (ICP-AES and ICP-MS). This could be related to the limitation of the instrument and anomalous low concentration of the element in the sample analyzed.

Some major elements are below detection limit. $Na_2O$ is below detection limit for serpentinites. $TiO_2$ is below detection limit for quartz veins and serpentinites and shows an enrichment in amphibolite and talc tremolite schists. $P_2O_5$ and BaO are below detection limit for all lithologic units analyzed. Ce, Dy, Er, Eu, Gd, Lu, Th, U, Y and Yb are below detection limit in serpentinites. Other trace elements and base metals Ag, As, Cd, Ta, Tb, Th, Tm, U, Li and Tl are below detection limit in serpentinite, tremolite talc schist, talc tremolite schist and amphibolites.

### 5.3. Major elements

Major elements are elements which are found > 1 wt. % concentration. Due to this fact always they are presented in weight percent. The information from these elements is useful to understand the history of the rocks.

#### 5.3.1. Variation of major elements on the lateritic column

These variations are related to surficial weathering and silicification. The deposit is formed by surficial weathering and chemical precipitation. To see the variation of major elements along the lateritic profile Bivariant plots are produced. The samples plotted are only serpentinites. These samples collected from the fresh, oxide zone and saprolite zone. Based on table 5.2 $SiO_2$ shows increment from fresh serpentinite to saprolite zone sequentially.

From Bivariant plots the following relationship is observed. On Fig 5.1 a shows $Al_2O_3$ inflation pattern with increment up to oxide zone and its value decline to the saprolite zone. This is due to the immobile nature of aluminum in oxidized environment. The highest $Al_2O_3$ is observed in

oxide zone. Ni (Fig 5.1 b) is positively correlated with $SiO_2$ and highest value is observed in lower saprolite zone. This is due mobility of Ni in residual medium and percolation of nickel down to the saprolite zone precipitation of Nickel in alkaline environments. $Fe_2O_3$ (Fig 5.1 c) shows inflation pattern with an increment up to oxide zone and decline in saprolite zone. MgO and $Cr_2O_3$ (Fig 5.1 d and e) shows a negative correlation with $SiO_2$ since MgO and $Cr_2O_3$ is remains in residual environment. Alkalis (Fig 5.1 f-h) show a horizontal trend due to low concentration of these elements in a peridotite. All CaO, $Na_2O$ and $K_2O$ are mobile in oxidizing environment. The absence of scattering is due to low concentration of these elements is due to low concentration in parent rock peridotite). $TiO_2$ (Fig 5.1 i) shows a very low concentration and liner pattern. This tells that the magma that form this rocks is low –Ti Thoeliitic.

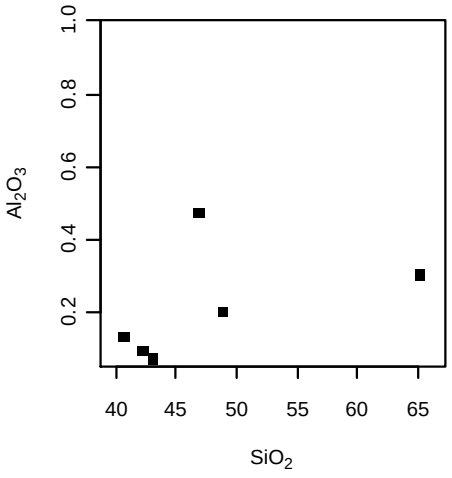


(a)

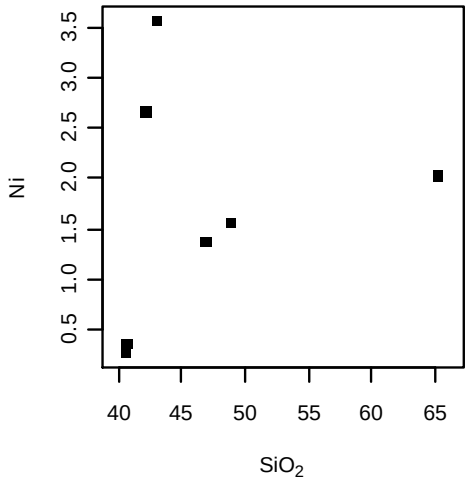


(b)

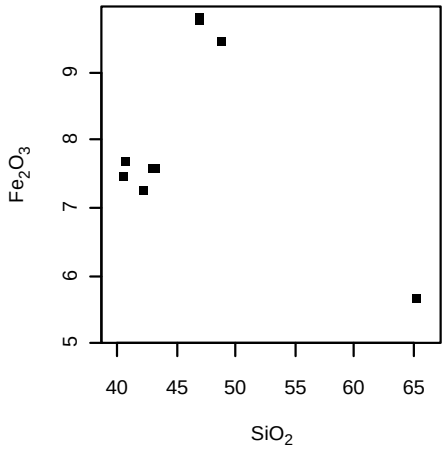


(c)

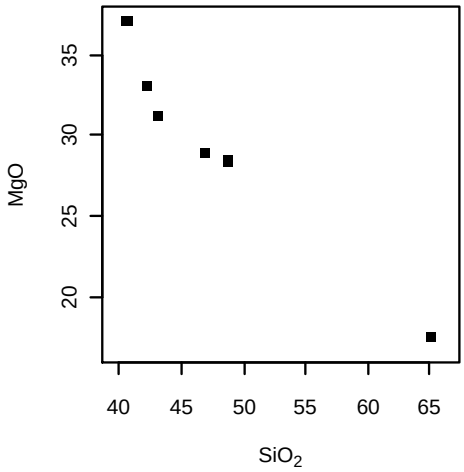


(d)

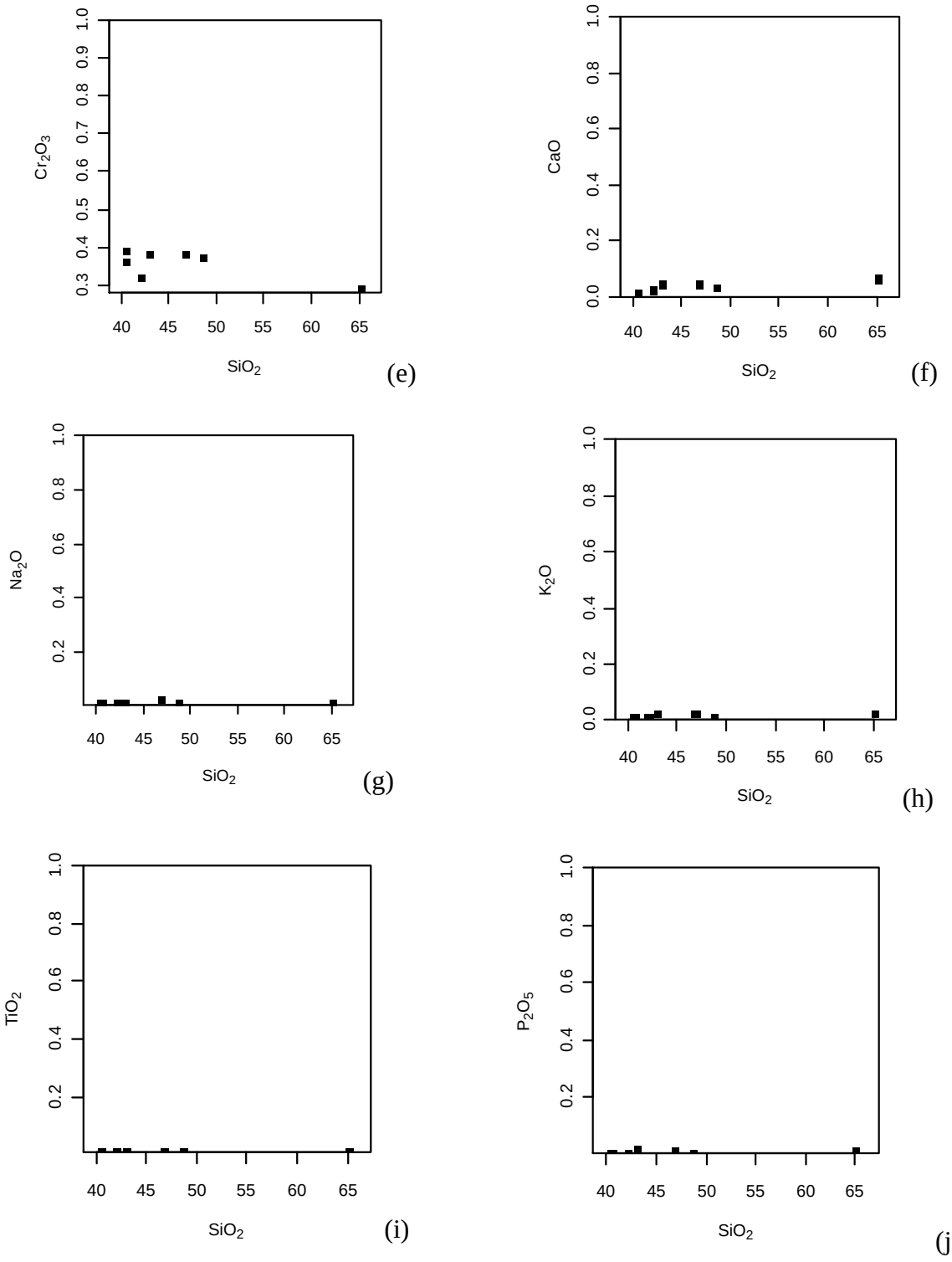


*Fig 5.1 Bivariant plots of silica with major oxides for fresh and altered serpentinites; concentration of x and y axis are is in wt. %.*

### 5.3.2. Zircon as a petrogenic indicator

Silica is highly mobile under metamorphism. The rocks found in the area are metamorphosed. Zirconium is one of the immobile elements and incompatible element (Alene and Barki, 1997). It is relatively remain not affected during metamorphism (Pearce and Cann, 1973; Green, 1980). Zircon shows enrichment when the magma is differentiated (Alene and Barki, 1997).

$SiO_2$ (Fig 5.2 a) shows a vertical constant relationship with Zr. This is due to uniformity of Zr in the rocks with variable $SiO_2$ concentration. This tells during differentiation and surficial silicification Zr remains constant. $Al_2O_3$ (Fig 5.2 b) show a linear horizontal trend for the serpentinites which Closer to x-axis on which the concentration of Al is very small. This tells the absence of surficial enrichment of Al in serpentines. Another trend observed is a linear vertical trend from serpentinites to tremolite schist and then to talc schist. This is because of the increment of Al during differentiation. The concentration of Al in amphibolites is small which could be related to fractionation of Al containing minerals during crystallization of talc schist and tremolite schist. MgO (Fig 5.2 c) shows a vertical pattern similar to $SiO_2$. But, in this case MgO concentration is declining and Zr remains constant. The decrease in MgO concentration is due to the crystallization of olivine (foresterite). $P_2O_5$ , $Na_2O$, $K_2O$ plots on Fig 5.2 d – f shows a linear vertical constant trend due to the depletion P, Na and $K_2O$ on the source. TiO2 (Fig 5.2 i) shows a linear pattern closer to X- axis due to similar low concentration of Ti on different lithologies. This is due to low Ti thoeliite affinity of the rocks in the study area. Similar to $Al_2O_3$ on Fig 5.2 b CaO on Fig 5.2 f shows a vertical line for magmatic differentiation and horizontal line for surficial alteration. This is due to the absence plagioclase crystallization on magmatic evolution from ultra-basic to basic composition. This is followed by crystallization of Ca bearing plagioclases in amphibolites. Fractionation of clinopyroxene and olivine resulted the decline in concentration of Ni (Fig 5.2 j) from (0.33 – 0.12 %Ni). But the concentration of Cr positively correlated with Zr. Plots of Nb and V (Fig 5.2 i and m) shows a positive correlation with Zr. This is because both elements are incompatible and remain in the liquid during crystallization. Due to less mobility of these elements as compared to others they form a line and cluster on the plots. Other elements $SiO_2$, MgO, $Fe_2O_3$, Ni, V and Cr (see fig 5.2) are scattered due to higher mobility.

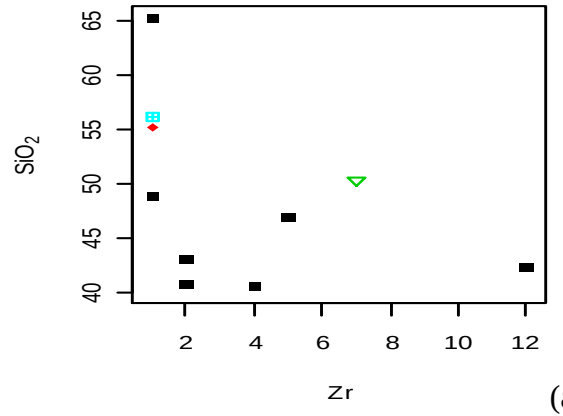


(a)

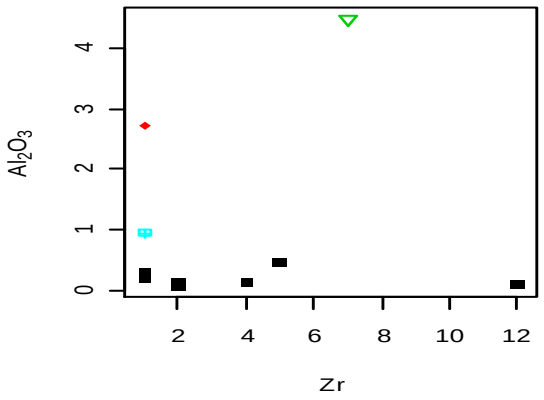


(b)

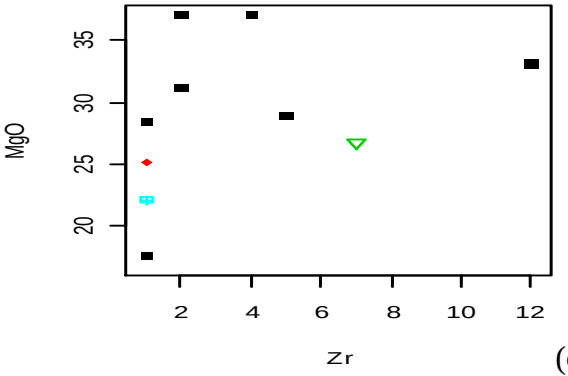


(c)

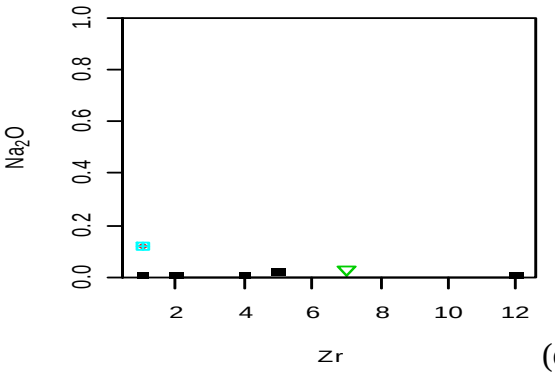


(d)

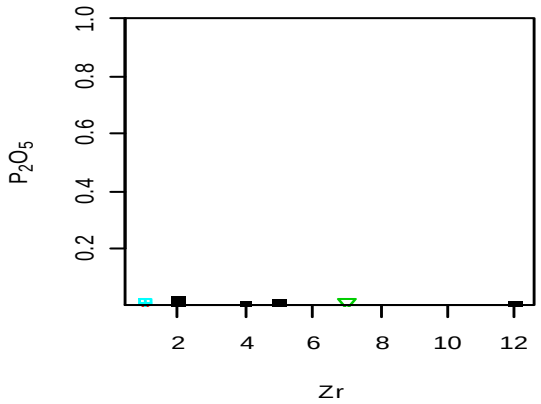


(e)

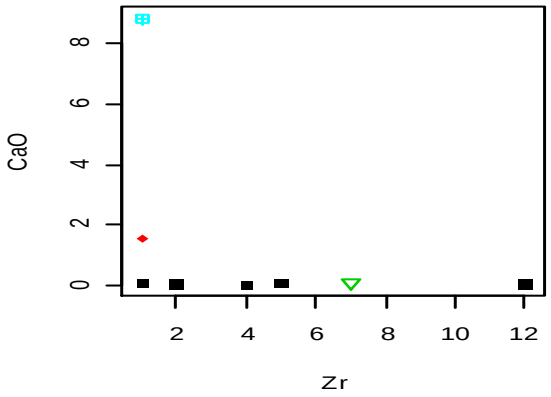


(f)

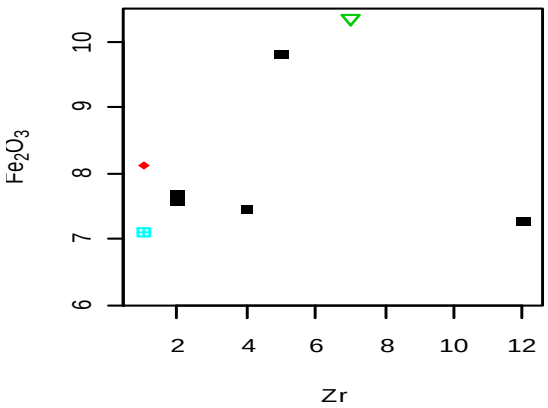


(g)

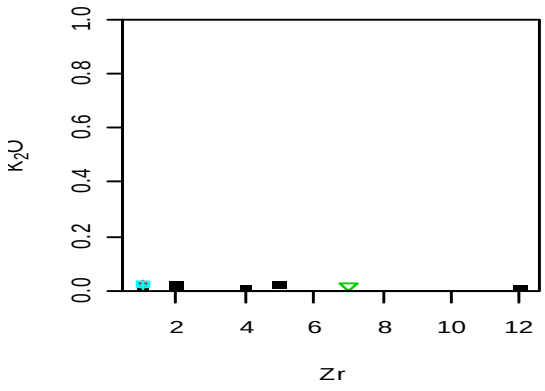


(h)

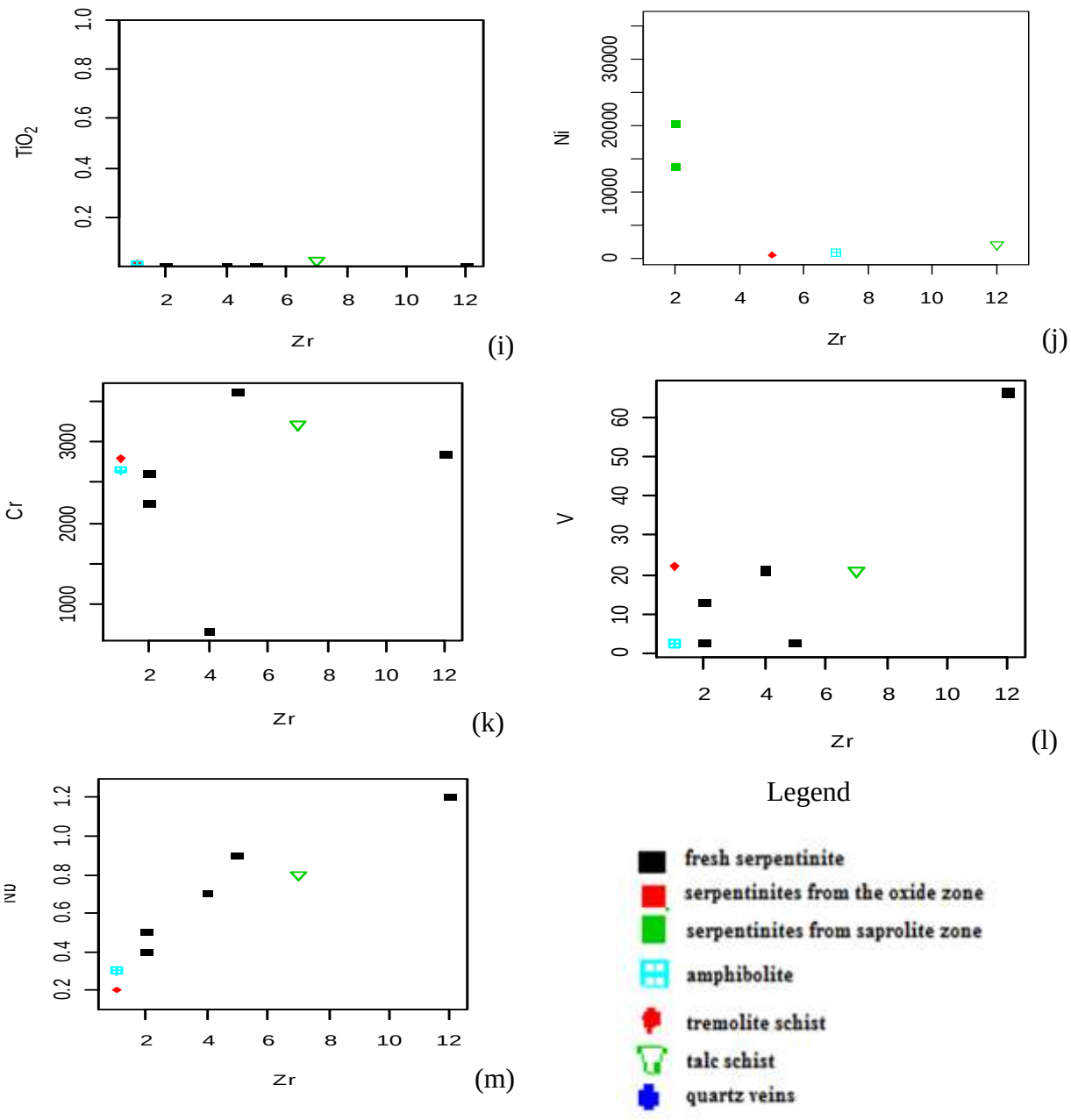


*Fig 5.2 Bivariant plots of Zr with other major and trace elements. The units are ppm for both X and Y axis.*

### 5.3.3. Alteration effect

Alteration can change the composition of a rock (Humphris and Thompson, 1978; Gillis et al., 1992). Loss on ignition of the host and the country rocks is displayed on table 5.2. From this data serpentinites shows higher loss on ignition than talc and tremolite schist (see fig 5.3). This is because serpentinites are more prone to alteration than talc and tremolite schists. Serpentinites

and talc tremolite schist contains hydrous minerals. While amphibolites and quartz veins doesn't contain a hydrous minerals. Therefore the LOI of serpentinites and talc tremolite schists is higher than the LOI of amphibolites and quartz veins. Alteration affected the concentration of mobile elements than immobile elements. To see this binary plots of $Al_2O_3$ and $Na_2O$ with respect to LOI is made (fig 5.3 a and b). These elements are immobile and mobile respectively.

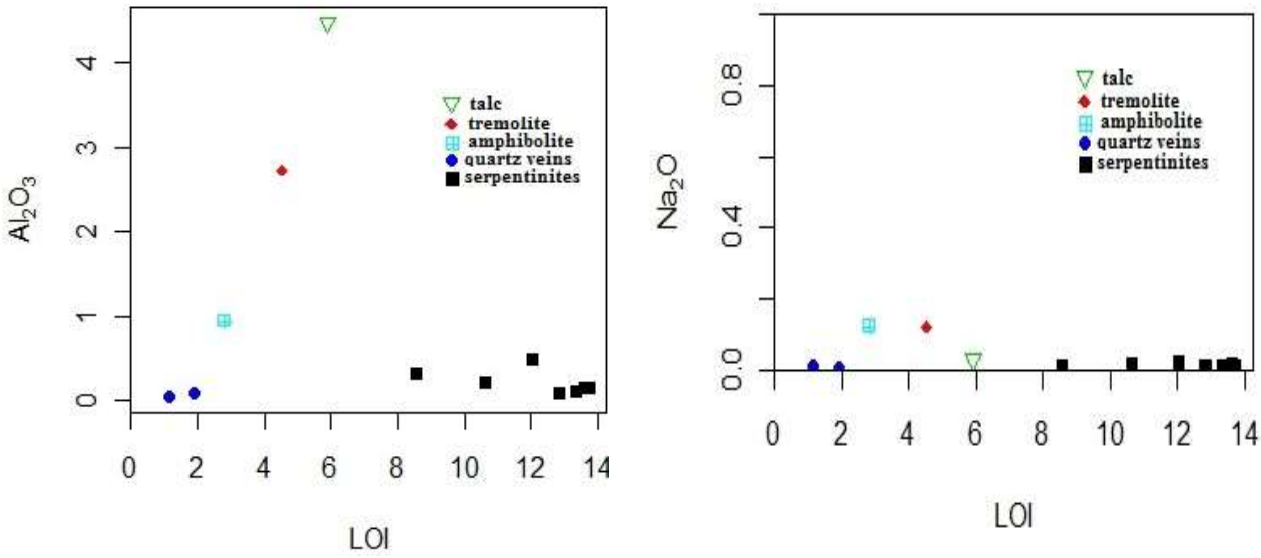


*Fig 5.3 LOI of the host rock and country rocks. The units are Wt. % for both X and Y axis.*

### 5.4. Trace element geochemistry

Trace elements are very informative for understanding the petrogenesis than major elements.

#### 5.4.1. Trace element with zircon

High field strength elements like Nb and Th are plotted on Bivariant diagram of Fig 5.4.a and b respectively. Both Nb and Th show a positive correlation with Zr. This is because of the accumulation of these elements on the melt during magma differentiation. Incompatible rear earth elements La and Nd are plotted on Fig 5.4 c and d respectively. They show a similar positive correlation with Zr. also shows a positive correlation with Zr due to accumulation on the melt. Sr on Fig 5.4 e, Eu on Fig 5.4 f shows a similar positive correlation with Zr. Because these elements are incompatible and remain in the melt during crystallization of serpentinite, tremolite talc schist and talc tremolite schist. Their concentration is higher in amphibolites. Since, they are compatible to the crystal phase during crystallization of plagioclase. These elements can substitute Ca in magmatic system. The mineral constituents of amphibolites are dominantly

hornblende and epidote. Epidote is a metamorphic equivalent of plagioclase. In plagioclase is calcium containing feldspar. Therefore, Sr and Eu concentration is higher in amphibolite as compared to other lithologies.

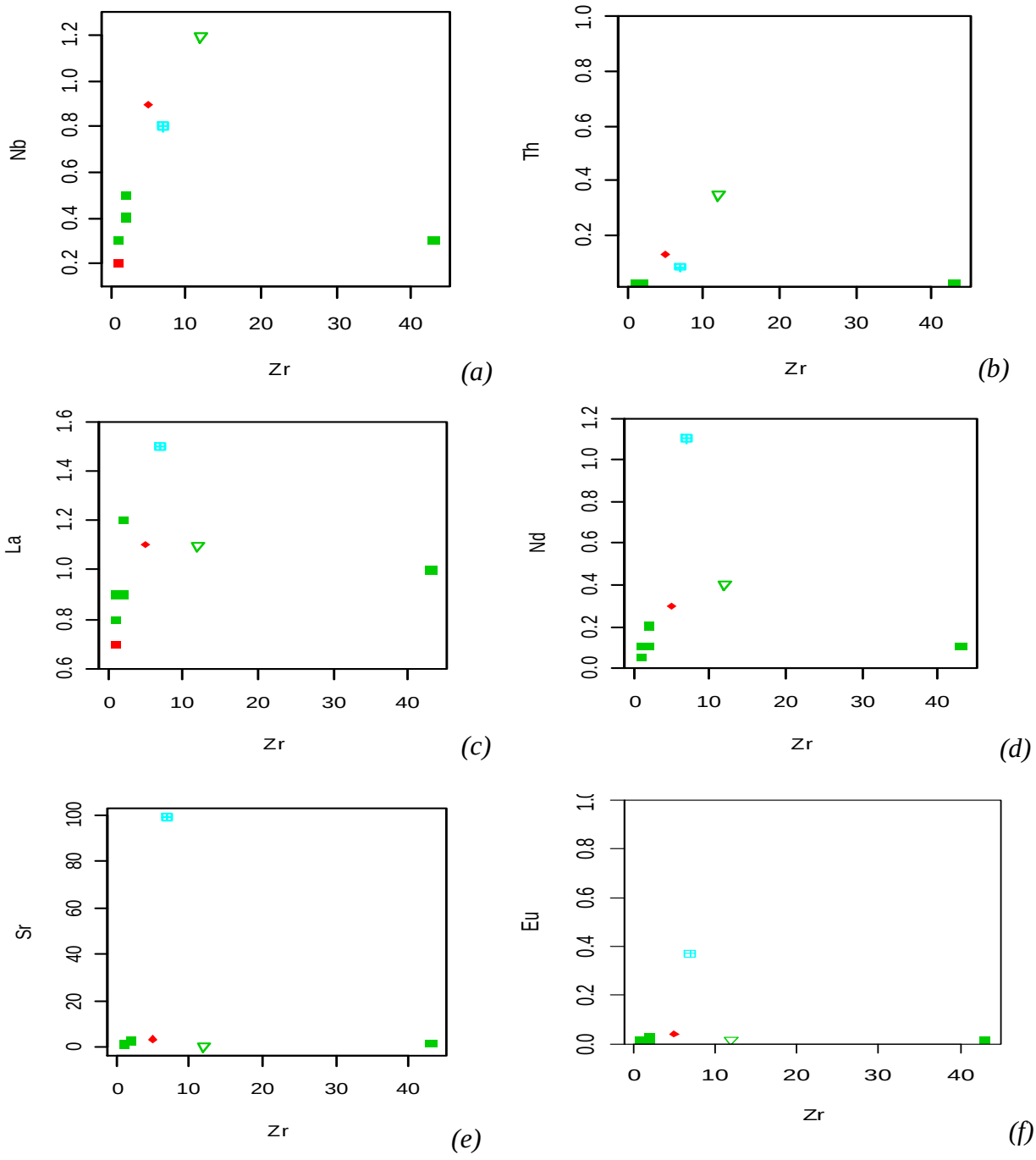


*Fig 5.4 high field strength and incompatible rear earth element vs. Zr plot. All units are in ppm. Legend is similar as Fig 5.2.*

Large ion lithophile elements Ba and Sr are plotted against $SiO_2$ on fig 5.5.a and b respectively. From Ba Vs. $SiO_2$ plot, Ba in the serpentinite shows scattering due to positive correlation with silicification. Ba concentration of the fresh serpentinite and tremolite talc schist is similar and lower than silicified serpentinites. This is related to the removal of Ba during metamorphism. Ba in fresh serpentinites and tremolite talc schist is lower than amphibolite and tremolite schist. Sr on other hand is not scattered and forms a liner pattern in serpentinites, tremolite talc schist and talc tremolite schist. Since Sr is mobile in surficial and metamorphic environment it could be removed during metamorphism or the concentration of Sr is small as explained with Zr in Fig 5.4 e. Sr shows high concentration in amphibolite. This is due to the presence of Ca phases in amphibolite.

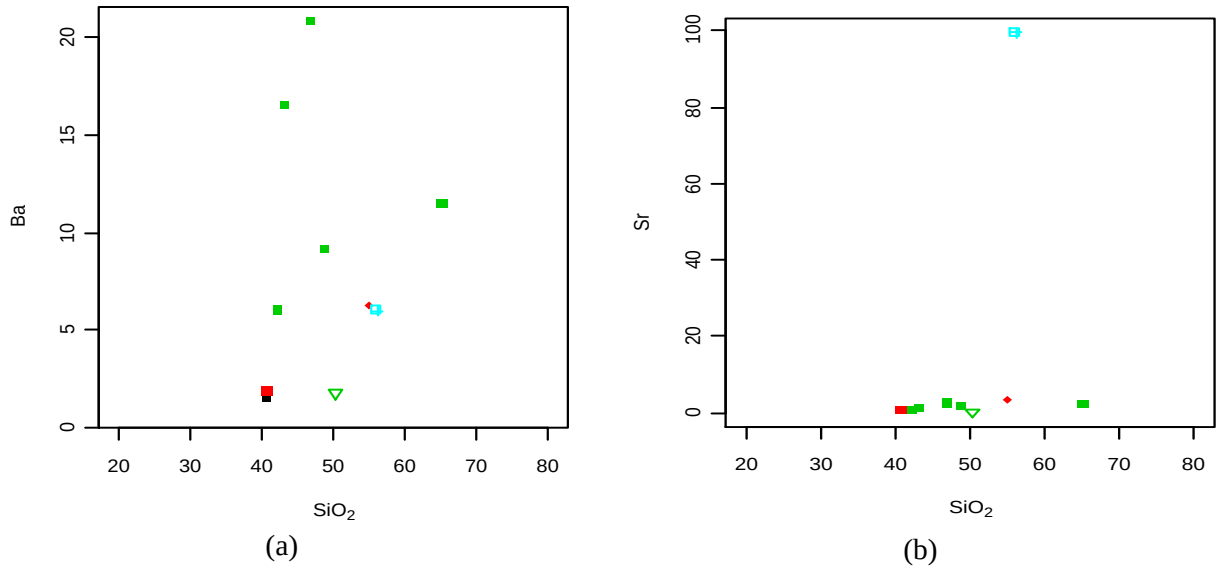


*Fig. 5.5 Bivariant plot of large ion lithophile elements (Ba) and silica (SiO2). All concentration are in ppm and symbol is similar as Fig 5.2.*

### 5.4.2. Trace element ratios

Fig 5.6 displays trace element trace element ratios of Ti/Sm, Ti/Eu with Zr/Sm and shows a positive correlation. Positive correlation of Ti/Eu, Ti/Sm and Zr/Sm shows the absence of amphibole intervention on the magma evolution. If amphibole involves in the system it will selectively retain Ti and result negative Ti/Eu and Zr/Sm relationship (Sun and McDonough, 1989; Rollinson, 1993). The linear pattern resulted for both trace element ratios showing the absence of selective enrichment of trace elements. This evidence tells similar origin of all mafic and ultramafic rocks present in Ula Ulo.

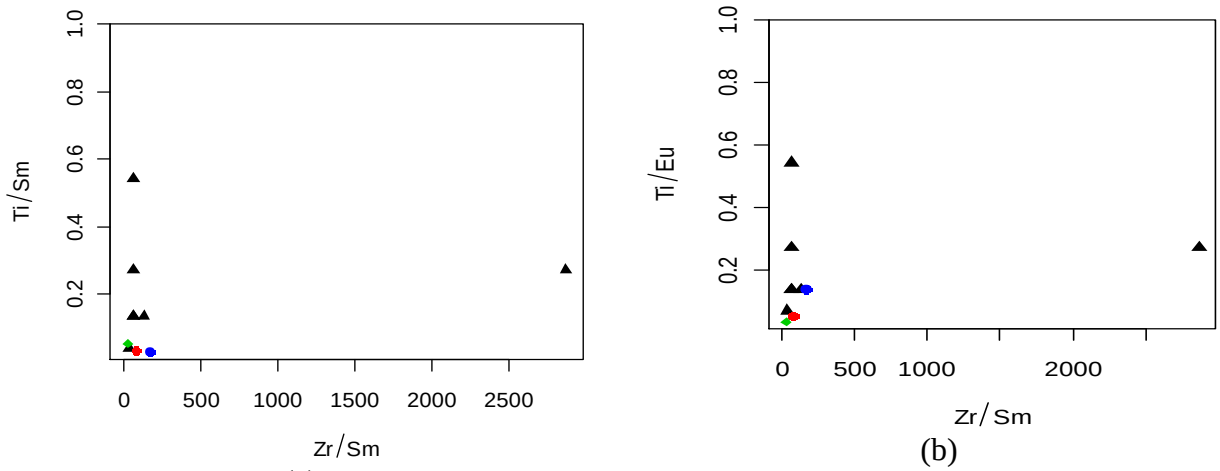


*Fig 5.6 Trace element ratios of Ti/Sm (a) and Ti/Eu (b) Vs. Zr/Sm. Concentrations are in ppm and symbol is similar as Fig 5.2.*

Spider diagrams are helpful for presenting many samples on one plot and to see the correlations between samples (Brownlow, 1996). Fig 5.7a and b are primitive mantle normalized (Sun and McDonough, 1989) LILE and HFSE plot of serpentinites (Fig 5.7 a), and talc schist, tremolite schist and amphibolite (Fig 5.7 b). On Fig 5.7a serpentinites shows a slight enrichment of LILE and depletion of HFSE. The enrichment of LILE is due to the assimilation and dehydration of the subducting slab (Taylor et al., 1994). Immature arc setting shows a slight enrichment of LILE (Worku and Schandelmeir, 1996). Serpentinites are Ce depleted suggesting no interaction of see water during crystallization. Pb spike is due to contribution of subducting slab. Relatively flat trend observed on the right side of the plot due to immobility of HFSE as compared to LILEs (Humphris and Thompson, 1978; Gillis et al., 1992).

On Fig 5.7b tremolite schist, talc schist and amphibolite are plotted. All shows slight enrichment of LILE and depletion of HFSE. They have similar trend due to similar source. Amphibolite shows positive Sr and Eu anomaly due to accumulation of plagioclase. Talc schist in another hand shows negative Sr and Eu anomaly due to fractionation of plagioclase. All serpentinites, talc schist, tremolite schist shows strong negative Ti anomaly due to Ti depleted sources. Ti depletion is due to melting above the subducting slab (Furnes et al. 2015). Adola boninites shows Ti depletion (Alene and Barker, 1995; Woldehimanote and Behrman, 1995). Variation on LILEs (Cs, Rb, Ba and Th) is observed between serpentinites and other lithologic elements. This due to the variation on the contribution of the subducting slab. But,


*Fig 5.7 Spider plot of Large ion lithophile elements and high field strength elements (Sun and McDonough, 1989); (a) spider plots of serpentinites, (b); spider plot of tremolite schist (■), talc schist (■) and amphibolite(■).*

All units shows LILE Enrichment (Ba/Yb)n is 2.92 (serpentinite), 1.2(talc schist), 3.84 (tremolite schist) and 3.2 (amphibolite). Because these LILEs are fluid mobile and easily assimilated from the subducting slab as compared HFSEs. The absence of variation on the high field strength elements is due to similarity of sources. Low Ti/Zr is observed in all samples analyzed similar to modern boninites (Woldehimanote and Behrman, 1995).

Chondrite normalized REE plot (fig 5.8) of Boynton (1984) is used to see the selective fractionation, enrichment and depletion of REE. Two type's trends are observed. These are REE

Depleted (Fig 5.8a, b and c) and LREE (Fig 5.8 d) enriched patterns. As displayed on table 5.2 REEt of serpentinite, talc schist and tremolite is by far lower than amphibolite. This is due to the presence of considerable variations in LREE. As the ratio indicates High La/Yb ratio is observed in amphibolite. The contribution of the subducting slab is higher in amphibolite than the serpentinite, talc schist and tremolite schist. High LREE enrichment is observed in Bonine Island due to metasomatic enrichment (Hickey and Frey, 1982).

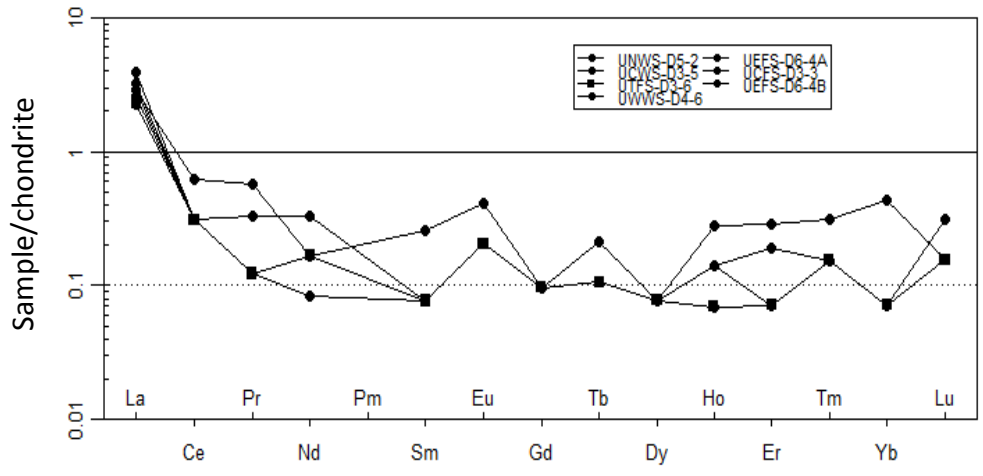


(a)

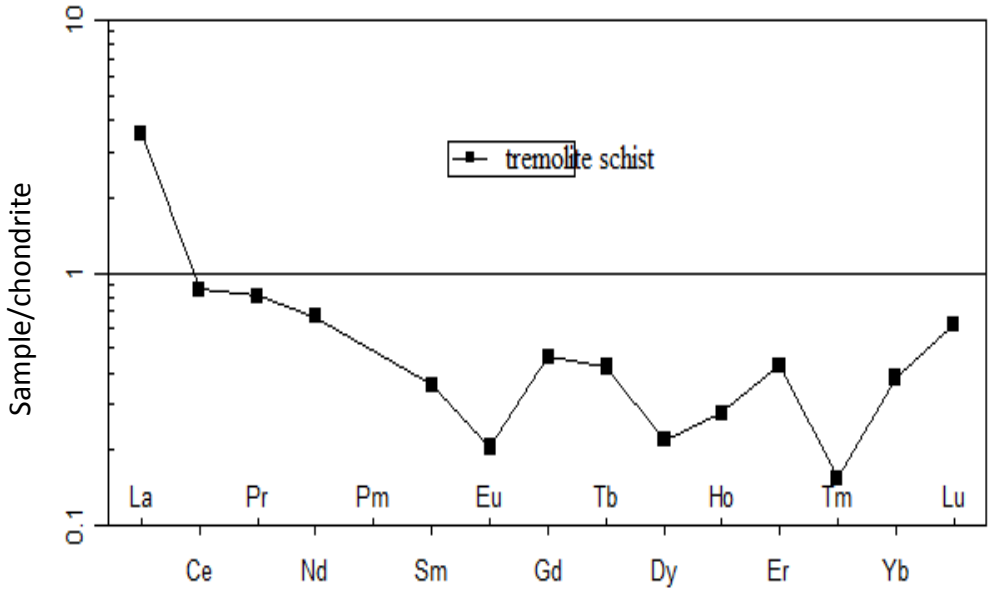


(b)

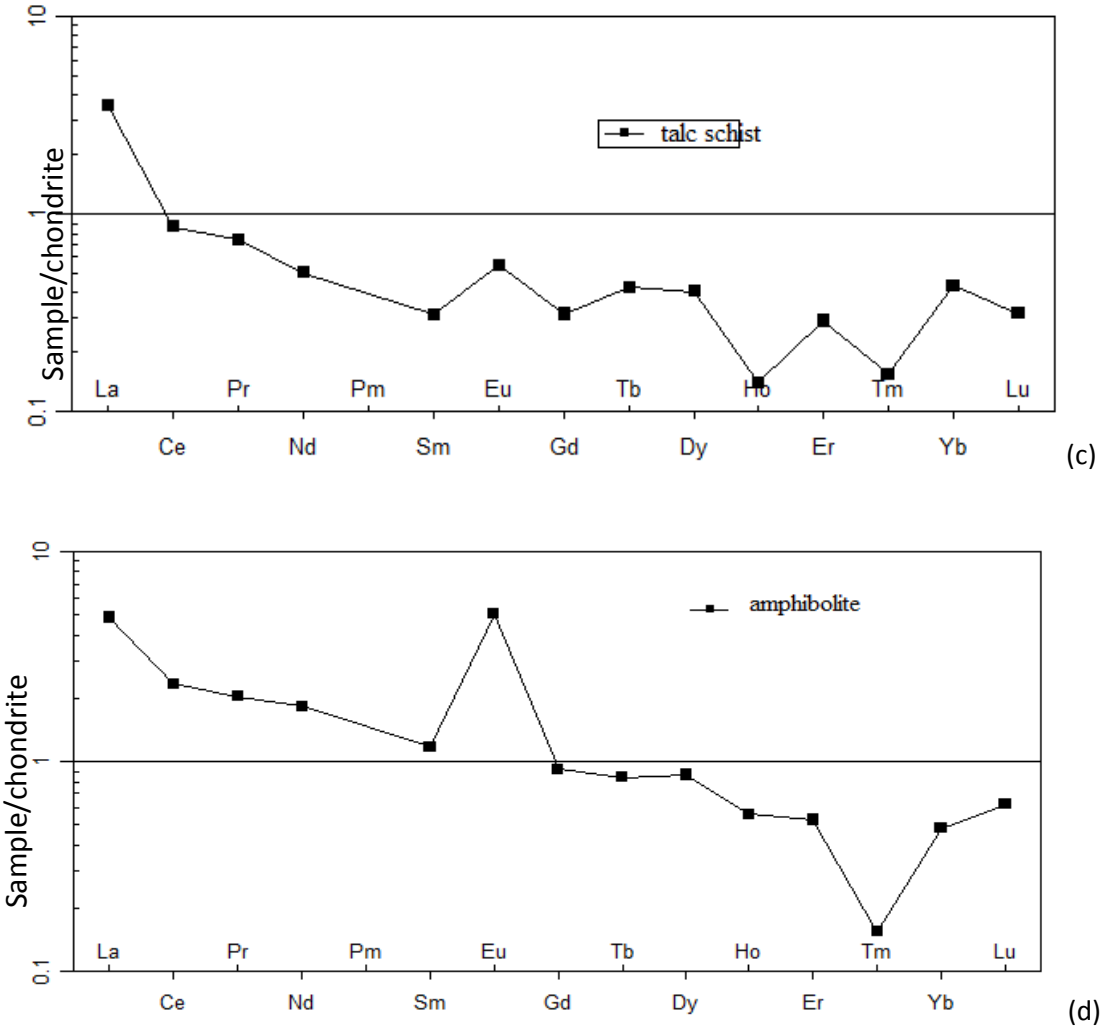


*Fig 5.8 Chondrite normalized REE pattern*: serpentinite *(a), tremolite schist (b), talc schist (c) and amphibolite schist (d).*

Low Ti/Yb (< 0.2) is observed for the serpentinite, talc schist, tremolite schist and amphibolite. Therefore no garnet phase is present during melting and indicates show melting. If garnet present it will selectively deplete Yb and result higher value (Furnes et al., 2015). Serpentinites (Fig 5.8a) shows a linear trend without prominent negative or positive anomaly of Eu. This indicates the absence of plagioclase phase during melting and crystallization of serpentinites. Tremolite schist (Fig 5.8b) shows a slight prominent Negative anomaly of Eu. This is due to fractionation of plagioclase. Talc schist (Fig 5.8c) show slight accumulation of plagioclase (Ottonello et al., 1984; Trubelja et al., 1995). Amphibolite (Fig 5.8d) shows a strong positive Eu anomaly due

accumulation of plagioclase. Additionally amphibolite show a strong negative Tm anomaly due to fractionation of Ni, Cr and Mn containing minerals like olivine and clinopyroxene.

| **Lithology** | **(La/Sm)c.n** | **(La/Yb)c.n** | **REEt** |
|---|---|---|---|
| Serpentinite | 8.1 | 4.2 | 0.7 – 1.84 |
| Talc schist | 10.6 | 6.6 | 2.69 |
| Tremolite schist | 9.1 | 3.7 | 2.79 |
| Amphibolite | 3.7 | 8.1 | 6.18 |

Table 5.3 chondrite normalized LREE and HREE ratios *of serpentine, talc schist, tremolite schist and amphibolite.*

### 5.4.3. Tectonic discrimination

Fig 5. 9a is Miyashiro (1974) $SiO_2$-$FeO_t$/MgO classification of magma series. On the plot all, serpentinte, talc schist, tremolite schist and amphibolites fall on calc alkaline magma series. This also supported by (Fig 5.9 b) which is Shervais (1982) Ti- V discriminating diagram of basalts. This classification widely used for ophiolite sequences which experiences metamorphism. On the plot all the rocks fall on low alkaline thoeliitic island arc thoeliitic bonnieite. Tectonic discrimination diagrams of Woods (1980) based on immobile elements is presented on fig 5.9c and d. On fig 5.9 d and e most the lithologies fall on Arc – basalts. Based on all these information the tectonic setting of Ula Ulo is island arc boninite andesite. These are high magnesium andesite. Previous works of Kozyrev et al. (1985) described Megado terrain as inter arc /back arc basin. Alene and Bekri (1997) studied Moyale Meta basic rocks and described Moyale terrain as immature island arc. Beraki et al. (1989), classified Adola belt as immature island arc.

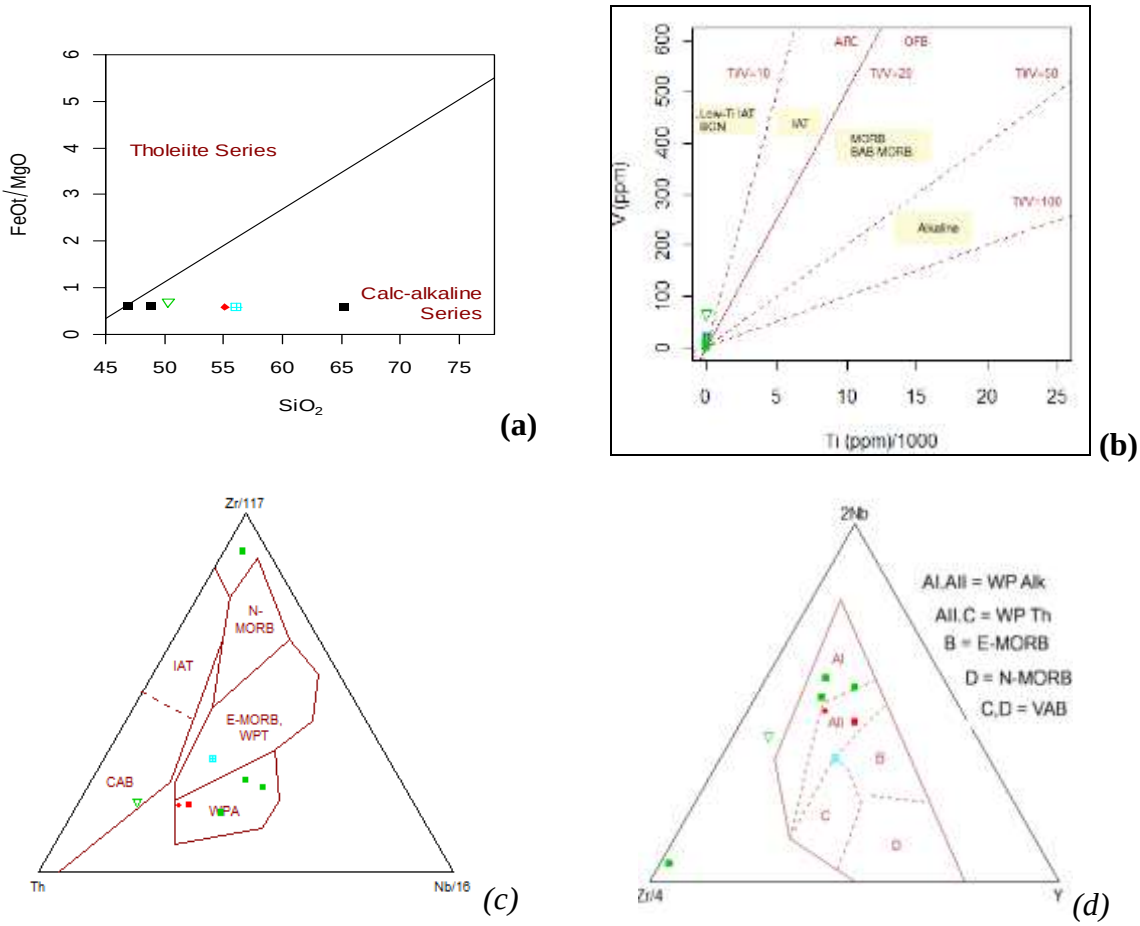


*Fig 5.10 chemical classification and tectonic discrimination diagrams: (a) Miyashiro (1974) SiO2-FeOt/MgO classification of magma series, (b) Shervais (1982) discriminating diagram of basalt and tectonic discrimination plots (c and d) (Woods, 1980)*

Correlation of Ula Ulo serpentinites, talc schist, tremolite schist and amphibolite shows a closer similarity to adola boninites and adola arc related (Wolde et al., 1996).

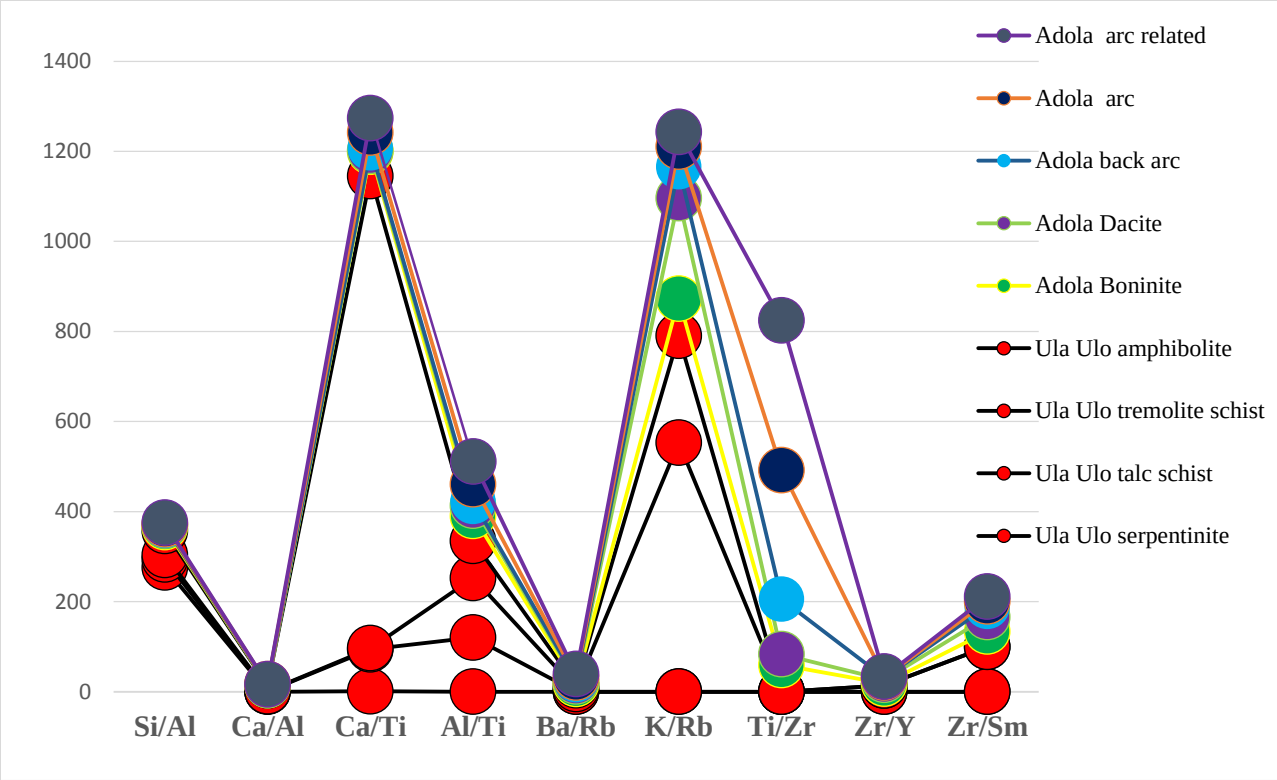


*Fig 5.11 comparison and correlation with adola belt rocks.*

### 5.5. Geological history of Ula Ulo metamorphic terrain

The study area experienced multiple phases of deformation and metamorphism. These deformation and subsequent metamorphism resulted in the formation of different structures and metamorphic rocks. Lithological units found in the study area have volcanic and sedimentary protolith. Rocks from volcanic protolith include serpentinites, talc tremolite schist, tremolite talc schist and amphibolites. Meta sedimentary rocks are quartzite, meta-psmmite and graphite schist.

Serpentinites are formed from the accretion of oceanic lithosphere (Moores, 1970; Coleman, 1971; van der Ent et al, 2013). Serpentinization occurred at the interaction of oceanic lithosphere and sea water (van der Ent et al, 2013). These interactions resulted in the transformation of anhydrous mafic minerals (dominantly olivine and pyroxene (Winker, 1979)) to hydrous magnesium silicates. Mineralogical constituents of Ula Ulo serpentinites are identified by thin section, polished section and XRD analysis. The phases observed on XRD are antigorite, lizardite, olivine and talc (fig 6.6). Thin section investigation shows relict olivine. Chromite and magnetite are opaque minerals observed by polished section. Antigorite, lizardite and talc are

formed by hydrothermal alteration of mantle peridotite (Mustard et al. 2005; Schulte et al. 2006). The experiment of Dietrich and Peters (1971) on antigorite tells about the first appearance of antigorite in metamorphic terrains. The first appearance of antigorite indicated metamorphic facies of upper limit of pumpellylite and the beginning of greenschist. But antigorite can persist for elevated temperature and pressure. Therefore, the metamorphic facies of Ula Ulo serpentinites is greenschist facies to amphibolite facies. wolde et al. (1996) stated the grade of metamorphism of Adola metamorphosed mafic/ ultramafic rocks as greenschist to lower amphibolite facies.

Based on whole rock analysis $SiO_2$ and MgO composition of unaltered fresh serpentinite is 40.6 % and 37.1 % respectively. Based on this composition these serpentinites are classified as ultramafic rock (Le Maitre, 1989). MgO/FeO (5.5) is higher as other ultramafic rocks worldwide (Winker, 1979). CaO concentration is trace (0.01) due to the absence of Ca-bearing minerals (clinopyroxene). Since relict olivine grains observed in thin section and clinopyroxene is absent the possible protolith of Ula Ulo serpentinites is peridotite. Peridotitic protolith is suggested by Jelenc (1966) which is in positive argument current finding.

During Serpentinization of ultramafic rocks the presence and absence of $H_2O$, $CO_2$ and CaO control the new mineral to be formed (Greenwood, 1967; Johannes 1969; Winker, 1979) (see equation below).

2 serpentine + 3 CO2 = 1 talc + 3 magnesite + 3 $H_2O$

1serpentinite + 2 quartz = 1 talc + 2 $H_2O$

5 serpentine + 2 diopside = 1 tremolite + 6 forsterite + 9 H20

If $H_2O$ is the only fluid in the system mainly antigorite, lizardite with minor talc are formed. But talc in Ula Ulo serpentinites reaches up to 52.1 % (fig 5.9). Therefore, this talc is formed by the alteration of serpentinite in presence $CO_2$. Tremolite is not observed in phase investigation and in thin section. This indicates the protolith of serpentinites is Ca - difficent. TAS and AFM classification (fig 5.9 and fig 5.10 a) of the serpentinite shows picrobasalt (ultramafic) and thoeliitic affinity respectively.

Tremolite talc schist and talc tremolite schists bound serpentinite. In thin section these rocks show talc and tremolite. Whole rock composition of tremolite talc schist is $SiO_2$ (55.1%) and

MgO (25.2). according to Le Maiter (1989) this rocks are compositionally a mafic rock. Compared to the serpentinites (0.01%) the concentration of CaO (1.56%) is higher. This is due to the presence of Ca- bearing minerals (diopside) in the protolith. Their MgO/FeO is 3.4 which is lower than the serpentinite. On TAS classification the composition falls on basaltic andesite. AFM plot shows thoeliitic affinity. Therefore, the protolith of this rock is basalt. On the other hand, talc tremolite schists show a chemical composition of $SiO_2$ (50.3 %), MgO (26.8 %), FeO (9.32 %, CaO (0.06 %). According to Le Maitre (1989) this rock is mafic rock. It is classified as basalt and thoeliitic on TAS and AFM plot respectively. The protolith of this rock is basalt.

Amphibolites are analyzed using thin section and whole rock geochemistry. Amphibolite is a common name used for metamorphic rock containing principally hornblende and epidote. In thin section the dominant minerals are epidote and hornblende. Replacement of plagioclase by epidote is observed in different field of views. The presence of epidote is an indication of low grade metamorphism (greenschist facies). Trace elements Eu, Sr, Nb show strong positive anomalies. This is because of plagioclase and supporting basaltic origin. Its chemical composition is $SiO_2$ (56.1 %), FeO (6.45%), MgO (22 %), and CaO (8.8 %). Based on this result the rock is classified as mafic rock (Le Maitre, 1989). The difference between this and the other rocks is its high CaO concentration. This is related to the presence of Ca-bearing minerals dominantly plagioclase and clinopyroxene. On TAS and AFM classification, it is classified as basaltic andesite and thoeliitic respectively.

In general all the rocks hosting and confining the deposit are metavolcanic rocks with basic chemistry. The grade of metamorphism is low grade greenschist facies for all lithologic units. Based on their geochemical signatures these rocks are thoeliitic in composition. All the lithologic units show Low Ti, P and Yb concentration. This depletion supports of volcanic arc settings (Alene and Barker, 1997). Ti/Zr ratio of all lithologic units is very small (< 0.001). Adola thoeliite are high Ti/Zr ratio (150 – 300) if Ti/Zr ratio is very low the rocks are bonnieite instead of thoeliite (Wolde et al., 1996). Therefore, metavolcanic rocks of Ula Ulo are bonnieite instead of thoeliite. $Al_2O_3/TiO_2$ and $CaO/TiO_2$ ratios are serpentinites (38, 3), tremolite talc schist (802, 458), talc tremolite schist (1316, 17) and amphibolite (45, 431). Studies on bonnieite by Sun and Nesbitt (1978), Hickey and Frey (1982), and Sun et al. (1989) characterized bonnieite as

$Al_2O_3/TiO_2$> 20 and $CaO/TiO_2$> 17. Except serpentinites (low $CaO/TiO_2$) other lithologic units are bonnieite. The low $CaO/TiO_2$ ratio in the serpentinite is related to low clinopyroxene content.

Based on present work the tectonic setting of the study area is volcanic arc setting (fig 5.10 b, c and d). The Megado belt is studied by several researchers and the following tectonic interpretations were given accordingly. Kozyrev et al. (1985) described Megado terrain as inter arc /back arc basin. Alene and Beraki (1997) studied Moyale Meta basic rocks and described Moyale terrain as immature island arc. Beraki et al. (1989) classified Adola belt as immature island arc. In fig 5.10 b on Shervais (1982) discriminating diagram all the rocks fall on low Ti bonnieite. This is also mentioned by Berhe (1990) who discussed the presence of bonnieite in Adola belt and inferred the tectonic setting as supera- subduction environment. Wolde et al. (1996) indicated the tectonic setting of Megado thoeliite and bonnieite as volcanic arc setting. Four tectonic environment are correlated to different units of adola belt, continental basement, island arc, back arc and MORB which are correlated as Awata gneisses, meta-igneous complex of Daba, Megado and Kenticha belt, and Reji amphibolite respectively (woldehaimanot et al, 1995).

# Chapter VI

# Nickel mineralization of Ula Ulo ultramafic bodies

## 6.1. Ore zone and ore bodies

The mineralization is confined within the Megado belt mafic – ultramafic rocks. The host rock is serpentinite. The mineralized portion is bounded by the talc tremolite schist in its eastern and southern side. The deposit is formed by lateritic weathering and down depth percolation and enrichment of the saprolite zone. The weathering liberated the nickel from the primary host (olivine and pyroxene). Percolation and repercipitation of nickel as nickel silicate minerals formed the deposit. The boundary between the serpentinite and talc tremolite schist is sharp and distinct. The ore body limits within the host rock is delineated based on the assay values. The shape of the ore body is circular to elliptical body. The central part is the unmineralized barren serpentinite. The nickel concentration in this central part is only 0.236 wt %. This is below cutoff grade in current market. Because the minimum grade mined from laterite by the current state is 0.99 Wt. % at Muurin Murrin, Australia (Mudd, 2010). The ore body is internally zoned into three parts (Fig 6.1). These are identified based on the grade and the style of the mineralization. They are stockworked ore body, coated ore body and veined ore body. They are found as eccentric hallow circles form core to the rim of the ore body. The thickness of the ore body is variable along the strike of the mineralization. It is thicker at the middle part of the ore body along the strike. The mineralization found as dissemination throughout the host rock and as distinct garnierite veins. The disseminated mineralization covers a larger aerial extent. Vein mineralization is confined only to the outer rim of the ore body. The presence of intensive weathering removed the upper cap zone and exposed the saprolite zone. Therefore, the over burden of the mineralization is shallow and is up to 1-1.5 meter. Relative overburden variation is observed throughout ore body. Thicker overburdens are observed at the central – core part of the ore body. This is because of the presence of thick cap and oxide zones.

### 6.1.1. Ore Zone one

This zone covers the inner circular belt. The overburden in this zone is relatively thick due to the presence of the ferric cap (Fig 5.2a). The cap is very reddish in color and contains concretion of

iron minerals. Samples taken from this zone (UCWS-D3-5 and UCFS-D3-3) indicates slight Fe and Cr enrichment.

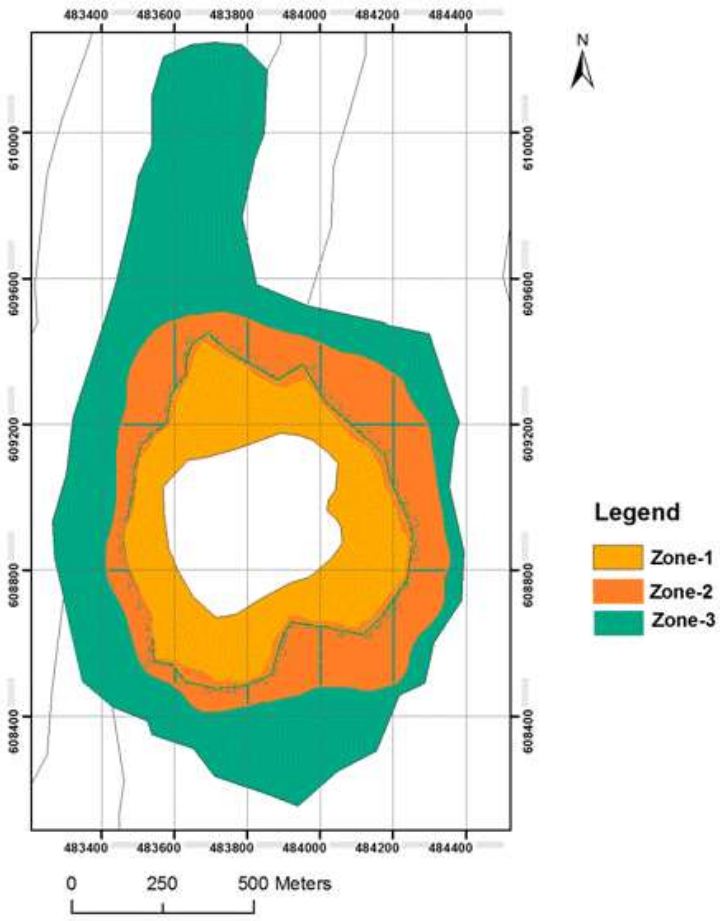


*Fig 6.1 Geological map of ore body morphology and zones*

This enrichment is related to residual enrichment. In this zone the mineralization found as disseminated patches. Associated magnetite and silica veins are also present. Webs of veins form box work pattern. The term stockwork is used to describe the style of mineralization. The garnierites are green to grey in color. The nickel concentration in this zone is 0.869 wt%. The boundary of this zone with the barren serpentinite is zigzag. The boundary of the zone with zone two is gradual and relatively flat. The thickness of the zone is narrow (between 10 – 15 meters). It is wider in the north western part where the topography is relatively flat. Towards the eastern part the zone is narrow covering only 10 meter. From ore petrographic studies thin magnetite

veins forms meshes of magnetite (Fig. 6.2b, c and d). These magnetite sometimes cross chromite grains.

(a)

(b)

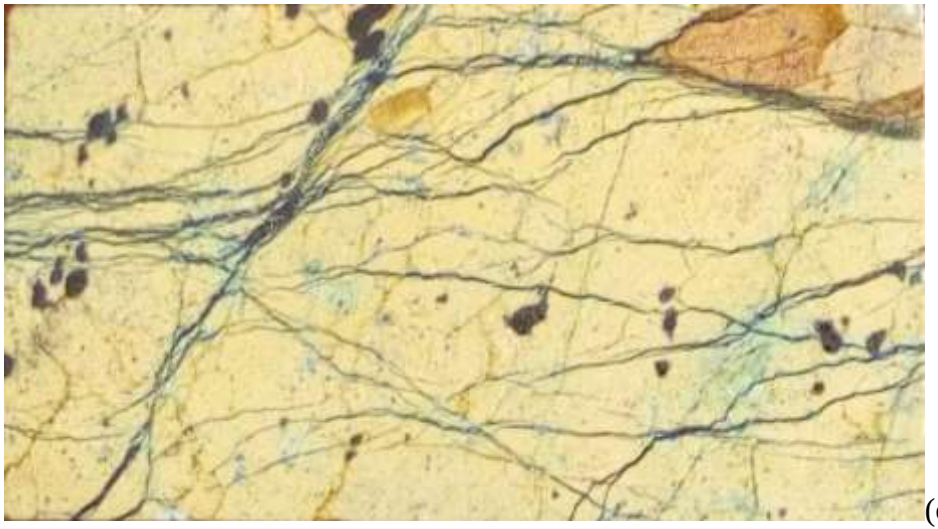

(c)

*Fig 6.2 field photographs and polished section showing; (a) ferric cap, (b) and (c); disseminated mineralization outcrop and(d) polished section showing disseminated garnierite mineralization and associated magnetite veins and chromite clusters (the longest dimension is 42 mm).*

### 6.1.2. Ore Zone two

This zone (fig 5.3 a) is the intermediate zone between the stockworked and veined ore body. The mineralization is found as coatings and disseminations (fig 6.3 b, c and d). The color of garnierites is deep green (fig. 6.3 d). The average nickel concentration that is calculated from samples is 3.12 wt %. The concentration is higher when there is a coating. Relatively the eastern slope is higher grade (3.96 wt. %) than the western (1.98 wt. %) and the northern slope (2.52 wt. %). This zone covers wider portion of the ore body. It is narrower in the west where veined type

mineralization covers the most. The boundary with both zone one and zone three is gradual. The presence and proportion of garnierite veins delineate the boundary between zone two and three.

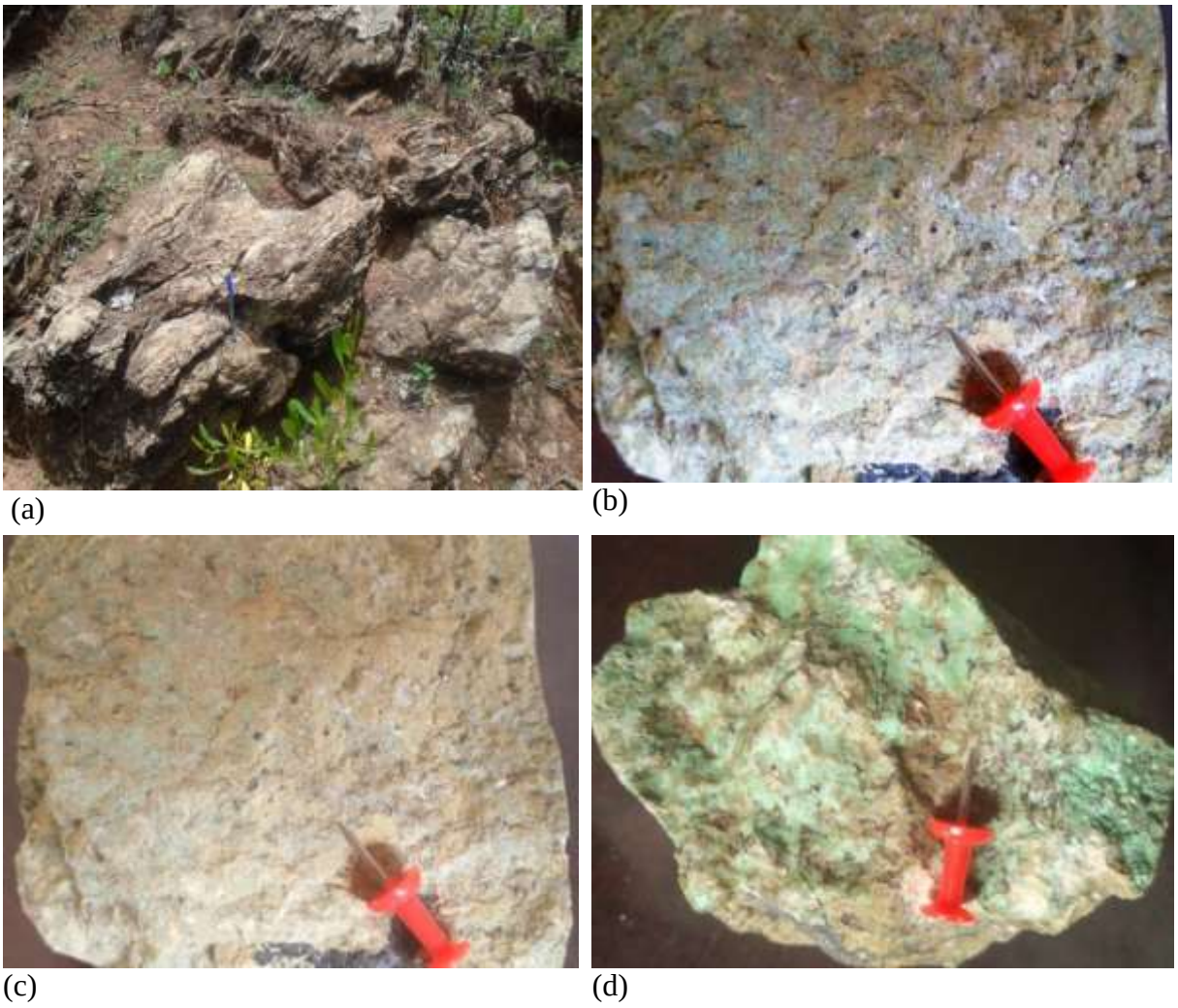


*Fig 6.3 field photograph and hand specimen photograph showing zone two garnierites: (a) field photograph, (b) and (c) hand specimen photograph of disseminated type and (d) coating type.*

### 6.1.3. Ore Zone three

Zone three is a zone in which both silica veins and garnierite veins (fig 6.4a and b) are intensively present. The color of garnierite veins is green while the silica veins are milky white. Analysis of silica veins (UNV-D5-1) showed that low nickel concentration. Since these silica veins are formed after the formation of host rock they crossed the host rock and garnierite veins. Veins show both box work, furrow and trihedron pattern. The grade is similar with zone two which is 3.12 wt %. It covers the portion between the country rock (talc tremolite schist) and zone two. Chromite grains are present (Fig 6.4 e). while magnetite veins are not present.

(a)

(b)

(c)

(d)

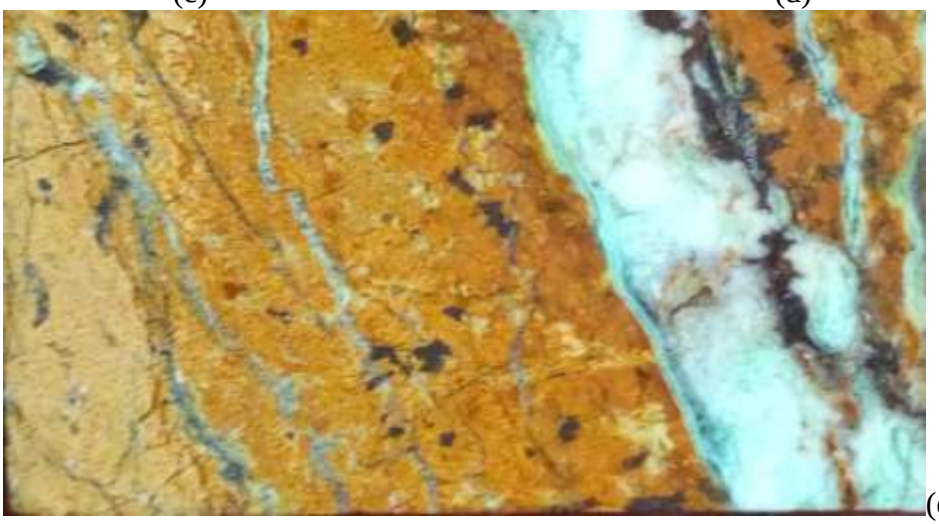

(e)

*Fig 6.4 field photographs, hand specimen and polished section photographs showing veined serpentinites specimens and outcrop*: *(a) specimen of garnierite vein, (b) disseminated mineralization, (c) and (d) are out crop photos in the northern part and western slope of the mineralization and (e) polished section photograph (the longest dimension is 42 mm).*

## 6.2.Mineralogy

### 6.2.1. Introduction

XRD pattern interpretations of serpentinite minerals (lizardite, antigorite and chrysotile) are done by different scholars (e.g. Brindly and Hang, 1973; Brindly and Maskimoic, 1974; Wicks and O' Hanely, 1988; Wells et al 2009 and Gail et al, 2012). All serpentinite minerals show peaks at 7.32 Å, 4.61 Å, 3.66 Å and 1.54 Å. These peaks are at 2θ values of 12, 19, 24 and 60 respectively. Discrimination of these minerals is done by Biittner and Saage (1982) as follows. Antigorite shows clear peak at 2θ 58.80 and 1.57 Å. Lizardite instead shows a peak at 61.50 2θ (1.57 Å). The dominant phases are identified based on specific peaks. These are chrysotile (d=2.45 Å), lizardite (d=2.51 Å) and antigorite (d=2.55 Å).

Garnierite show basal spacing at 7 Å and 10 Å. If they are serpentinite-like and talc – like respectively (Brindley and Hang, 1973). Pecorite and nepouite are two end members of serpentinites like garnierite. They show 7.36 Å and 7.31 Å low intensity peak respectively (Y. Song et al., 1995).In their classification, Villanova et al (2014) classified garnierite into five major classes based on XRD patterns and presented structural formulas (fig 6.5 and table 6.1).

| Type | XRD | Chemical formula |
|---|---|---|
| I | 7 Å | Mg1.73Ni1.37Fe0.03Si3.92O10(OH)2 |
| II | 7 Å and minor talc-like impurities 10 Å | Mg1.58Ni0.92Al0.05Fe0.03Si2.17O5(OH)4 |
| III | 7 + 10 Å | Ni1.79 Mg0.57Si2.31O5(OH)4·n(H2O) |
| IV | 10 Å | Mg1.56Ni1.53Si3.94O10(OH)2·(H2O) |
| V | 12 Å | Mg5.76Ni1.69Si12.22O15(OH)2·6(H2O) |

*Table 6.1 XRD basal spacing's and associated chemical formulas of garnierite's (Villanova et al (2014))*

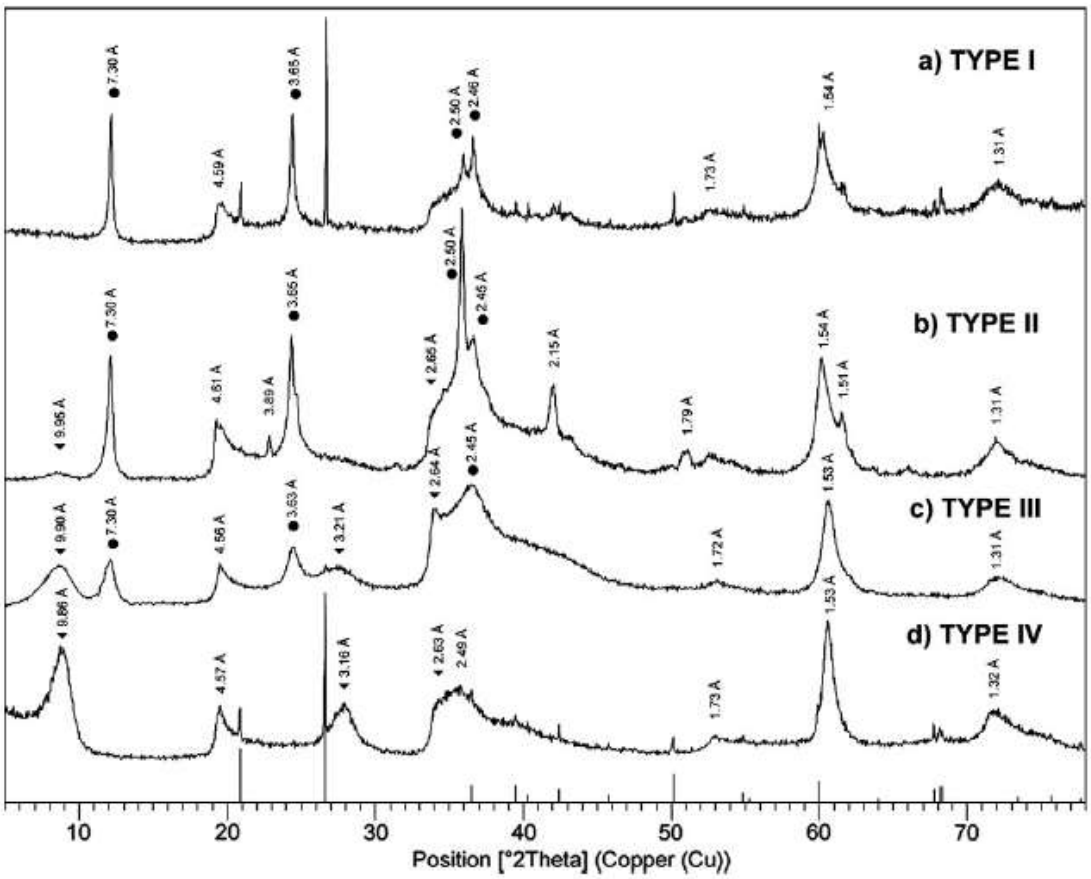


*Fig 6.5 XRD pattern of garnierite's (Villanova et al (2014))*

### 6.2.2. Mineral assemblage

The mineralogical composition of the host rock was characterized using thin section and XRD analysis. The samples collected from the ore zone are used to characterize the ore and gangue minerals. Under thin section investigations olivine and serpentine minerals are identified. Serpentine minerals show two kinds of textures. These are vein and acicular texture. Serpentine minerals identified by XRD (fig 6.6) include Antigorite ($H_{6.2}Mg_{48}O_{147}Si_{34}$) and lizardite ($Al_{0.22}Fe_{0.15}H_4Mg_{2.79}O_9Si_{1.84}$). Other silicate minerals detected are olivine and Talc ($H_2Mg_3O_{12}Si_4$). In proportion Antigorite takes the highest proportion 56.7%. This is followed by lizardite (24.3%), olivine (16.2%) and talc (2.8 %).

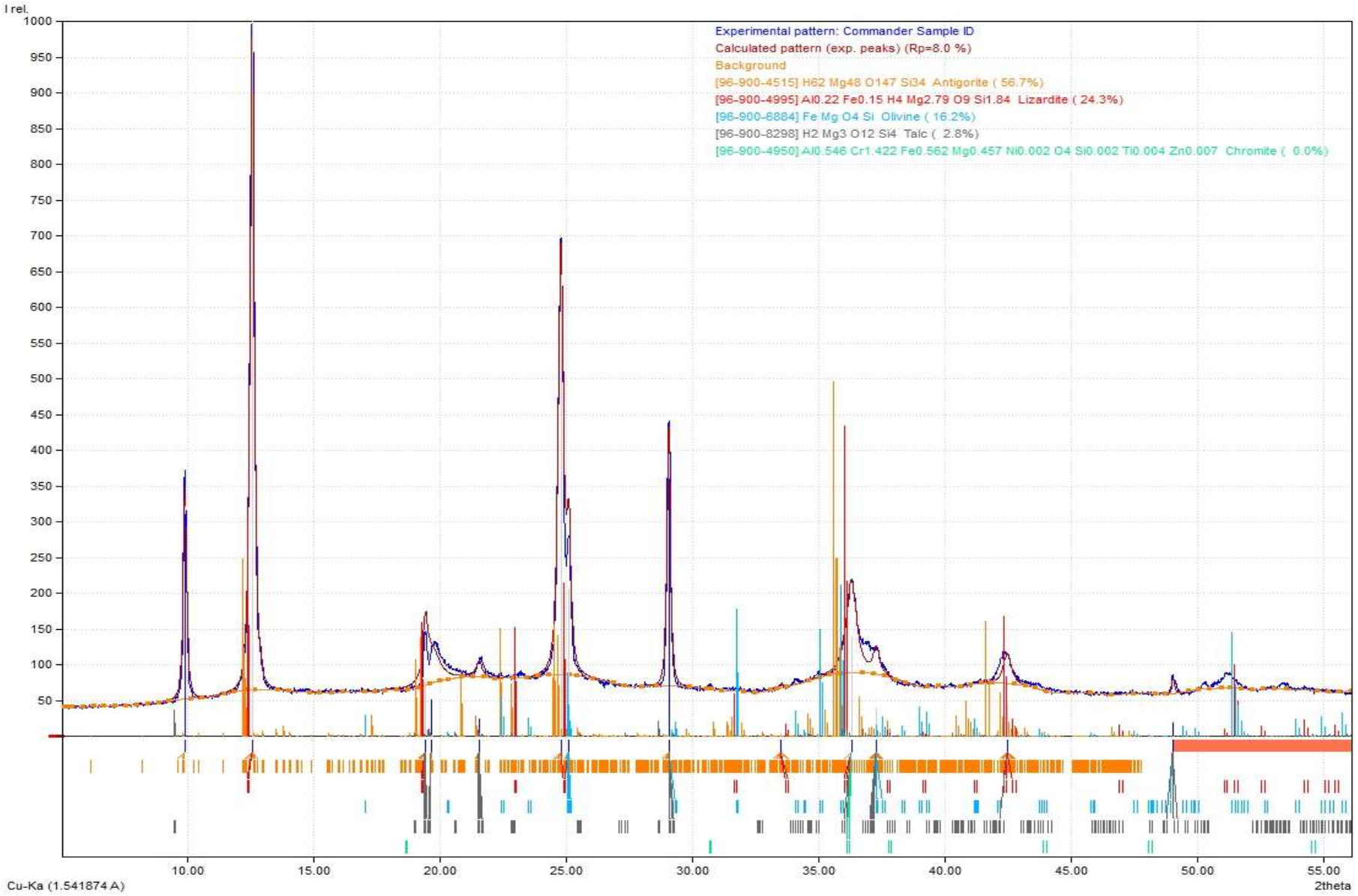


*Fig 6.6 XRD pattern of the host rock (GAR -02)*

The ore minerals identified are garnierite, chromite and magnetite. The gangue minerals are serpentine and talc minerals. Relict olivine crystals are always presents as a reddish spot. Garnierite can only be discriminated by XRD. Textural interpretation is made based on the inter relationship between the grains

**Chromite:** chromite minerals has higher reflectance than magnetite. Its color is milky white. The relief is lower than magnetite. The chromite grains are massive and euhedral (fig 6.7 a). These massive crystals are sometimes fractured and filled by magnetite veins (fig 6.7 b). Since magnetite infill's and replaces chromite. Chromite is older than magnetite. Based on petrographic investigation the modal proportion of chromites on the host rock ranges from 2 % to 15 % and 0 % - 2% in zone one and zone three respectively.

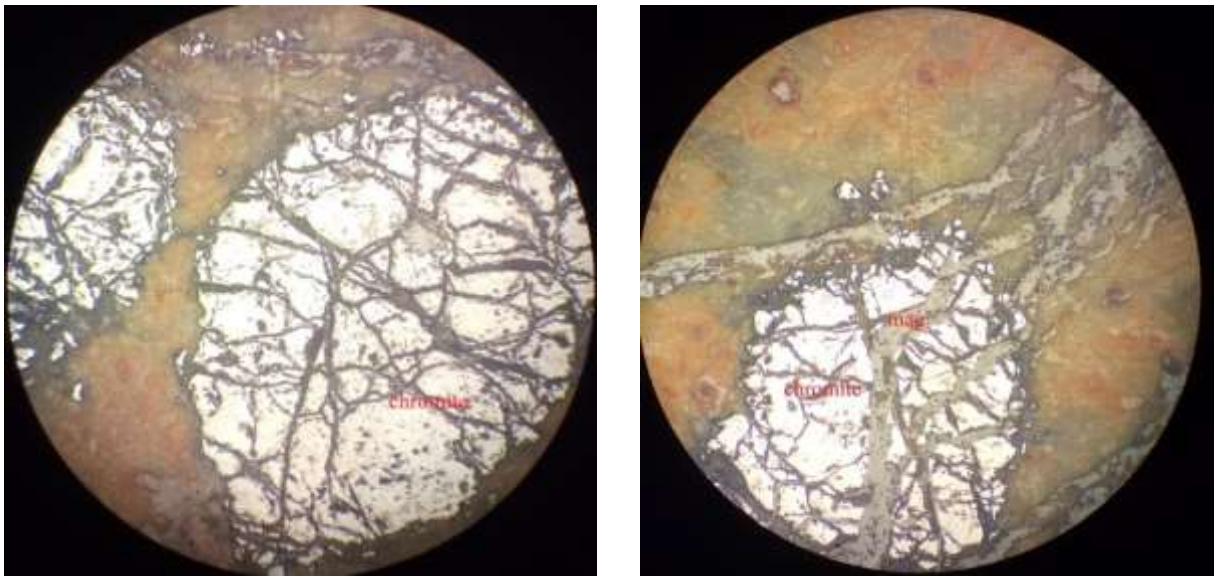


(a) (b)

*Fig 6.7 photo micrograph showing chromite grains and magnetite veins: (a) euhedral chromite grain and (b) magnetite veins crossing chromite (cross polar, 10X)*

Based on Match software interpretation (fig 6.6), the chemical composition of this chromite is $Al_{0.724}Cr_{1.152}Fe_{0.648}Mg_{0.431}$ $Mn_{0.007}Ni_{0.004}O_4$ $Ti_{0.022}$ $V_{0.012}$. Magnesium chromites ($CrMgO_4$) are observed in veins of garnierite.

**Magnetite:** Magnetite is gray low reflectance crystals (fig 6.8). Their relief is higher than chromite and gangue minerals. Magnetite is found as vein fillings and discrete grains. Meshes of magnetite are also common. These meshes are merged and form massive veins. This mineralization is confined to zone one and zone three of the ore body. Based on petrographic

investigation the modal proportion of magnetite in the ore zone ranges from 3 % to 5 % and 0 % - 3 % in zone one and zone three respectively.

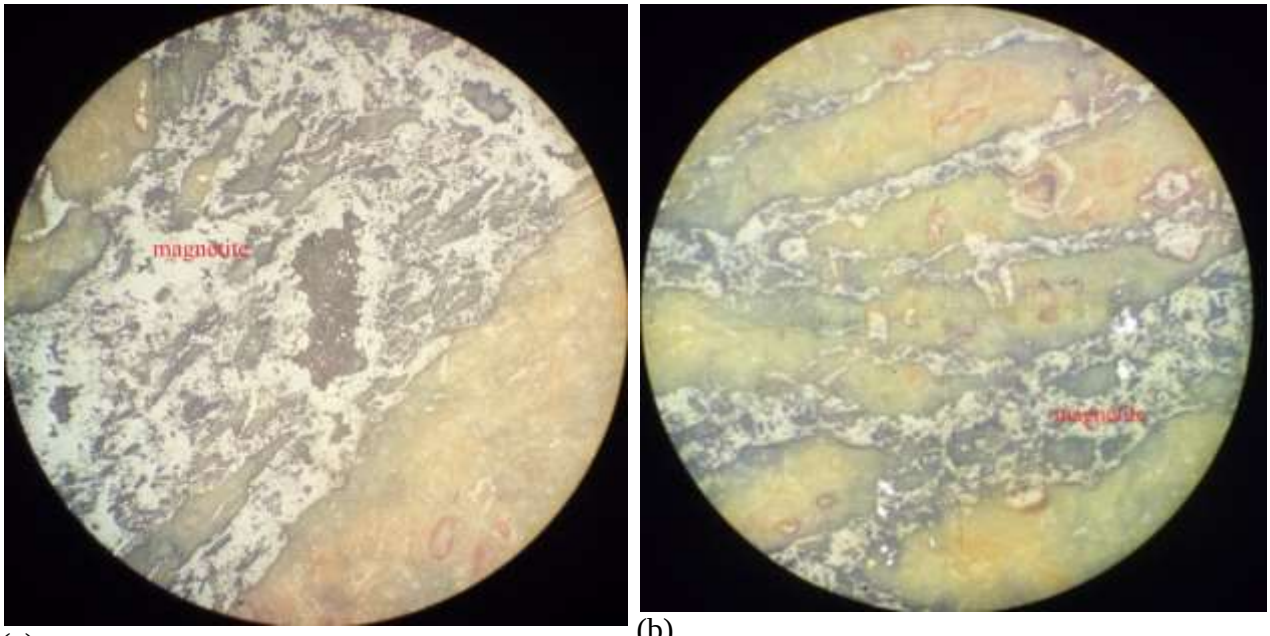


(a) (b)

*Fig. 6.8 photomicrographs showing vein and meshes of magnetite within the garnierite*

**Garnierite**: garnierite is common name used for nickel bearing silicate minerals. These nickel silicates are an aggregate of many elements. Mostly the primary constituents are Si, Mg and Ni. It is not possible to be discriminate garnierites by both transmitted light and reflected light petrography. Therefore XRD interpretations are used for phase identifications. Four types of garnierites and garnierite vein is analyzed by XRD. This garnierites are taken from the oxide part, upper saprolite part with silica veins, middle saprolite part without silica, lower saprolite disseminated mineralization and lower saprolite veined part of the lateritic profile. The results of the analysis of these parts are presented on fig 6.9 a- e respectively. Fig 6.9 a is a XRD pattern of garnierite containing tints of garnierite and veins of magnetite (GAR-03). Fig 6.9 b is a garnierite containing the disseminated mineralization with silicification (GAR-04). Fig 6.9 c is a XRD pattern of garnierite found as disseminated type without magnetite and quartz veins (GAR-06). Fig 6.9 d is a plot of garnierite found as silicified dissemination on the lower saprolite zone (GAR-05). Fig 6.9 e is a garnierite found as a discrete vein (GAR-01).

The mineral phase identified and the chemical formula is variable. Yellowish mottled magnetite vein containing garnierites (fig 6.2 b and fig 6.9 a) shows mineral phases of The associated

phases identified are Antigorite ($H_{58}Mg_{45}O_{138}Si_{32}$), quartz (12.7%), chromite (4.2%), talc 2M ($Mg_3O_{12}Si_4$) (2.5%) olivine ($MgNiO_4Si$) (1.5%) and magnetite (0.7%). The nickel in this garnierites found as $Ni_2Si$ (0.2%), $Ni_2Si$ $Ni_2Si$ (0.3 %), $Ni_2O_4Si$ (1.2%) (fig 6.9 a).

The second is garnierite found in transition zone of oxide zone and saprolite zone (fig 6.2a and fig 6.9 b). The analysis of this garnierite resulted talc ($H_2Mg_3O_{12}Si_4$) (47.7 %), antigorite - T ($Mg_{48}O_{147}Si_{34}$) (37.9%), Lizardite – 1T ($H_6Mg_3O9Si_2$), $N_2Si$ (5.0%), $Ni_2Si$ (5.0%) and NiSi NiSi (0.2%). The third is disseminated garnierite found in middle part of the saprolite zone. This garnierite didn't contain silica and magnetite veins (fig 6.2 a and fig 6.9 c). The analysis showed that talc ($H_2Mg_3O_{12}Si_4$)(88.2%) and $Al_{3.8}Si_{32.2}O_{72}$)($H_2O$)0.68(11.8%).

The fourth garnierite is coated garnierite in lower saprolite (fig 6.4 b and fig 6.9 d). The analysis shows talc ($H_2Mg_3O_{12}Si_4$) (52.1%), antigorite ($H_{58}Mg_{45}O_{13}Si_{32}$) (27.6%), Lizardite ($Al_{0.22}Fe_{0.15}H4Mg_{2.79}O_9Si_{1.84}$)(14.2%), $NiSi_2$ $NiSi_2$ (4.0%) and $Ni_2Si_2$ $Ni_2Si_2$ (2.1%). The last sample is analyzed from the bottom of the lateritie profile (fig 6.4 a and fig 6.9 e). the chemistry of this garnierite is talc ($H_2Mg_3O_{12}Si_4$) (79.9%), chlorite ($Al_2Cr_{0.2}Fe_{0.1}H_{79}Mg_9O_{18}$) (3.2%), $NiSi_2$ $NiSi_2$ (1.2%), Magnesium chromite ($CrMgO_4$) (1.0%) and $Ni_2Si$ (0.1%).

### 6.2.3. Mineral paragenesis

Paragenesis is timewise relationship between the mineral assemblages. Fig 6.10 presents paragentic sequences of ore and gangue minerals. Relict olivine grains are the first mineral to be crystallized from the magma.

Mineralogy of the ore can be summarized as talc-like and serpentinite like ore minerals. These minerals are willmesite and Kerolite- pimmilite. In terms of distribution willmesite covers the largest proportion. On the garnierite veins only talc- like phase is detected. On the outer zone also the talc-like phases are dominant. The proportion of talc from the internal zone to the rim increases. Talc is formed from serpentine minerals during alteration. Observing the dominant phases from the internal zone to the outer the paragentic sequences is adopted. Antigorite, olivine, chromite and lizardite are contemporary. These are the initial phases followed by magnetite, willmesite and kerolite. Finally lizardite - nepouite series is formed

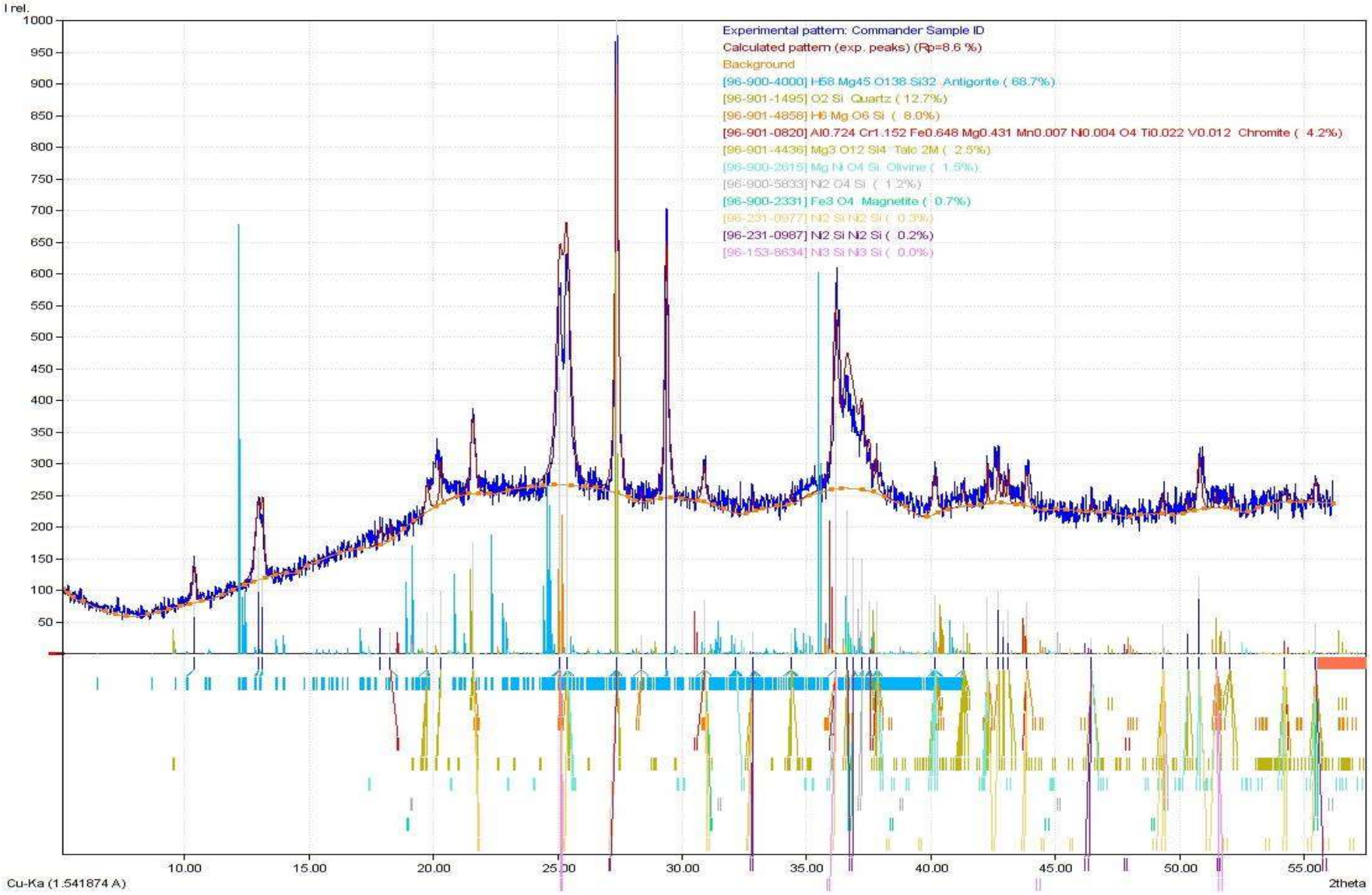


*Fig 6.9 a XRD pattern garnierite containing tints of garnierite and veins of magnetite (GAR-03)*

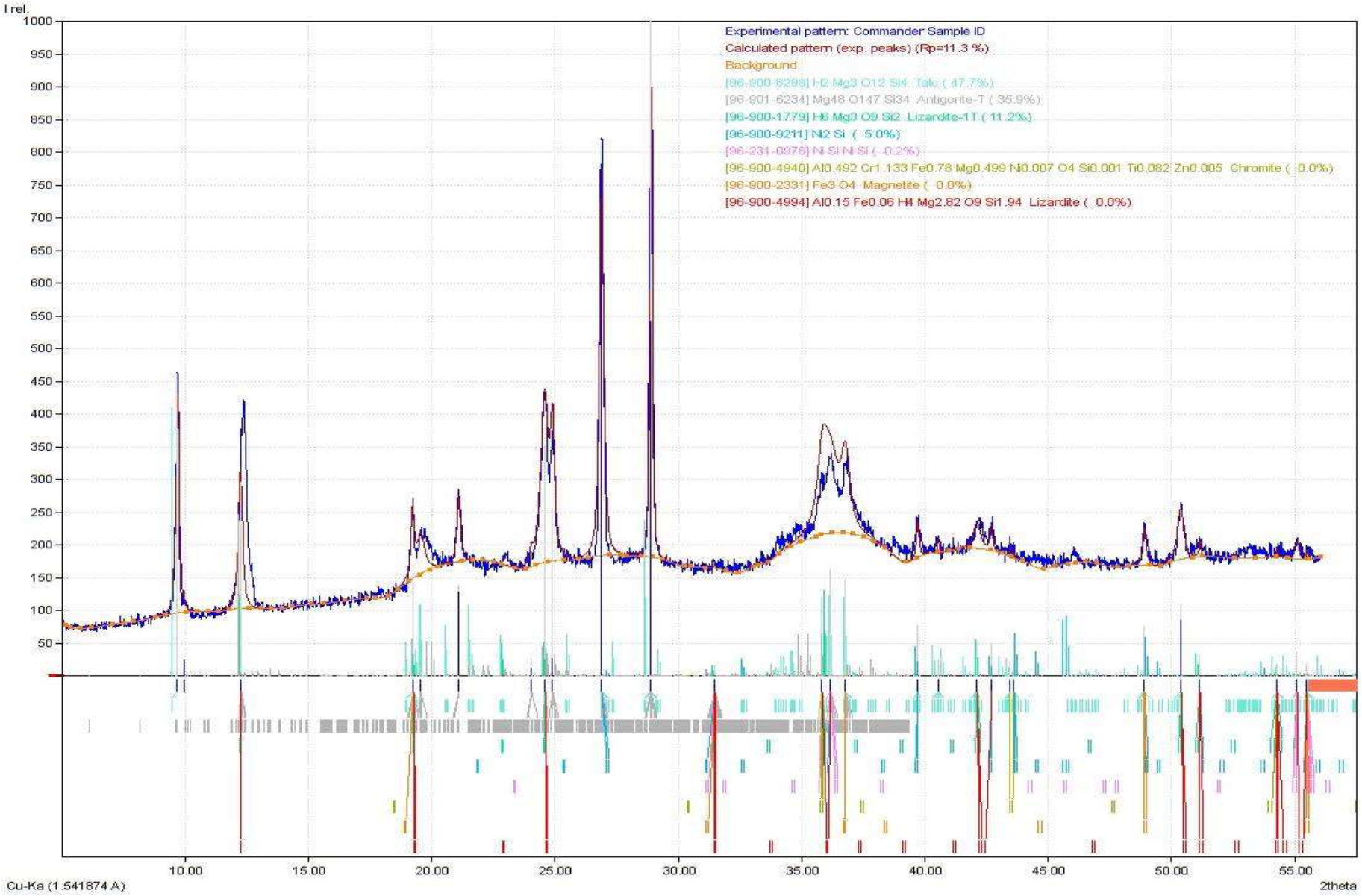


*Fig 6.9 b XRD pattern of garnierite containing the disseminated mineralization with silicification (GAR-04)*

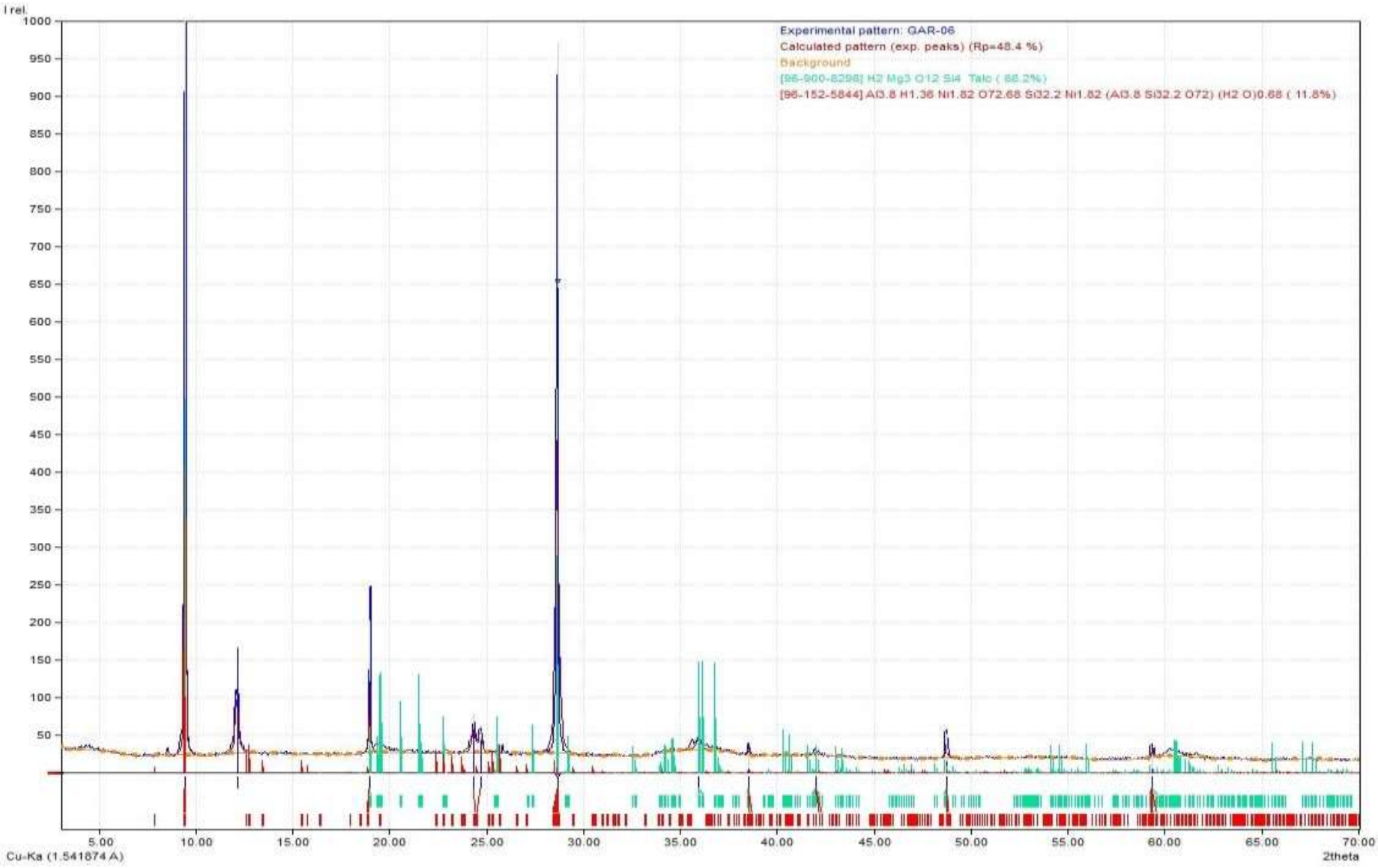


*Fig 6.9 c is a XRD pattern of garnierite found as disseminated type without magnetite and quartz veins (GAR-06)*

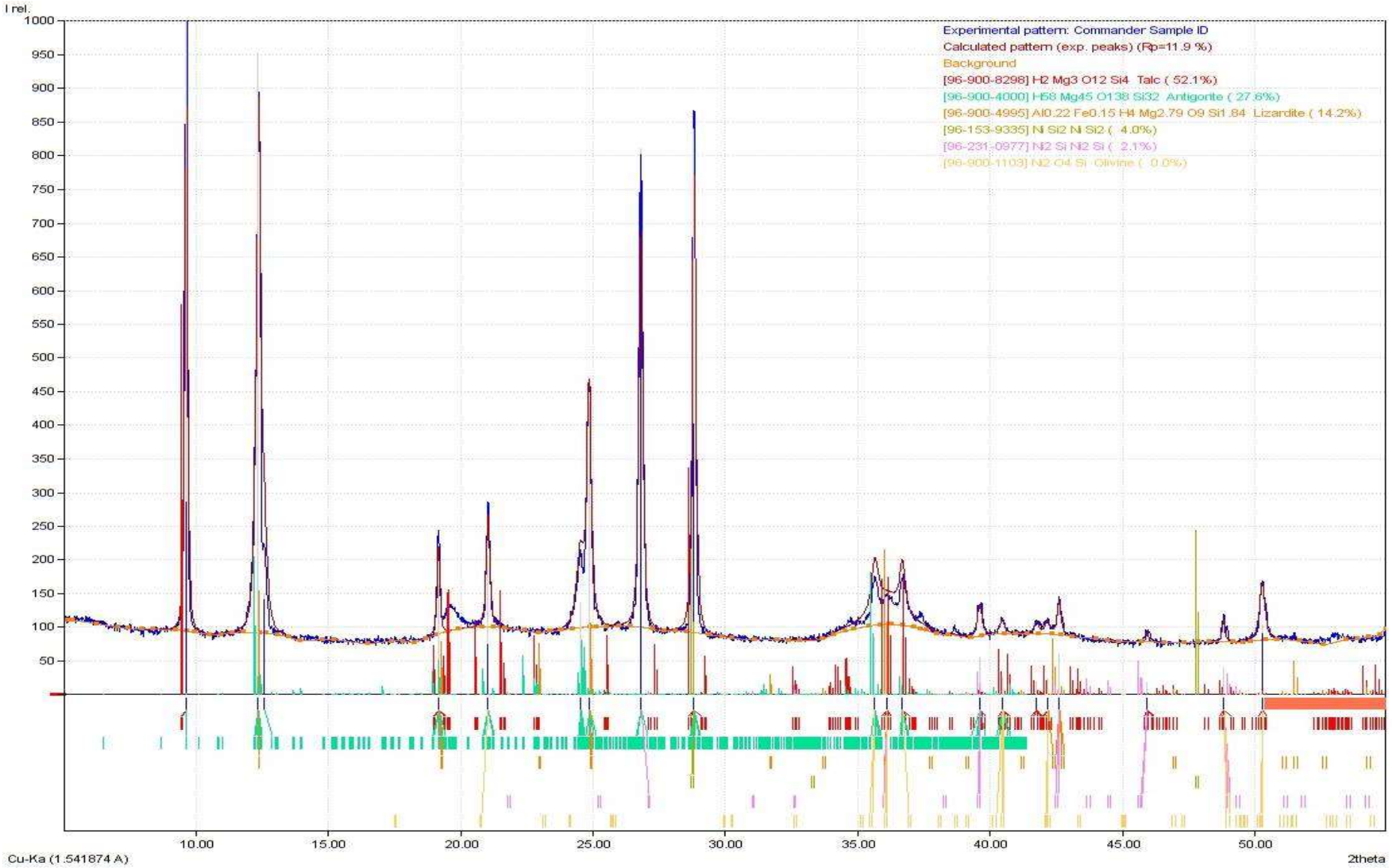


*Fig 6.9 d XRD plot of garnierite found as coating on the lower saprolite zone (GAR-05)*

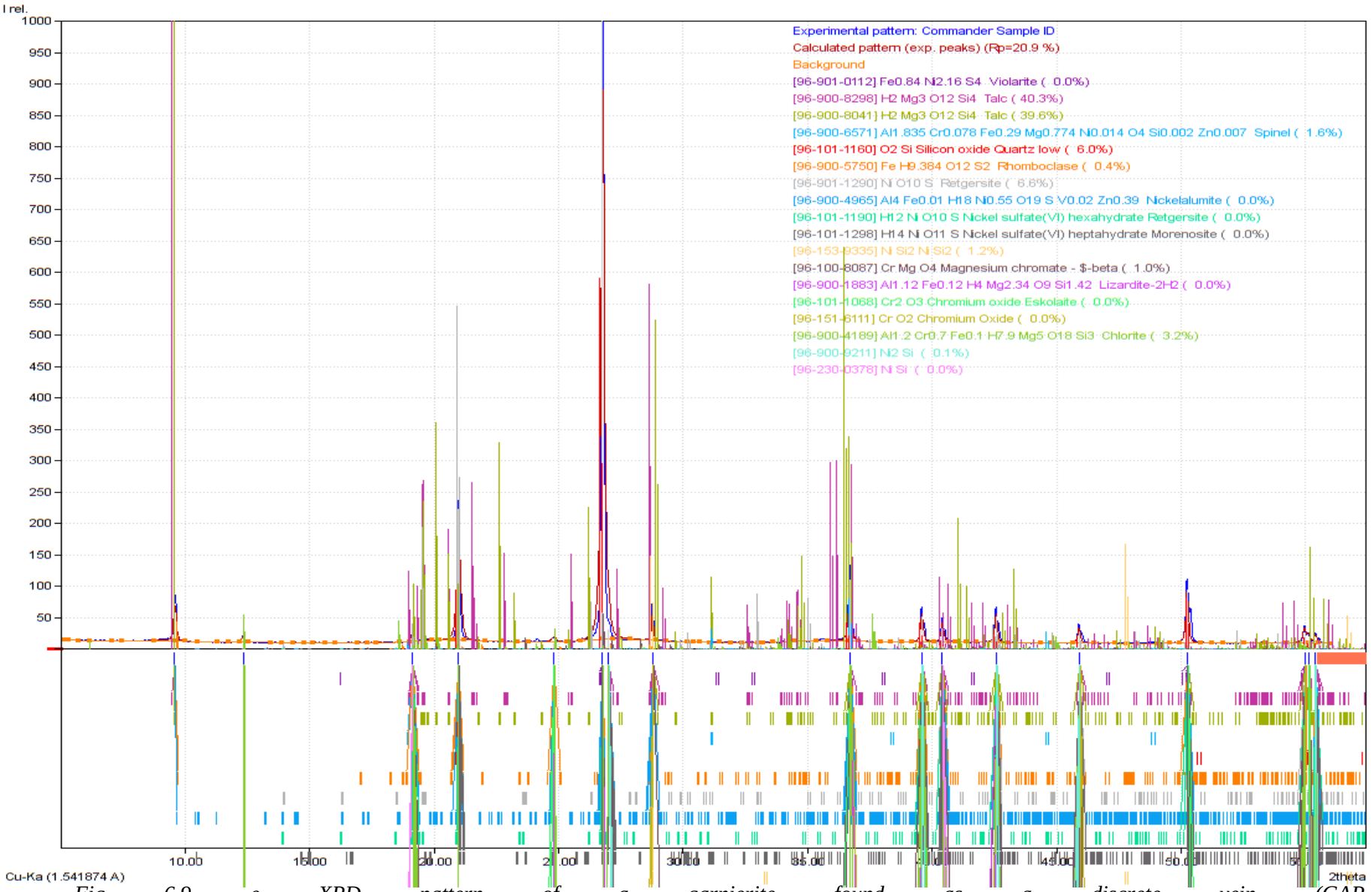


*Fig 6.9 e XRD pattern of a garnierite found as a discrete vein (GAR-01)*

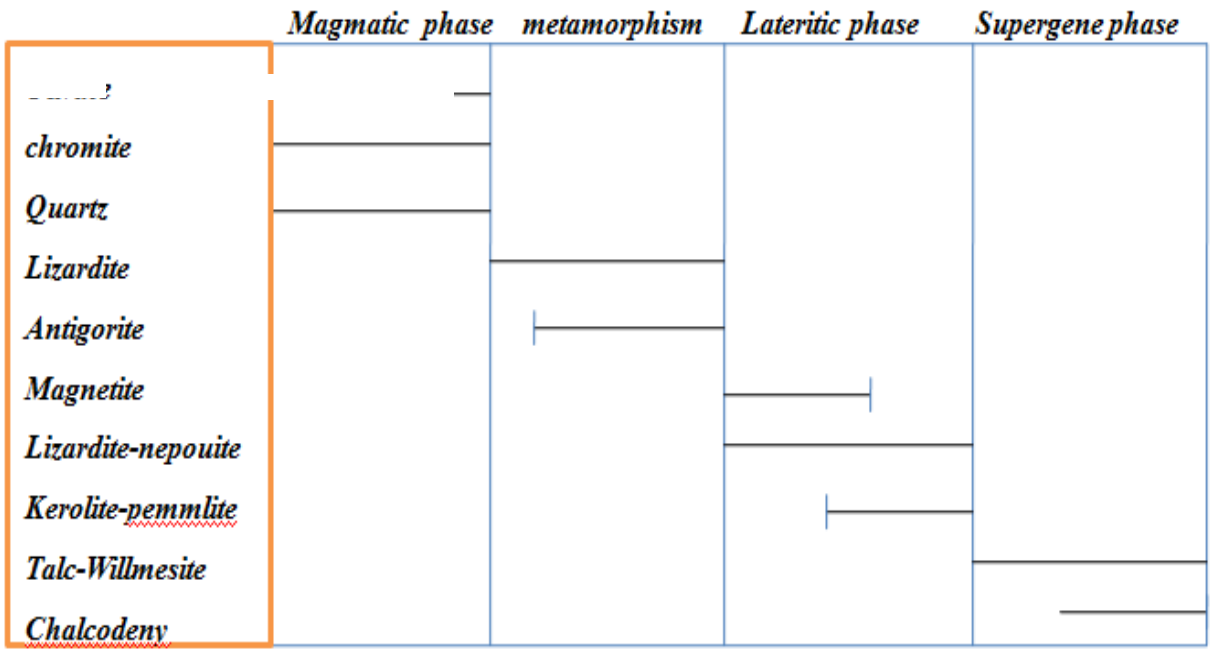


*Fig 6.10 paragentic sequence of the ore and gangue mineral of the deposit*

Textural interpretation are made base on the ore petrography. Colloform texture (fig 6.11a and b) is observed on the garnierite veins. Worm like grains is contained within this garnierite veins. The color of this worm like grains is green. Gangue minerals surrounded these grains.

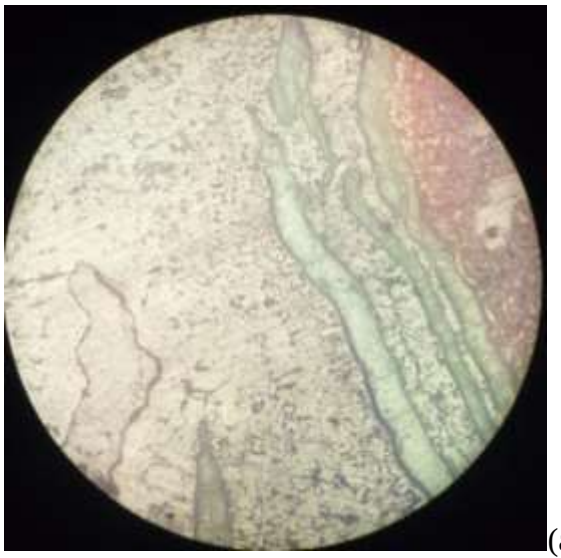
(a)
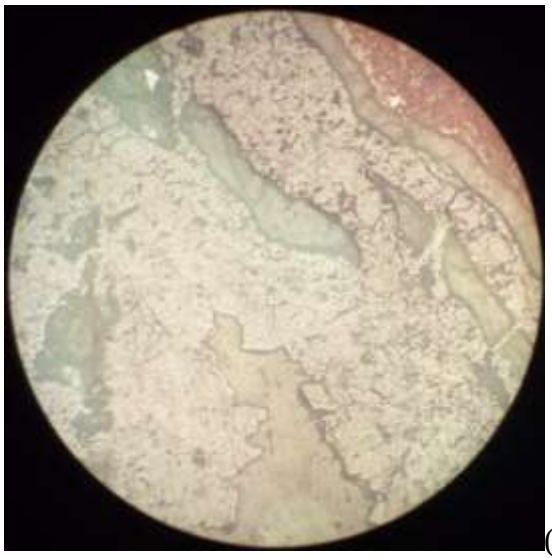
(b)

*Fig 6.11 Colloform textures of the garnierite mineralization*

### 6.3. Resource estimation

In order to calculate the resources in the area, thickness and density of the host rock is required. The deposit is classified in to two polygons as shown in fig 6.12. The first polygon, area 1, is designated for zone one while the other polygon, area 2, is used for zone two and zone three. Area 1 is 180,000 $m^2$ and Area 2 is 946,000 $m^2$. The density of the ore body is taken to be that of the density of serpentinite which is 2.6 $g/cm^3$.

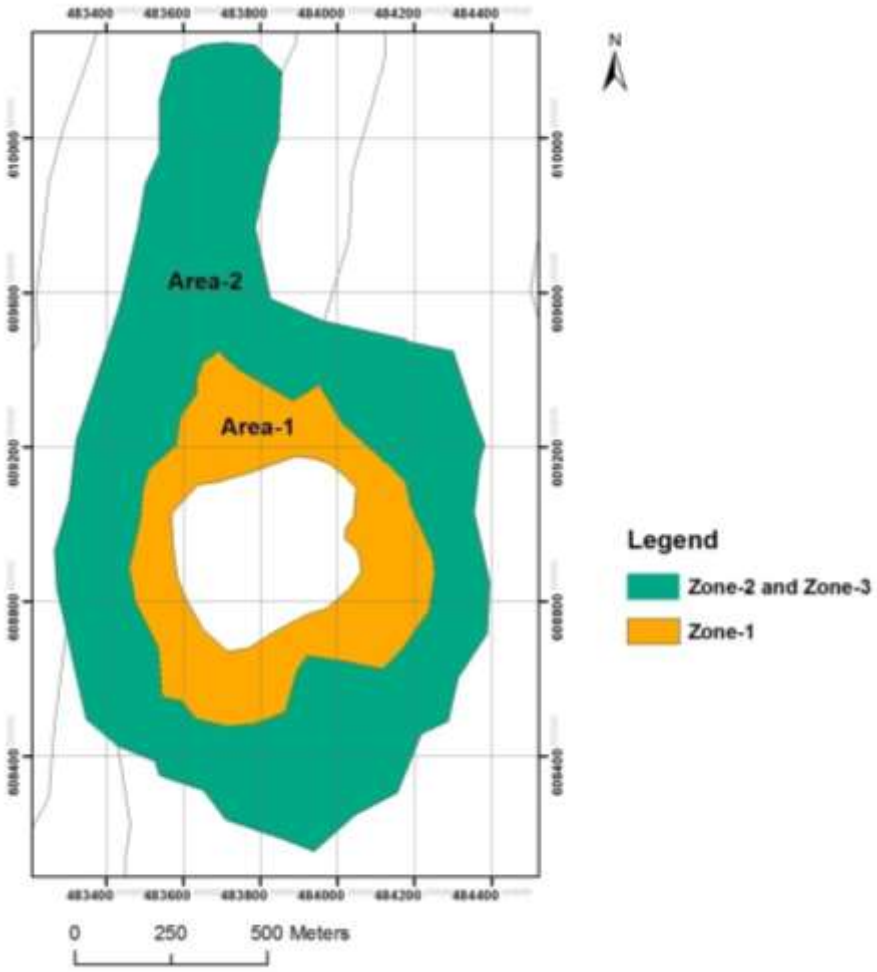


*Fig 6.12 ore body blocks of the deposit*

Therefore the tonnage is calculated as follows:

Tonnage 1 = area 1* depth * density
= 180000$m^2$ * 5.93 m* 2.6 $g/cm^3$
= 2,775,240 ton

Tonnage 2 = area 2* depth * density
= 946000$m^2$ * 5.93 m * 2.6 $g/cm^3$
= 1,4585,428 ton

Reserve is estimated based on the grade of the ore deposit. Two groups are identified based on assay results. The grade of zone one is 1.848 wt% while the grade of zone two and three is 2.02 w%. Therefore reserves are:

| ore bodies | tonnage (ton) | Grade (wt. %) | Metal (Nickel) (Kg) |
|---|---|---|---|
| **block 1** | 2775240 | 1.848 | 51286.4 |
| **block 1** | 14585428 | 2.02 | 294626 |

To estimate the resource and reserve simple computation based on field observation and area calculation using ArcGIS is done. The amounts of samples collected are small (8 samples). Therefore the level of confidence is small and the resource classified as inferred resource (fig 6.13).

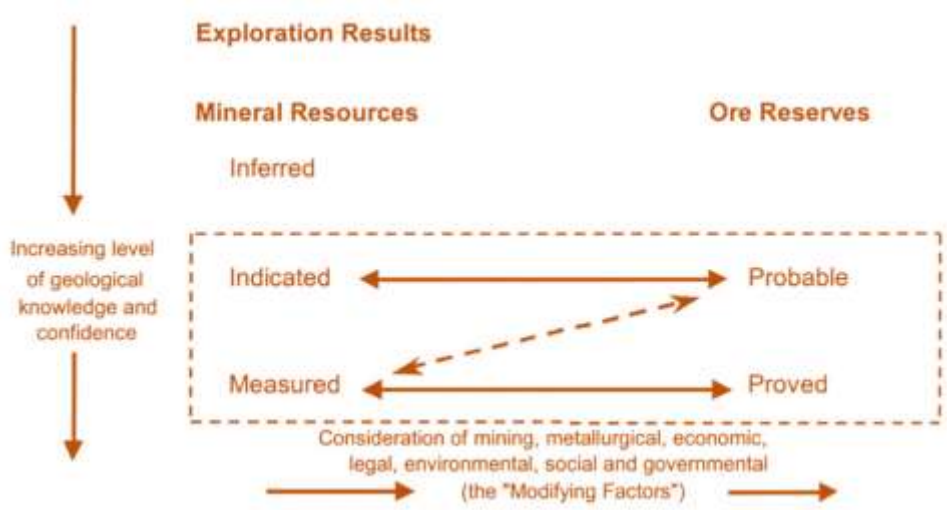


*Fig 6.13 JORC resource and reserve classification (JORC, 2012)*

Valicu and Yehwalwork (1967) calculated the reserve of mineralization. The calculation is done to cross checks previous exploration working in Ula Ulo and other serpentinite occurrences of adola belt. The calculation is done by Polygon method. The overburden is 1 meter. The maximum depth of the mineralization is 5.93 meter. The minimum and average Ni tenore are 0.82 and 1.60 % respectively. Classification of the resource is done as tenor > 0.5 % and > 0.82 % (fig. 4.12). They estimated the resources as 2,973,981 ton and 47,730 Ni metal. The calculation is done based on 50*50 M interval and the resource is inferred.

# Chapter- VII

# Discussion

## 7.1. Garnierites of Ula Ulo nickel deposit

Ula Ulo serpentinite hosted nickel deposit is zoned in to three zones as discussed on section 6.1. These ore zones show distinction in terms of the garnierite type. Zone one found as the top layer of the lateritic profile followed by zone two and finally zone three. Based on the XRD interpretation using Match software the following interpretations are made for garnierites those are found in three zones separately.

**Zone one garnierite:** the garnierite in these zone found as $Ni_2Si$ (0.2%), $Ni_2Si$ $Ni_2Si$ (0.3 %), $Ni_2O_4Si$ (1.2%). The associated phases identified are Antigorite ($H_{58}Mg_{45}O_{138}Si_{32}$), quartz (12.7%), chromite (4.2%), talc 2M ($Mg_3O_{12}Si_4$) (2.5%) olivine ($MgNiO_4Si$) (1.5%) and magnetite (0.7%). The ore mineralogy can be summarized as talc and serpentine like garnierite. This is because both phases are identified. According to Villanova et al (2014) these garnierite are type – III garnierites (table 6.1 and fig 6.5). These garnierites are the aggregate of talc like and serpentine like garnierite. Nickel containing antigorite are not encountered in well-known deposits (Brindley and Maksimovic, 1974). Therefore the ore minerals are dominantly talc-like with small serpentine. These ore minerals are generalized as kerolite (Brindley and Hang, 1973). But according to Brindley and Maksimovic (1974) the ore mineral end members are talc - willmesite and kerolite – pimmilite. These minerals show a basal spacing both at 7 and 10 angstrom (fig 6.9 a and b). The XRD plots shows ragged vibrating graph which is related to low crystalline nature of the garnierite.

**Zone two garnierite:** garnierite in this zone (fig 6.9 c and d) is found as dissemination and coating. Both types are investigated separately. The dissemination type is covering the larger proportion. In this zone the mineral phases detected are (35.9 %) antigorite ($Mg_{48}O_{147}Si_{34}$), quartz (11.2 %), lizardite ($H_6Mg_3O_9Si_2$), (47.7) talc ($H_2Mg_3O_{12}Si_4$), (5.0 %) $Ni_2S$ and (0.2 %) NiSi. The mineralization is found as nickel silicate. The garnierite type is talc-like and serpentine-like. According to Villanova et al (2014) these garnierite are type – III (table 6.1 and fig 6.5). Talc-like and serpentinite-like garnierites are discriminated by Brandley and

Maksimovic (1974). Talc-like garnierite is willmesite. Serpentinte-like garnierite is lizardite - nepouite. The concentration of talc in the host rock is only 2.8 %. The current concentration indicates the presence of recrystallization of serpentine minerals to talc during weathering and precipitation.

**Zone three garnierite:** in this zone the mineralization is found as a vein and dissemination. In the vein (fig 6.9 e) talc and multi element nickel enrichment is found. The chemical formulas are $H_2Mg_3O_{12}Si_4$ and $Al_{3.8}H_{1.36}Ni_{1.82}\,O_{72.68}\,Si_{32.2}\,Ni_{1.82(}Al_{3.8}\,Si_{32.2}O_{72)}\,(H_2O)_{0.68}$ respectively . The type of garnierite found in the vein is only talc like (fig 6.9 e). According to Villanova et al (2014) this garnierite is type – IV garnierite (table 6.1 and fig 6.5). Therefore the ore mineral is willmesite (Brandily and Maksimvoc, 1974). It shows one prominent basal spacing (peak) at 10 angstrom. The phases found in the disseminated part (fig 6.9 c) are talc, antigorite, lizardite, $Ni_2Si$ and $NiSi_2$. Talc is the dominant phase 52.1%. This is followed by antigorite (27.6 %) and lizardite (14.2%). The mineralization is 4 % $NiSi_2$ and 2 % $Ni_2Si$. The ore mineral end members are talc - willmesite and kerolite – pimmilite.

### 7.2. Genesis of the Ula Ulo nickel deposit

In Adola greenstone belt there are several occurrences of serpentinites. Some of these serpentinite bodies are nickelfirous. Ula Ulo is one of these nickel serpentinite bodies. The concentration of nickel in primary protolith rock defines the development of lateritic supergene mineralization. A study by Jelenc (1964) stated that the development of nickel mineralization in Ula Ulo, kilta and Tulla is the result of development of residual soil. Based on the present study the genesis of Ula Ulo nickel deposit is explained as follows.

Mineral deposits are formed by the interaction of more than one type of ore forming processes. Through these processes a given mineral occurrences is enhanced to a level of economically exploitable mineral deposit. The concentration of nickel in Ula Ulo fresh and altered (silicified) serpentinites is 2643 ppm and 1.38 – 3.57 % respectively. Background and threshold concentration of nickel in Adola region is 15 – 25 ppm and 100 ppm respectively (Kozyrev et al. 1985). The enrichment of nickel from fresh serpentinites (2643ppm) to silicified and altered serpentinites (3.57 %) is done by surficial process. While enrichment of Ni in fresh serpentinites above the background and threshold of adola serpentinites is related to the magmatic processes.

Magmatic process can create a variation on a concentration of certain metal based on the source of magmas. A magma that forms Ula Ulo serpentinites is high Mg ultramafic magma possibly originated from partial melting of mantle. Elemental abundance nickel in mantle is $4.56 \times 10^3$ which higher than oceanic crust ($2.79 \times 10^2$) and continental crust ($5.29 \times 10^1$) ((Taylor, 1982 cited from Brownlow (1996)). Hence a magma that is formed by partial melting of mantle has higher nickel concentration than magma originated from reworked oceanic crust and continental crust. When this magma crystallizes it forms ultramafic rocks. This ultramafic rocks contains higher proportion Mg – containing minerals. These are olivine and pyroxene. In these ultramafic rocks and mafic minerals nickel and magnesium found as Mg-Ni solid solutions (Rosell et al., 2015). Therefore, olivine (foresterite) and serpentinites can hold Ni concentration up to 0.4 % Ni (Lelong et al., 1976; Butt and Nickel, 1981; Elias, 2006; Thorne et al., 2009, 2012b; Wells et al., 2009 cited from Salah (2014)). From this instance it is clear that the anomalous Ni concentration in Ula Ulo serpentinites is due to Mg – Ni solid solution. While the important factor for the presence of this solution is the concentration of nickel in the primary magma.

Through petrographic and mineralogical investigations it is observed that the ore minerals and mineral assemblage of Ula Ulo nickel deposit are not related to magmatic nickel sulfide deposit. Because, rock forming and ore minerals found in the host rock and mineralized portion are antigorite, lizardite, talc, nepouite, pimmilite and willmesite. Instead they are garnierite (Brindly and Hang, 1973; Brindly and Maskimoic, 1974; Wicks and O' Hanely, 1988; Wells et al 2009 and Gail et al, 2012).

Garnierites are hydrous magnesium silicates which are formed by weathering and chemical precipitation of ultramafic rocks (Brindley and Hang, 1973; Brindley and Maskimoic, 1974; Springer, 1974; Springer, 1974; Brindley, 1978; Wicks and O' Hanely, 1988, Villanova-de-Benavent et al., 2014). New Caledonia and flacondo are two interesting examples of lateritic nickel deposits (Villanova-de- Benavent et al., 2014). The host rocks and the ore minerals of the deposits are serpentinites and garnierites which are similar to Ula Ulo lateritic nickel deposit.

The genesis of Falcondo lateritic nickel deposit in Dominican Republic is similar to Ula Ulo. Its genesis is summarized by Rosell et al. (2015). The deposit is formed by weathering of serpentinites. During weathering of the serpentinites nickel accumulated on the residual

weathering medium. This nickel in the residual limonitic zone is percolated down to the saprolite zone and precipitated as garnierites and nickel rich serpentinites (Rosell et al. (2015). The ore minerals of Flacondo garnierite mineralization are lizardite – nepouite, chrysotile-pecorite, kerolite – pimmilite and sepiolite-flacondite (Rosell et al., 2015).

The protor materials of the deposit are serpentinites which are currently hosting the mineralization. These serpentinites are exposed to the surface and subjected to weathering. This weathering disintegrates the host rocks and released Ni to the top part of the ridge. As observed during chemical analysis the top part of the ridge is barren from nickel mineralization. From field observation the possible cause for this is hypothesized. This is the lateritic profile developed on top part of the ridge is eroded away and the barren bed rock is exposed. This bed rock is similar to the bed rock that we get below the saprolite zone of the mineralized part of the ridge.

The first zone is where limonitic goethite, residual chromite and ferric cap are present. Oxides of this zone show enrichment of FeO (+2.1 %), $Al_2O_3$ (+0.34%) and $CrO_2$ (+0.3).The associated phases identified are Antigorite ($H_{58}Mg_{45}O_{138}Si_{32}$), quartz (12.7%), chromite (4.2%), talc 2M ($Mg_3O_{12}Si_4$) (2.5%) olivine ($MgNiO_4Si$) (1.5%) and magnetite (0.7%). The ore mineral found as Ni – Si and Ni – $O_4$- Si. Both are nickel silicates found as exsolution in olivine and serpentinites (Maynard, 1983). Nickel silicates are talc and serpentinite like garnierites. The ore minerals identified are kerolite (Brindley and Hang, 1973) or talc - willmesite and kerolite – pimmilite (Brindley and Maksimovic, 1974). Based on Villanova et al (2014) these garnierite are type – III. These type III garnierites have an equal proportion of talc like and serpentine like garnierites.

Zone two and three found bellow the residual zone and characterized by garnierite veins, disseminated garnierite patches and quartz coating. During field observations some physical variations are observed between zone two and zone three garnierites. But, Different literatures showed that these two zones are assumed as a single zone saprolite zone (Wei Fu et al., 2014; Ougra, 1977; Eliopoulos, 2014). Saprolite zone contains mainly nickel silicates (Rosell et al., 2015). Similarly in Ula Ulo the saprolite zone considered as a single zone. The mineral phases identified from the garnieritized serpentinite are antigorite ($Mg_{48}O_{147}Si_{34}$), (11.2 %), lizardite ($H_6Mg_3O_9Si_2$), (47.7) talc ($H_2Mg_3O_{12}Si_4$), (5.0 %) $Ni_2S$ and (0.2 %) NiSi while in the garnierite veins $H_2Mg_3O_{12}Si_4$ and $Al_{3.8}H_{1.36}Ni_{1.82}\ O_{72.68}\ Si_{32.2}\ Ni_{1.82}\ (Al_{3.8}\ Si_{32.2}O_{72})\ (H_2O)_{0.68}$ are found. One clear difference with the zone one is the nickel mineralogy in this saprolite is only Ni-Si. This

indicates the mineralization found in this zone is only as hydrous nickel silicate (Maynard, 1983). The other point is only talc like garnierites are observed in garnierite veins. The ore minerals of the saprolite zone of Ula Ulo deposit are both talc –like and serpentine like garnierites. While the garnierites veins are only talc-like. According to Villanova et al (2014) saprolite garnierites and vein garnierites are type – III and type- IV respectively. This means saprolite garnierite are both talc like and serpentine like garnierite (Type-III) while in the garnierite veins are only talk garnierite (Type – IV).Their corresponding ore minerals are lizardite – nepouite and willmesite respectively (Brandily and Maksimvoc, 1974). .

The studies of garnierites in New Caledonia (Dublet et al., 2012) mentioned about the precipitation of nickel in the limonitic oxide zone and saprolite zone. From the study, nickel is precipitated on the limonitic zone as Fe- Ni solid solution whereas in the saprolite zone as cluster of separate phase. In Ula Ulo nickel precipitation occurs in acidic zone (oxide zone) as Ni-goethite and serpentinite like garnierites. This is similar to precipitation of nickel in limonitic zone of New Caledonia. Relatively immobile nickel will substitute mobile Mg in the serpentinite (Dublet et al., 2012). Therefore, the serpentinites show depletion of magnesium while nickel is enriched. Change in concentration of MgO is – 8.2 % while Ni concentration elevated from 2630 ppm to 1.1 %. In saprolite zone the dominant phase is encrustation and vein precipitation. Therefore, the change in concentration is Ni (+3.3%) and Mg (- 4%).

Model (fig 7.1) is developed for Ula Ulo lateritic deposit based on field observation, mineralogical and chemical analysis. The genesis of the mineralization is summarized as the following:

1. Anomalous nickel concentration found in protor serpentinites and olivine
2. weathering disintegrated the serpentinites and librated the nickel
3. On residual oxide zone weathered serpentinites adsorb the nickel in the places where Mg is leached out.
4. Meteoritic water dissolves the oxide zone and nickel percolated down to the saprolite zone.
5. On the saprolite zone nickel precipitated as garnierite veins and encrustation on saprolite serpentinites.

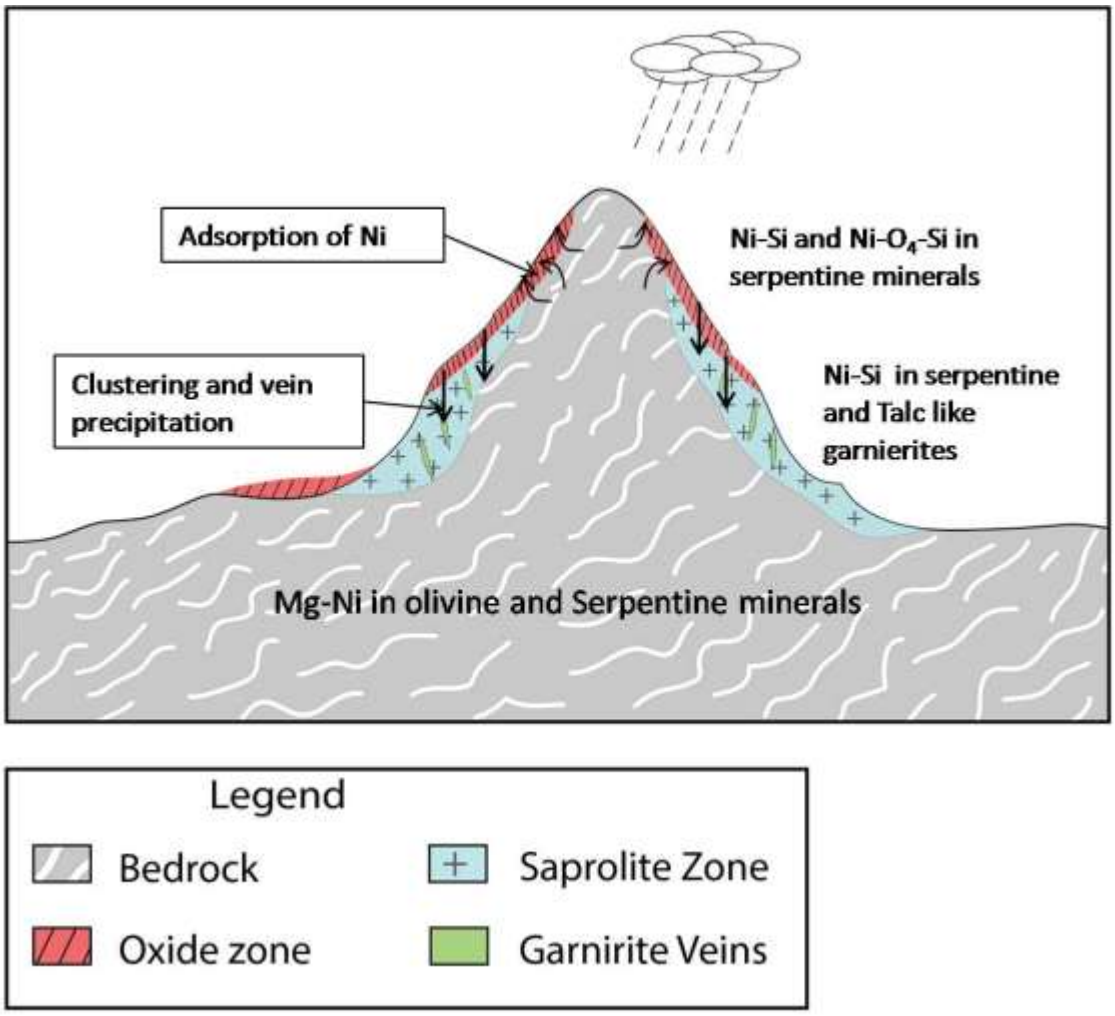


*Fig 7.1 Idealized ore deposit model of Ula Ulo lateritic nickel deposit*

# Chapter- VIII

# Conclusion and recommendation

## 8.1. Conclusion

The methodologies adopted for the research are geological fieldwork, petrography, ore mineralogy and geochemistry. These methods give valuable information to address the objective of the research. The major findings of the research are the following:

1. The geology of the area is characterized as the following. All the lithologic units studied are metamorphic rocks. These rocks are volcanic and sedimentary protolith. Volcanic protolith rocks are serpentinite, talc tremolite schist, tremolite talc schist and amphibolites. Sedimentary origins are quartzite, graphite schist and meta psmmite. The grade of metamorphism is green schist facies. Metavolcanic rocks are boninite Thoeliite. The tectonic setting is volcanic arc.
2. Ula Ulo nickel deposit is hosted and confined by serpentinite. The country rocks of the deposit are talc tremolite schist and tremolite talc schist. The mineralization on the ore body found as dissemination, coating and discrete veins. The mineral assemblage of the ore zone is chromite + magnetite + lizardite-nepounite+talc-willmesite.
3. The deposit is zoned into two zones. These are oxide zone and saprolite zone. In the oxide zone garnierites found as Ni – serpentine and Ni – talc. In the saprolite zone only nickel silicates are found. The ore minerals of the oxide zone are mainly serpentine like garnierite with small talc like. While in saprolite the ore minerals are dominantly talc like serpentinites with small serpentinite like garnierites. Both talc- like and serpentine like garnierites present in Ula Ulo Lateritic nickel deposits.
4. The genesis of the mineralization is summarized as the following:

    1. Anomalous nickel concentration found in protor serpentinites and olivine
    2. weathering disintegrated the serpentinites and librated the nickel
    3. On residual oxide zone weathered serpentinites adsorb the nickel in the places where Mg is leached out.

4. Meteoritic water dissolves the oxide zone and nickel percolated down to the saprolite zone.
5. On the saprolite zone nickel precipitated as garnierite veins and encrustation on saprolite serpentinites.

**5.** The reserve of the deposit is estimated based on conventional approach of resource estimation. Based on the estimation two separate blocks are identified. These are Bloke 1 is 2775240 @ 1.848 Ni % and Block 2 is 14585428 @ 2.02 Ni.

### 8.2. Recommendation

1. Some rational examples of currently active mines are presented on table 6.2 (table 6.2) (Mudd, 2010). As presented on the table 6.2 the tonnage and grade of lateritie deposits of the world is closer to Ula Ulo nickel deposit based on the current resource estimation and by previous works of Valicu and Yehwalwork (1967). After the last exploration working by Bentor (1967) and Valicu and Yehwalwork (1967) no exploration is done in Ula Ulo nickel deposit. some companies like Canadian based Artena have done feasibility study for mining in 1974, suddenly the progress stopped and no works have done till now. At least at this level of understanding this research shows a green light for subsequent exploration and the deposit could be economical at current state of nickel price and sophistication of technology. Both factors can minimize the cut off grade and increase profitability.

| **Project** | **Country** | **Ore (Mt)** | **Ni (%)** | **kt Ni** | **Company** |
|---|---|---|---|---|---|
| Murrin murrin | Australia | 330 | 0.99 | 3267 | Minara resource |
| Falcondo | Dominican Republic | 72.3 | 1.53 | 1110 | Xstrata |
| Doniambo | New Caledonia | 142.3 | 2.48 | 3526 | Eramet |
| Goro | New Caledonia | 124.3 | 1.46 | 1815 | Vale Inco JV |
| Loma de Niquel | Venezuela | 40.5 | 1.46 | 591 | Anglo American |
| Codemin | Brazil | 10.6 | 1.29 | 137 | Anglo American |

*Table 7.1 some examples of active lateritic mines and their corresponding resource (Mudd, 2010).*

2. From scientific point of view, extrusive ultramafic rocks like serpentinite can document the history of orogeny and mineral transformation from low grade to high metamorphic grades.
3. As observed in polished sections, chromite and magnetite mineral grains present within the serpentinites. This minerals are an ore mineral of Cr and Fe respectively. so these oxide mineralization need to be studied.
4. Other fascinating scientific problem I have seen is the structural elements found in the metasediments. The study of this structures could fill the gap on understanding Legadembi – Aflata shear zone.
5. There are many ultramafic occurrences in Adola belt. For example closer to Ula Ulo, there are Kilta on the south and kenticha in the east. These ultramafic rocks could host a mineralization and industrial minerals. Therefore it is advisable to see also other occurrences next to Ula Ulo.

# References

Abdelsalam, M. G., Tsige, L., Yihunie, T. and Hussien, B. (2008). Terrane rotation during the East African Orogeny: evidence from the Bulbul Shear Zone, south Ethiopia. *Gondwana Research*. ***14*(3)**: 497-508.

Alene, M. and Barker, A. J. (1997). Geochemistry of meta-igneous rocks from southern Ethiopia: a new insight into Neoproterozoic tectonics of northeast Africa. *Journal of African Earth Sciences*. ***24*(3)**: 351-370.

Ashley, P. M. (1975). Opaque mineral assemblage formed during serpentinization in the Coolac ultramafic belt, New South Wales. *Journal of the Geological Society of Australia*. ***22*(1):**91-102.

Asrat, A., Barbey, P., and Gleizes, G. (2001). The Precambrian geology of Ethiopia: a review. *Africa Geoscience Review*. ***8*(3/4)**: 271-288.

Bas, M. L., Maitre, R. L., Streckeisen, A., Zanettin, B. and IUGS Subcommission on the Systematics of Igneous Rocks. (1986). A chemical classification of volcanic rocks based on the total alkali-silica diagram. *Journal of petrology*. ***27*(3)**: 745-750.

Bentor. (1967). A report to minstry of mines. Unpublished report, Addis Ababa.

Beraki, W.H., Bonavia, F.F., Getachew, T., Schmerold, R. and Tarekegn, T. (1989). The Adola fold and thrust belt, Southern Ethiopia: a re-examination with implications for Pan-African evolution. *Geol. Mag*. **126**: 647-657.

Berhe, S. M. (1990). Ophiolites in north-east and east Africa: implications for Proterozoic crustal growth. *Journal Geological Society London. **147**:41-57.*

Boynton, W. (1984). *Cosmochemistry of the rare earth elements.* Elsevier.

Brand, N.W., Butt, C.R.M., and Elias, M., 1998. Nickel laterites: classification and features *AGSO Journal of Australian Geology and Geophysics*. **17**: 81–88.

Berger, B. R. and Drew, L. J. (2002). *Mineral-deposit models In Deposit and geoenvironmental models for resource exploitation and environmental security*. Springer, Dordrecht. pp. 121-134.

Brindley, G.W. (1978). The structure and chemistry of hydrous nickel-containing silicate and aluminate minerals. *Bull. BRGM* . **3**:233–245.

Brindley, G. W. and Hang, P. T. (1973). The nature of garnierites-I. *Clays and Clay Minerals*.

***21***:27-40.

Brindley, G. W., and Maksimovic, Z. (1974). The nature and nomenclature of hydrous nickel-containing silicates. *Clay Minerals*. ***10*(4)**: 271-277.

Brownlow, H.A. (1996). *Geochemistry*. Prentice-Hal, Inc, New Jersey, USA.

Butt, C. R. and Cluzel, D. (2013). Nickel laterite ore deposits: weathered serpentinites. *Elements*. ***9*(2)**: 123-128.

Butt, C.R.M. and Nickel, E.H.(1981). Mineralogy and geochemistry of the weathering of the disseminated nickel sulfide deposit at Mt. Keith, Western Australia. *Econ. Geol*. **76**: 1736–1751.

Burisch, M., Gerdes, A., Walter, B. F., Neumann, U., Fettel, M. and Markl, G. (2017). Methane and the origin of five-element veins: mineralogy, age, fluid inclusion chemistry and ore forming processes in the Odenwald, SW Germany. *Ore Geology Reviews*. ***81***:42-61.

Bu¨ttner, W. and Saage, R. (1982): Rapid XRD Determination of the chrysotile/lizardite ratios in asbestos-bearing serpentinites. TMPM (Tschermaks Mineralogische und Petrographische Mitteilungen). **30**:177–187.

Central Stastical Agency (2007). Oromia statistical data. unpublished report, Addis Ababa.

Chater, A.M. (1971). The geology of the Megado area of southern Ethiopia. Unpublished Ph.D. Thesis. University of Leeds, England. 178pp.

Clark, A.M.S. (1978). Chemical and mineralogical development of the Sidamo nickeliferous serpentinites (Ethiopia). *Miner. Deposita.* **13**: 221–234.

Coleman, R. G. (1971). Plate tectonic emplacement of upper mantle peridotites along continental edges. *Journal of Geophysical Research*. **76**:1212–1222

Cornwall, H. R. (1949). *Nickel Deposits of North America*. USGS, Washington, DC.

Cox, D. P., and Singer, D. A. (1986). *Mineral deposit models*. US Government Printing Office,

Dill, H. G. (2010). The “chessboard” classification scheme of mineral deposits: Mineralogy and geology from aluminum to zirconium. *Earth-Science Reviews*. ***100*(1-4)**: 1-420.

Donaldson, M.J. (1981). Redistribution of ore elements during serpentinization and talc – carbonate alteration of some archean dunites, western australia. *Econ. Geol.* **76**: 1698-1713.

Dublet G., Juillot F., Morin G., Fritsch E., Fandeur D., Ona-Nguema G. and Brown, Jr., G. E. (2012). Ni speciation in a New Caledonian lateritic regolith: A quantitative X-ray

Absorption spectroscopy investigation. *Geochim. Cosmochim. Acta*. **95**: 119 – 133.

De Wit, M.J. and Chewaka, S. (1981). Plate tectonic evolution of Ethiopia and the origin of its mineral deposits: an overview. In: Chewaka, S., De Wit, M.J. (Eds.), Plate Tectonics and Metallogenesis: Some guidelines to Ethiopian Mineral Deposits Ethiopian Institute Geological Surveys, Bulletin, 2, pp. 115–129.

Dietrich, V. and Peters, T. (1971). *Schweiz. Mineral. petri. Mit.*. **51**: 329-348.

Eckstrand, O. R. (1975). The Dumont serpentinite; a model for control of nickeliferous opaque mineral assemblages by alteration reactions in ultramafic rocks. *Economic Geology*. ***70*(1):** 183-201.

Elias, M. (2006). Lateritic nickel mineralization of the Yilgarn craton. *Society of Economic Geologists, Special Publication.* **13**:195–210.

Eliopoulos, D. G., Economou-Eliopoulos, M., Apostolikas, A. and Golightly, J. P. (2012). Geochemical features of nickel-laterite deposits from the Balkan Peninsula and Gordes, Turkey: The genetic and environmental significance of arsenic. *Ore Geology Reviews*. ***48***: 413-427.

Evans, B. W. (2010). Lizardite versus antigorite serpentinite: Magnetite, hydrogen, and life (?). *Geology*. ***38*(10)**: 879-882.

Filippidis, A. (1982). Experimental study of the serpentinization of Mg-Fe-Ni olivine in the presence of sulfur. *The Canadian Mineralogist*. ***20*(4)**: 567-574.

Freysinnet, P., Butt, C.R.M. and Morris, R.C. (2005). Ore-forming processes related to lateritic weathering. *Econ. Geol.* **100th Anniversary Vol**.: 681–722.

Galí, S., Soler, J. M., Proenza, J. A., Lewis, J. F., Cama, J. and Tauler, E. (2012). Ni enrichment and stability of Al-free garnierite solid-solutions: A thermodynamic approach. *Clays and Clay Minerals*. ***60*(2)**:121-135.

Gaudin, A., Decarreau, A., Noack, Y. and Grauby, O. (2005). Clay mineralogy of the nickel laterite ore developed from serpentinised peridotites at Murrin Murrin, Western Australia. *Australian Journal of Earth Sciences*. ***52*(2)**: 231-241.

Ghebrehab, W. (1992). The geological evolution of the adola precambrian greenstone belt, southern ethiopia.*Journal of african earth sciences*. **14(4):** 457-469.

Ghebreab, W., Yohannes, E. and Giorgis, L. W. (1992). The Lega Dembi gold mine: an example of shear zone-hosted mineralization in the Adola greenstone belt, Southern Ethiopia.

*Journal of African Earth Sciences (and the Middle East)*. ***15*****(3-4)**: 489-500.

Gichile, S. (1992). Granulites in the Precambrian basement of southern Ethiopia: geochemistry, PT conditions of metamorphism and tectonic setting. *Journal of African Earth Sciences (and the Middle East)*. ***15*****(2)**: 251-263.

Gilboy, C.F. (1970). The geology of the Gariboro region of southern Ethiopia. Unpublished Ph.D.Thesis, University of Leeds, England. 212pp.

Gillis, K. M., Ludden, J. N. and Smith, A. D. (1992). Mobilization of REE during crustal aging in the Troodos ophiolite, Cyprus. *Chemical Geology*. ***98***: 71-86.

Green, T. H. (1980). Island arc and continent-building magmatism—A review of petrogenic models based on experimental petrology and geochemistry. *Tectonophysics*. ***63*****(1-4)**: 367-385.

Greenwood, H. J. (1963). *J. Petrol.* **4**: 317-351.

Hermela (1977). A report on Adola serpentinites. Unpublished report. Ministry of mines, Addis Ababa.

Hickey, R. L. and Frey, F. A. (1982). Geochemical characteristics of boninite series volcanics: implications for their source. *Geochimica et Cosmochimica Acta*. ***46*****(11)**:2099-2115.

https://en.climate-data.org/location/508527/ accessed on 2.3.2018.

http://www.insg.org/whatnickel.aspx accessed 28.1.2018.

Humphris, S. E. and Thompson, G. (1978). Trace element mobility during hydrothermal alteration of oceanic basalts. *Geochimica et Cosmochimica Acta*. ***42*****(1)**: 127-136.

Irvine, T. and Baragar, W. (1971). A guide to the chemical classification of the common volcanic rocks. *Canadian journal of earth sciences* **8**(5):523-548.

Jelenc, D.A. (1963). A report on nickel exploration on southern Ethiopia written to Ministry of Mines and energy. Unpublished report, Addis Ababa

Jelenc, D.A. (1964). A report on nickel exploration on southern Ethiopia written to Ministry of Mines and energy. Unpublished report, Addis Ababa.

Jelenc, D.A. (1965). A report on nickel exploration on southern Ethiopia written to Ministry of Mines and energy. Unpublished report, Addis Ababa.

Jelenc, D.A. (1966a). A Report on Mineral Occurrences of southern Ethiopia. Unpublished report, Ministry of Mines and Energy, Addis Ababa.

Jelenc, D.A. (1966b). A report on nickel exploration on southern Ethiopia written to Ministry of

Mines and energy, Ministry of Mines and Energy, Addis Ababa.

Johnson, P. R. and Woldehaimanot, B. (2003). Development of the Arabian-Nubian Shield: perspectives on accretion and deformation in the northern East African Orogen and the assembly of Gondwana. *Geological Society, London, Special Publications*. ***206*(1)**: 289-325.

Johannes, W. (1968). *Contr. Mineral. Petrol.* **19**:309-315.

Code, J. O. R. C., & Joint Ore Reserves Committee. (2012). The JORC code and guidelines. *Australasian code for reporting of exploration results, mineral resources and ore reserves prepared by The Australasian Institute of Mining and Metallurgy (AusIMM), Australian Institute of Geoscientists and Minerals Council of Australia.[Online] Dostępne w: www. jorc. org [Dostęp: 10.07. 2015]*.

Kazmin, V. (1975). The Precambrian of Ethiopia and some aspects of the geology of the Mozambique Belt. *Geophysical Observatory Bulletin*. **1**: 14

Kazmin, V., 1972. Geology of Ethiopia; explanatory note to the geological map of Ethiopia, 1:2,000,000. Unpublished technical report, Ministry of Mines, Addis Ababa.

Kazmln, V. (1978). Geology of the Ethiopian Basement and possible relation between the Mozambique and the Red Sea Belts. Egypt. J. Geo/.. **22(1)**: 73-86.

Kazmin, V., Shlferaw, A. and Balcha, T. 1978. The Ethiopian basement: Stratigraphy and possible maner of evolutlon. *Geo/. Rdsctu*, **54667(2**), 531.

Keays, R. R. (1995). The role of komatiitic and picritic magmatism and S-saturation in the formation of ore deposits. *Lithos*. ***34*(1-3)**: 1-18.

Kozyrev, V., Girma, K., Safanov, T., Bekele,W.M., Tuliankin, V., Bestujev, A., Baijapov, A., Tewolde, M.T., Gurbanvich, G., Kaitukov, M,.Arijapov, A. (1985). Regional geological and exploration work for gold and other minerals in the Adola Goldfields. Ethiopian Mineral Resources Development Corporation. Unpublished report. Addis Ababa.

Levitte, D. and Kent, G. (1968). A report on Nickeliferous laterites of Sidamo. Unpublished report, Addis Ababa.

Longo, F. (2014). Garnierites and garnierites: Textures, mineralogy and geochemistry of garnierites in the Falcondo Ni-laterite deposit, Dominican Republic. *Ore Geology Reviews*. ***58*:** 91-109.

LeMaitre, R.W. (Ed.), 1989. *A Classification of Igneous Rocks and Glossary of Terms.* Blackwell, Oxford, 193 pp.

Lelong, F., Tardy, Y., Grandin, G., Trescases, J.J. and Boulange, B.(1976). Pedogenesis, Chemical weathering and processes of formation of some supergene ore deposits. **In:** Wolf, K. H. (Ed.), *Handbook of stratabound and stratiform ore deposits -I- Principles and general studies Supergene and Surficial Ore Oeposits; Texture and Fabrics v. 3*. pp. 93–133. Elsevier, Amsterdam.

Marsh, E., and Anderson, E. (2011). *Ni-Co laterites–a deposit model*. US Geological Survey Open- File Report 2011-1259.

Maynard, J. B. (2012). *Geochemistry of sedimentary ore deposits*. Springer Science & Business Media.

Mengesha, T., Tadiwos, C., and Workenesh, H. (1999). Explanation of geological map of Ethiopia, scale 1: 2,000,000. Unpublished technical report, EIGS, Addis Ababa.

Meschede, M. (1986). A method of discriminating between different types of mid-oceanic ridge basalts and continental tholeiites with the Nb–Zr–Y diagram. *Chem. Geol*. **56**: 207–218.

Ministry of Mines (1964). A report on Adola Nickel exploration results. Unpublished report, Addis Ababa.

Misra, K. (1999). *Understanding mineral deposits*. Kulwer academic publisher, Dordrecht, Netherlands, 845pp.

Moody, J. B. (1976). Serpentinization: a review. *Lithos*. ***9*(2)**: 125-138.

Moores, E. M. (1970). Ultramafics and orogeny, with models of the U.S. Cordillera and the Tethys. *Nature*. **228**:837–842.

Mudd, G. M. (2010): Global trends and environmental issues in nickel mining: Sulfides versus laterites. *Ore Geology Reviews*. **38:** 9–26.

Naldrett, A. J. (1999). World-class Ni-Cu-PGE deposits: key factors in their genesis. *Mineralium deposita*. ***34*(3):** 227-240.

Naldrett, A. J. (2013). *Magmatic sulfide deposits: Geology, geochemistry and exploration*. Springer Science and Business Media, New York, 734 pp.

Pearce, J. A. and Cann, J. R. (1973). Tectonic setting of basic volcanic rocks determined using trace element analyses. *Earth and planetary science letters*. ***19*(2)**: 290-300.

Redman, B. A. and Keays, R. R. (1985). Archaean basic volcanism in the eastern Goldfields province, Yilgarn Block, western Australia. *Precambrian Research*. ***30*(2)**: 113-152

Ridely, J. (2013). *Ore deposit geology*. Cambridge university press, New York, 411pp.

Ripley, E. M. And Li, C. (2013). Sulfide saturation in mafic magmas: Is external sulfur required for magmatic Ni-Cu-(PGE) ore genesis?. *Economic Geology*. ***108*(1)**: 45-58.

Rollinson, H.R. (1993). *Using geochemical data: evaluation, presentation, interpretation*: Routledge.

Roqué-Rosell, J., Villanova-de-Benavent, C. and Proenza, J. A. (2017). The accumulation of Ni in serpentines and garnierites from the Falcondo Ni-laterite deposit (Dominican Republic) elucidated by means of μXAS. *Geochimica et Cosmochimica Acta*. ***198***: 48-69.

Schmerold, R. 1988. A report on the field trip to the Adola goldfield (Sidamo). Unpublished report. EIGS/TMEP Eth/86/034, Addis Ababa.

Shervais, J.W. (1982). Ti–V plots and the petrogenesis of modern and ophiolitic lavas. *Earth Planet. Sci. Lett.* **59**:101–118.

Song, Y., Moon, H. S., & Chon, H. T. (1995). New occurrence and characterization of Ni-serpentines in the Kwangcheon area, Korea. *Clay Minerals*. ***30*(3)**: 211-224.

Springer G. (1974) Compositional and structural variations in garnierites. *Can. Mineral*. **12**: 381–388.

Staude, S., Werner, W., Mordhorst, T., Wemmer, K., Jacob, D. E., and Markl, G. (2012). Multi-stage Ag–Bi–Co–Ni–U and Cu–Bi vein mineralization at Wittichen, Schwarzwald, SW Germany: geological setting, ore mineralogy, and fluid evolution. *Mineralium Deposita*. ***47*(3)**: 251-276.

Stern, R.J. (1994). Arc assembly and continental collision in the Neoproterozoic East African Orogen: implications for the consolidation of Gondwanaland. *Annual Review of Earth and Planetary Sciences*. ***22*(1)**: 319-351.

Sun, S. S. and McDonough, W. S. (1989). Chemical and isotopic systematics of oceanic basalts: implications for mantle composition and processes. *Geological Society, London, Special Publications*. ***42*(1)**: 313-345.

Solomon, T., Milesi, J. P., Deschamps, Y. (2003). Geology and mineral potential of Ethiopia: a note on geology and mineral map of Ethiopia. *Journal of African Earth Sciences*. ***36*(4)**: 273-313.

Tadesse, G. and Allen, A. (2005). Geology and geochemistry of the Neoproterozoic Tuludimtu

Ophiolite suite, western Ethiopia. *Journal of African Earth Sciences*. ***41*(3)**: 192-211.

Teklay, M., Kröner, A., Mezger, K. and Oberhänsli, R. (1998). Geochemistry, Pb□ Pb single zircon ages and Nd□ Sr isotope composition of Precambrian rocks from southern and eastern Ethiopia: implications for crustal evolution in East Africa. *Journal of African Earth Sciences*. ***26*(2)**: pp.207-227.

Thorne, R., Roberts, S. and Herrington, R.. (2012b). The formation and evolution of the Bitincke nickel laterite deposit, Albania. *Miner. Deposita.* **47**: 933–947.

Thornton, C. P. and Tuttle, O. F. (1960). Chemistry of igneous rocks--[Part] 1, Differentiation index. *American Journal of Science*. ***258*(9)**: 664-684.

Tolessa, S., Bonavia, F.F., Solomon, M., Awoke, H. and Eshete, T., 1991. Structural pattern of Pan- African rocks around Moyale, southern Ethiopia. *Precambrian Research*. **52**: 179–186.

Training for mineral explotation project (TMEP). (1993). Interim report on mineral exploration in Adola area, Sidamo, Ethiopia. Technical report, EIGS/UNDP Training for Mineral Exploration Project, Addis Ababa.

Tsgie, L. (2006). Metamorphism and gold mineralization of the Kenticha–Katawicha area: Adola belt, southern Ethiopia. *Journal of African Earth Sciences*. **45**:16‑32.

Tsige, L. and Abdelsalam, M.G. (2005). Neoproterozoic–Early Paleozoic gravitational tectonic collapse in the southern part of the Arabian-Nubian Shield: the Bulbul Belt of Southern Ethiopia. *Precambrian Research*. ***138*(3-4)**:297-318.

Van der Ent, A., Baker, A.J.M., van Balgooy, M.M.J. and Tjoa, A. (2013). Ultramafic nickel laterites in Indonesia (Sulawesi, Halmahera): Mining, nickel hyperaccumulators and opportunities for phytomining. *Journal of Geochemical Exploration*. **128**: 72–79

Vlacicu, Z.C. and Yewhalwork, M. (1967). Geological report on nickel deposits in sidamo province, Ministry of mines. Unpublished report, Addis Ababa.

Villanova-de-Benavent, C., Proenza, J.A., Galı´, S., Garcı´a-Casco, A., Tauler, E., Lewis, J.F. and Longo, F. (2014): Garnierites and garnierites: Texture, mineralogy and geochemistry in the Falcondo Ni-laterite deposit, Dominican Republic. *Ore Geol. Rev*. **58C**:91–109.

Walsh, J.. (1972). Geology of the Moyale area, Degree Sheet 14, Report No. 89. Ministry of Natural Resources, Geological Survey of Kenya, Kenya, 32 pp.

Wells, M. A., Ramanaidou, E. R., Verrall, M. and Tessarolo, C. (2009). Mineralogy and crystal chemistry of "garnierites" in the Goro lateritic nickel deposit, New Caledonia. *European Journal of Mineralogy*. ***21*(2)**:467-483.

Whittaker, E. J. W. and Zussman, J. (1956). The characterization of serpentine minerals by X-ray diffraction. *Mineralogical Magazine*. ***31*(233)**: 107-126.

Wicks, F.J. and O'Hanley, D.S. (1988): Serpentine minerals: structures and petrology. in ''Hydrous phyllosilicates'', S. Bailey, ed. *Mineralogical Society of America, Rev. Mineral.* **19**: 91–167

Wicks, F. J. and Whittaker, E. J. W. (1977). Serpentine textures and serpentinization. *Canadian Mineralogist*. ***15*(4)**:459-88.

Winkler, H.G.F. (1979). *Petrogenesis of Metamorphic Rocks, fifth ed.* Springer Verlag, New York, Heidelberg, Berlin, 348p.

Wolde, B., Asres, Z., Desta, Z. and Gonzalez, J. J. (1996). Neoproterozoic zirconium-depleted boninite and tholeiitic series rocks from Adola, southern Ethiopia. *Precambrian Research*. ***80*(3)**: 261-279.

Woldehaimanot, B. 1995. Structural Geology and Geochemistry of the Neoproterozoic Adobha and Adola Belts (Eritrea and Ethiopia).*Giessen Geolgische Schriften.* **54**: 218 pp.

Wood, D.A., Joron, J.L., Treuil, M., Norry, M. and Tarney, J. (1979). Elemental and Sr isotope variations in basic lavas from Iceland and the surrounding ocean floor. *Contrib. Mineral. Petrol.* **70**:319–339.

Worku, H., & Schandelmeier, H. (1996). Tectonic evolution of the Neoproterozoic Adola Belt of southern Ethiopia: evidence for a Wilson Cycle process and implications for oblique plate collision. *Precambrian research*. ***77*(3-4)**: 179-210.

Worku, H. and Yifa, K. (1992). The tectonic evolution of the Precambrian metamorphic rocks of the Adola Belt ( Southern Ethiopia). *J. Aft. Earth Sci.*. **14**: 37-55.

Yibas, B., Reimold, W.U., Armstrong, R., Koeberl, C., Anhaeusser, C.R. and Phillips, D. (2002). The tectonostratigraphy, granitoid geochronology and geological evolution of the Precambrian of southern Ethiopia. *Journal of African Earth Sciences*. ***34*(1-2)**: pp.57-84.

Yihunie, T. and Tesfaye, M. (2002). Structural evidence for the allochthonous nature of the Bulbul terrane in southern Ethiopia: a west-verging thrust nappe. *Journal of African*

*Earth Sciences*. **34**: 85–93.

Yibas, B. (2000). The Precambrian geology, tectonic evolution, and controls of gold mineralisations in southern Ethiopia. Unpublished Ph.D. Thesis, University of the Witwatersrand, Johannesburg, South Africa, 448 pp.

Yibas, B., Reimold, W.U., Anhaeusser, C.R. and Koeberl, C. (2000c). Geochemistry of the mafic rocks of the ophiolitic fold and thrust belts of southern Ethiopia: constraints on the tectonic regime during the Neoproterozoic (900–700 Ma). *Information Circular 349, Economic Geology Research Institute, University of the Witwatersrand*. **350**: 46 pp.

Yibas, B., Reimold, W.U., Anhaeusser, C.R. and Koeberl, C. (2003). Geochemistry of the mafic rocks of the ophiolitic fold and thrust belts of southern Ethiopia: constraints on the tectonic regime during the Neoproterozoic (900–700 Ma). *Precambrian Research*. ***121*(3- 4)**: 157-183.